Netrin-1 Trafficking in Human Neurons

by

Jhunam Sidhu

B.A., Whitman College, 2021

Thesis Submitted in Partial Fulfillment of the
Requirements for the Degree of
Master of Science

in the
Department of Molecular Biology and Biochemistry
Faculty of Science

SIMON FRASER UNIVERSITY
Summer 2024

Declaration of Committee

Name:	**Jhunam Sidhu**
Degree:	**Master of Science**
Title:	**Netrin-1 Trafficking in Human Neurons**
Committee:	**Chair:** **Dheva Setiaputra** Assistant Professor, Molecular Biology and Biochemistry
	Michael Silverman Supervisor Professor, Molecular Biology and Biochemistry
	Nancy Hawkins Committee Member Associate Professor, Molecular Biology and Biochemistry
	Michel Leroux Committee Member Professor, Molecular Biology and Biochemistry
	Lisa Julian Examiner Assistant Professor, Biological Sciences

Abstract

The secreted guidance cue netrin-1 orchestrates essential nervous system developmental processes such as axon pathfinding and synaptogenesis. However, little is known about the expression, transport, and localization of netrin-1 in human neurons. After optimizing human neuronal cultures derived from induced pluripotent stem cells (iPSC), I investigated the localization and intracellular transport of netrin-1. I demonstrated endogenous expression of netrin-1 within human iPSC-derived neurons via immunocytochemistry. I then studied the transport of fluorescently-labeled netrin-1 (netrin-1-mRuby3) via live cell imaging where netrin-1 traffics bidirectionally in neurons. Additionally, netrin-1 co-transports and co-localizes with the resident dense core vesicle protein chromogranin and KIF1A, the primary microtubule-based motor responsible for transport of this vesicle type. These findings are significant in the understanding of mechanisms behind netrin-1 function and regulation in human neurons.

Keywords: Netrin-1; KIF1A; Axonal transport; Dense core vesicles; iPSC-derived neurons; KAND

Acknowledgements

I would like to thank my supervisor, Dr. Michael Silverman, for his guidance and support throughout my time at Simon Fraser University (SFU). His mentorship has been instrumental in my development as a scientist, and I am truly grateful of the opportunities he has provided me. I would like to thank my committee members, Dr. Nancy Hawkins and Dr. Michel Leroux, for their insightful feedback and valuable contributions to my project. I would also like to thank my fellow lab member Andrew Wieczorek for his continual support. From my laboratory training to pushing me to think critically, Andrew's guidance has been indispensable towards my success and education. And finally, I would like to thank my other lab members, friends, and family for their help throughout my project. Thanks to the efforts of everyone in my life, I have grown tremendously both professionally and personally. I will always cherish my time at SFU and the relationships I have built here.

Table of Contents

List of Tables

List of Figures

List of Acronyms

AIS	Axon initial segment
BDNF	Brain-derived neurotrophic factor
CaM	Calmodulin
CHG	Chromogranin
c-MYC	Cellular myelocytomatosis oncogene
CNS	Central nervous system
DCC	Deleted in colorectal cancer
DCV	Dense core vesicle
DMEM	Dulbecco's modified eagle medium
DIV	Days *in vitro*
EHS	Engelbreth-Holm-Swarm
HSP	Hereditary spastic paraplegia
ICC	Immunocytochemistry
iPSC	Induced pluripotent stem cell
KAND	KIF1A neurological disorder
Klf4	Krupple-like factor 4
LB	Luria Broth
LTP	Long-term potentiation
MAP2	Microtubule-associated protein 2
NGN2	Neurogenin-2
NPC	Neural progenitor cell
NPY	Neuropeptide Y
NSC	Neural stem cell
Oct4	Octamer-binding protein 4
PBS	Phosphate-buffered saline
PH	Plekstrin homology
PLA	Proximity ligation assay
PLL	Poly-L-lysine

PLO	Poly-L-ornithine
Sox2	(Sex determining region Y)-box 2
STV	Synaptic transport vesicle
SVP	Synaptic vesicle precursor
TBS	Tris-buffered saline

Chapter 1. Introduction

1.1. Neuronal Transport

Active intracellular transport represents a fundamental process within eukaryotic cells, facilitating the movement of vital proteins and cargo with precision and efficiency. Unlike passive diffusion, active transport can move against concentration gradients and at greater speeds and distances. In eukaryotic cells, active transport proves essential for constructing the cytoskeleton, transporting proteins and organelles, cell division, and homeostasis (Ali & Yang 2020). Motor proteins facilitate active transport by converting chemical energy to mechanical energy to move essential proteins and other cargoes from their sites of synthesis to distal locations in the cell (Yildiz et al., 2004). They traverse microtubules and execute complex and coordinated activities necessary for cell survival. Active transport is particularly important for neurons due to their unique morphology. Comprised of a cell body, extending dendrites, and a long axon that can stretch up to one meter in a fully grown human, a neuron's strict structural polarity is crucial for its function of transmitting information over long distances. In a developing neuron, active transport aids in establishing distinct functional domains, supporting the development of axons and dendrites, and facilitating synaptogenesis (Vos & Hafezparast 2017). Throughout the life of a neuron, transport maintains homeostasis by shuttling proteins and organelles to their essential locations along axons and dendrites, while also removing cellular waste such as damaged organelles and oxidized proteins. As the axon largely lacks biosynthetic materials while being many orders of magnitude longer than the cell body, properly coordinated active transport is required to ferry essential cargo from the cell body to its most distal ends. Therefore, active transport stands as a key preliminary step to numerous cellular processes.

Active transport is necessary for establishing a neuron’s distinct domains and specialized functions. The three main parts of a neuron are the dendrites, the cell body, and the axon. The cell body of a neuron stores essential organelles and is the primary site of synthesis for proteins. A neuron will have multiple dendrites that protrude from the cell body and are responsible for receiving information from other neurons. Dendrites

house multiple post-synaptic sites. The post-synapse consists of receptors, channels, scaffolding proteins, and cytoskeletal elements specialized to receive the signal from neighboring neurons (Mendolesi 2022). The signal then generates an action potential which travels down the axon to trigger neurotransmitter release at pre-synaptic sites. The axon and pre-synaptic sites are also equipped with their own set of specific proteins and organelles that facilitate neurotransmitter release which then carries on the signal to the next neuron. The neuron establishes distinct dendrites and the axon during development. The neuron will first develop minor processes, one of which will become the axon and the rest dendrites (Banker 2018). During development, intracellular transport is regulated to control the movement of proteins, organelles, and cytoskeletal elements to establish axonal and dendritic polarity. For example, certain molecular motors will transport cargoes selectively into the axon (Scherer et al., 2020) or dendrites (Karasmanis et al., 2018). These cargoes will establish microtubule polarity and specialized structures like the pre- and post-synapse. Throughout the life of the neuron, active transport will work to maintain polarity, and traffic proteins to maintain pre- and post- synaptic function.

At any given time, hundreds of proteins and organelles are transported across the axon of a neuron via the dynamic active axonal transport system (Lasek et al., 1984). Active axonal transport is powered by motor proteins, such as various kinesins and cytosolic dynein, which travel along microtubules. Cargo undergoing axonal transport travels at a constrained number of specified speeds, which are categorized as ‘slow’ and ‘fast’ transport. Slow transport traffics a myriad of cytosolic and cytoskeletal proteins such as microtubules and metabolic enzymes (Nixon 1998). Slow transport only reaches rates of travel between 0.2-10 mm/day, orders of magnitude slower than fast transport (Roy 2020). Mechanisms behind slow transport are not well known, however, molecular motors such as members of the kinesin-1 family have been implicated (Terada et al., 2010; Glomb et al., 2023). Unlike the transport of cytoskeletal components via slow transport, organelles and vesicles are transported relatively rapidly by fast axonal transport. Fast transport characterizes the bidirectional transport of membrane vesicles and their contents over long distances (Hirokawa & Tanaka, 2015). Multiple kinesin families contribute to fast axonal transport, each with distinct transport characteristics. Organelles trafficked by kinesins and dynein traverse up to 400mm a day, with members

of the kinesin-3 family reaching steps 2.5 times faster than kinesin-1 (Hirokawa & Tanaka, 2015). Differences in certain motor characteristics, such as ATPase processivity in the motor domain and microtubule binding affinity, account for differences in molecular motor speed and run lengths (Mitra & Peterman 2020; Uemura et al., 2002). Dozens of different motor proteins exist and are necessary for the transport of the many proteins and organelles in a neuron. The differences in motor and transport characteristics fullfil different biological niches and are necessary for a versatile transport system. For example, the axonal growth rate of a given neuron is limited by its rate of slow transport (Stenoien & Brady 1999), while dysfunction in fast transport has been linked to various neurodegenerative diseases (Combs et al., 2019). Furthermore, a balance of fast and slow transport is necessary for the proper distribution of certain cargo such as secretory vesicles (Gumy et al., 2017). Axonal transport is a multifaceted task and underscores many critical processes in the development and function of a neuron.

The cytoskeleton of a cell maintains its structure and internal organization and acts as a highway for axonal transport. There are three main components of the cytoskeletal network, including the actin filaments, intermediate filaments, and microtubules (Fletcher & Mullins 2010). Microtubules are involved in many cellular processes, such as mitosis and cell mobility, and are the main substrate for kinesin and dynein motor-based transport (Cushion et al., 2024). Microtubules are found in all eukaryotic organisms (Goodson & Jonassan 2018), and are highly dynamic, constantly elongating and depolymerizing in response to cellular processes (Vorobjev et al., 1999). Microtubules are composed of heterodimers of α- and β- tubulin that self-assemble to form long and hollow structures (Goodson & Jonassan 2018). The α- and β-tubulin heterodimers assembly gives rise to the plus- and minus-ends of the microtubule (Figure 1.1). The β-tubulin end of the microtubule elongates quickly and is considered the “plus end.” The “minus end” is on the opposite side and significantly slower to elongate. In addition to this model of microtubule assembly, various microtubule modifications are employed for functional specificity. Tubulin subunits undergo post-translational modifications such as phosphorylation and acetylation, which affect the binding affinity of proteins to the microtubule to enhance or impede motor protein motility (Hammond et al., 2010). Microtubule binding proteins such as microtubule associate protein 2 (MAP2)

and Tau also regulate microtubule dynamics such as assembly and motor-based transport. MAP2 is neuronally specific and enriched in dendrites. It is necessary for dendrite elongation (Figure 1.1; Harada et al., 2002) and regulates cargo transport by inhibiting the motility of certain motor proteins, like kinesin-1 (Gumy et al., 2017; Hagiwara et al., 1994). Tau is enriched in axons and interacts with the cytoskeleton to regulate axonal transport through pathways such as stabilizing microtubule tracks and acting as a microtubule spacer to avoid overcrowding (Figure 1.1; Ebneth et al., 1998; Gaspard et al., 2016). While tau is necessary for the maintenance of the cytoskeleton, aggregations in tau produce "tauopathies" which disrupt axonal transport and contribute to several neurodegenerative diseases such as Parkinson's and Alzheimer's disease (Combs & Meuller 2020; Avila et al., 2012). Microtubules are essential structures for eukaryotic cells and in addition to functioning as a substrate for axonal transport, they also play a part in its regulation.

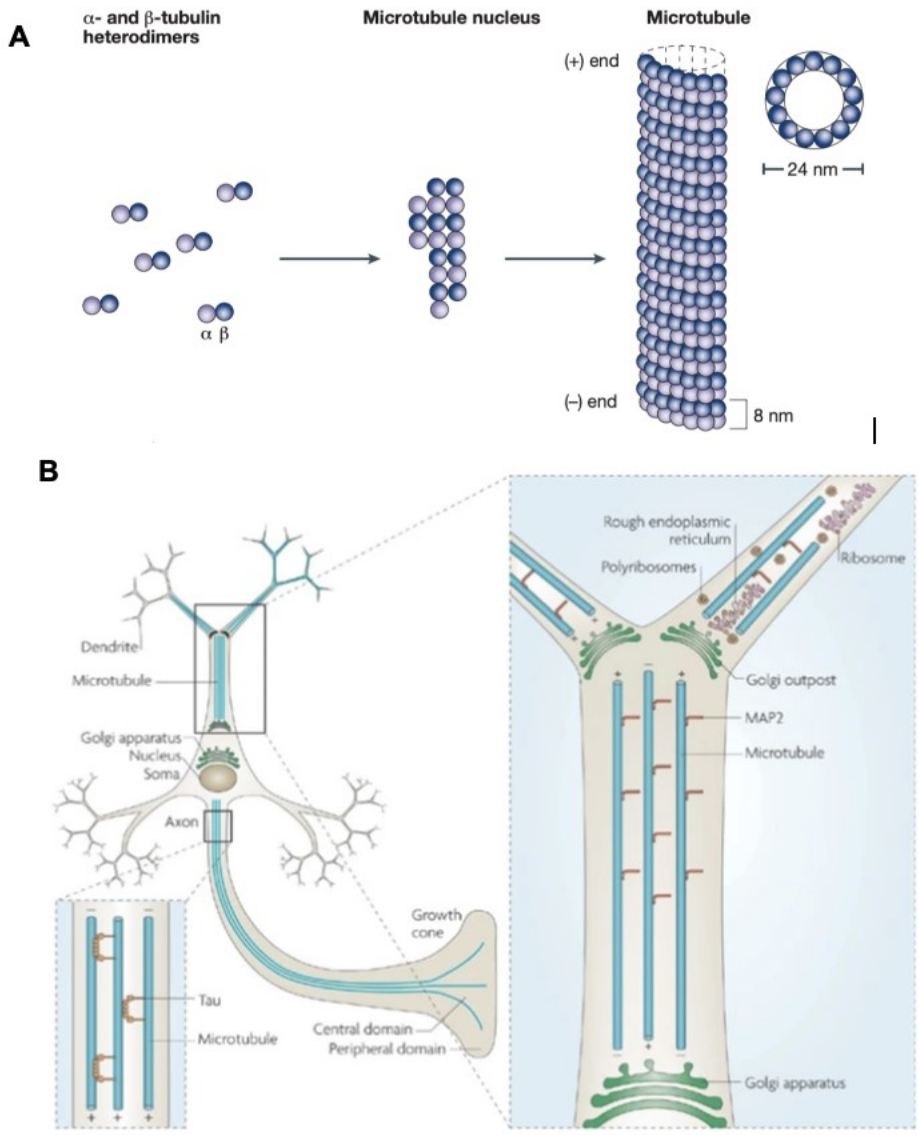

Figure 1.1 Microtubule organization and assembly

A. Microtubules are composed of heterodimers of both α- and β-tubulin which self-assemble to form protofilaments. Protofilaments are then assembled in parallel into sheets which then form the hollow microtubule tube. The plus end of the microtubule is marked by the exposed β-tubulin subunit. The minus end is marked by the exposed α-tubulin subunit. The microtubule undergoes elongation through the addition of new tubulin heterodimers. Microtubules are highly dynamic and will continuously undergo assembly and disassembly. (Jordan & Wilson 2004). B. Microtubules in the axon are arranged with the plus-end pointed away from the cell body. Tau is present in the axons and bound to the microtubules. In the dendrites, there are microtubules of mixed polarity, with microtubule-associated protein 2 (MAP2) bound to the microtubules. (Conde & Caceres 2009)

A distinct feature of fast axonal transport is the bidirectional movement of cargo, which is possible through the recruitment of motors with antagonistic directionality. Motors of different directionality are employed because of the strict orientation of microtubules within an axon, with plus ends strictly pointing away from the cell body and towards growth cones (Figure 1.1; Baas et al., 1988). Because motor proteins are largely either plus-end or minus-end directed (Duke 2002), movement both towards and away from the cell requires different motor types to be attached (Figure 1.2; Hendricks et al., 2010). Kinesin motor proteins are responsible for transport along microtubules in the plus direction while cytosolic dynein is responsible for transport in the minus direction (Abraham et al., 2018). To achieve transport in both directions, both kinesin and dynein motors will attach to the same cargo. While attached, the direction of transport is decided between kinesin and dynein through the dominance of one motor type. Some hypothesize that kinesins and dynein participate in a "tug-of-war" model driven by force-dependent kinetics (Hendricks et al., 2010), while others believe that bidirectionality can be achieved through the coordination of active and inactive states of the opposing motors (Bryantseva & Zhapparova 2012; Munoz & Klumpp 2022). Bidirectional behaviour can be considered inefficient, because motor proteins require ATP to function, and movement in both directions can delay the cargo delivery process. However, it may offer an advantage in avoiding roadblocks in the cytoskeletal network and in allowing time for cargo processing during transport (Hancock 2014). Bidirectional transport is a necessary and hallmark feature of fast axonal transport, that may offer distinct biological advantages.

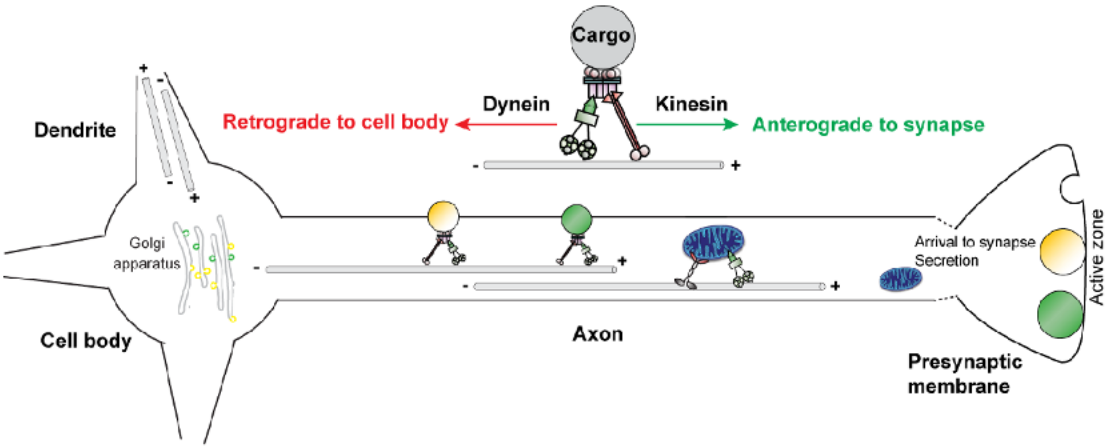

Figure 1.2 Bidirectional axonal transport
Bidirectional transport is essential for the proper distribution of organelles and proteins along a neuron's axon. Bidirectional transport is achieved through the recruitment of kinesin motor proteins working in the anterograde direction (away from the cell body) and cytosolic dynein in the retrograde direction (towards the cell body). The motor proteins carry cargo from the Golgi apparatus to their target destination along tracks of microtubules. (Made in Adobe Illustrator)

1.2. The Kinesin Superfamily and Cytoplasmic Dynein

Kinesins are a class of motor proteins found in eukaryotic cells that move along microtubules to traffic cargoes. The first kinesin identified, kinesin-1, was discovered in the axon of the giant squid (Vale et al., 1985). Since then, many more kinesin genes have been identified to construct the kinesin superfamily tree (Figure 1.3). The superfamily is broad and diverse, consisting of 45 KIFs and 15 families labelled kinesin-1 to kinesin-14B (Figure 1.3; Hirokawa et al., 2009). Kinesins are necessary for organelle and protein transport and chromosomal and spindle movements during cell division (Hirokawa et al., 2010). They move in a stepwise fashion with two motor head domains that bind to and move along microtubules to traffic cargo (Marx et al., 2010). Kinesin motor proteins consist of a conserved motor domain and unique stalk and tail domains which allow for specific dimerization and cargo binding (Figure 1.3). There are three categories of kinesins, defined by the position of their motor domain; N-terminal kinesins, C-terminal kinesins, and M-kinesins, where the motor domain is placed in the middle of the peptide. The three kinesin types are also somewhat functionally separated because of their structure. N-kinesins are microtubule plus-end directed, C-kinesins are minus-end

directed, and M-kinesins are described as microtubule depolymerizers (Konjikusic et al., 2021). Each of the families within the superfamily also has some degree of functional specificity in neuronal and CNS development and homeostasis. For example, members of the kinesin-6 family are responsible for the regulation of asymmetric vs symmetric cell division in the developing CNS, as well as the control of midbody formation during cytokinesis in cortical stem cells (Geng et al., 2018; Janisch et al., 2018). Members of the kinesin-4 and kinesin-2 family have been found necessary for axonal outgrowth and establishing microtubule polarity (Mukherjee et al., 2020; Van de Vaart et al., 2013). When it comes to the axonal transport of proteins and organelles, many kinesins are involved. For example, KIF1A, KIFC2, and KIF5C are all necessary for bidirectional axonal transport (Hirokawa et al., 2010; Hall & Hedgcock 1991; Saito et al., 1997; Kanai et al., 2000). Although members of the kinesin superfamily are closely related, they can vary greatly in form and function.

Kinesins have functional specificity in part because of their affinities for certain groups of cargo and their regulated localization. Unlike the conserved motor domain, the kinesin tail is varied and mediates cargo interactions. Mechanisms of cargo binding specificity are not well known however, evidence suggests that it involves specific interactions with the coiled-coil domain, the pleckstrin homology domain, and the recruitment of adaptor proteins (Jiang et al., 2019; Siddiqui et al., 2017; Figure 1.3). As a result of these interactions, kinesins are known to associate and traffic specific cargoes. However, there is some redundancy, with cargos such as mitochondria and synaptic vesicle precursors being transported by multiple motors (Hirokawa et al., 2010). Nevertheless, kinesin trafficking of these cargoes facilitates neuronal development with the elongation of axons and the polarization of neurons. Neuronal polarity is requisite for the proper function of the cell and is established early on by the differential allocation of cellular proteins and materials. By establishing distinct domains such as axons and dendrites, the neuron can receive and relay information, forming the basis for the development of the nervous system. KIF5, also known as conventional kinesin-1, exemplifies how kinesin-based transport can regulate these cellular processes. In the sorting of membrane traffic into axons and dendrites, KIF5 specifically localizes to axons because of interactions with unique features of the axon initial segment (Nakata &

Hirokawa 2003). Because kinesins exhibit specificity for cargo binding, regulating kinesin transport also regulates cargo localization. The complexity of the kinesin superfamily underscores its critical role in neuronal function.

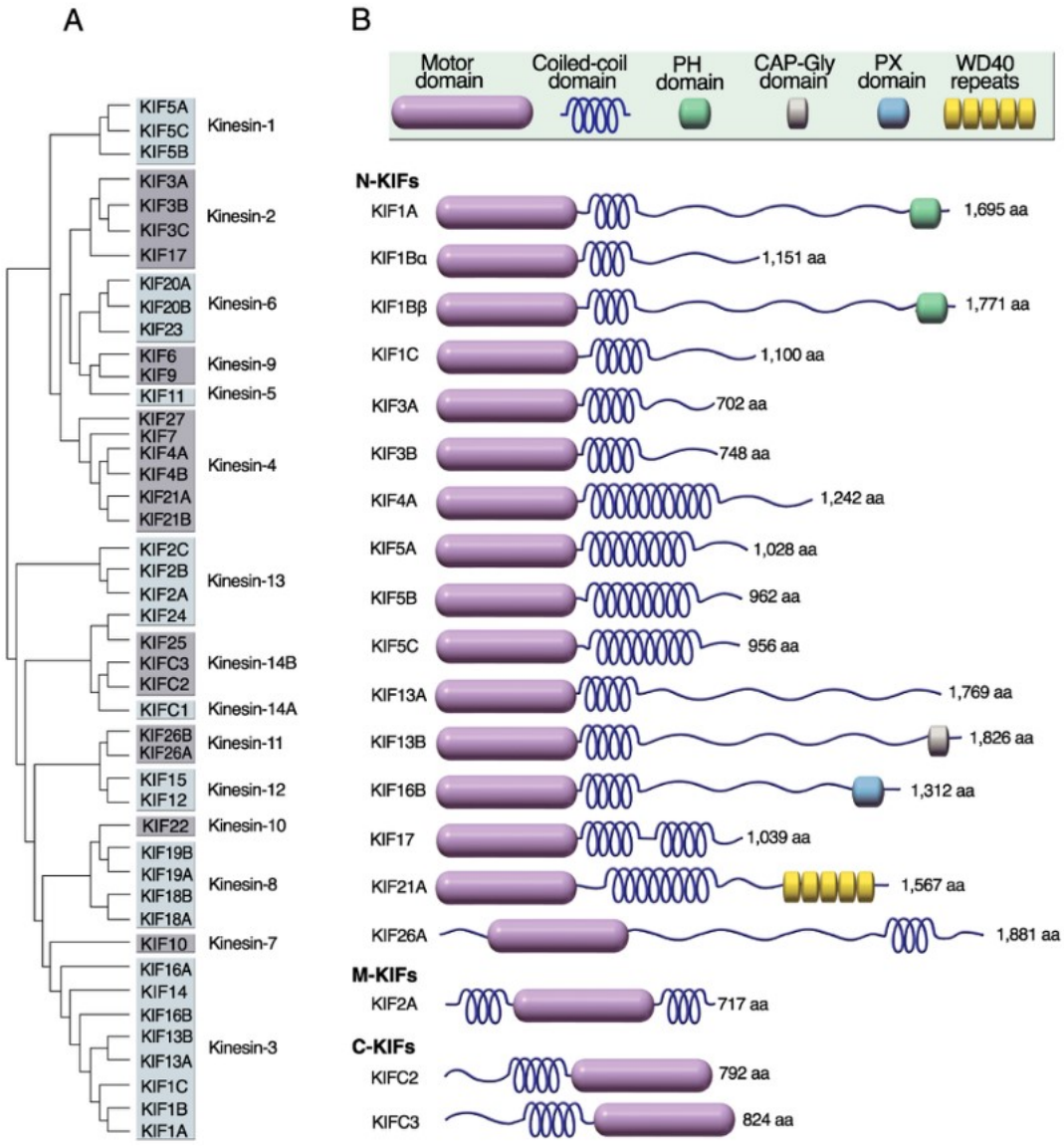

Figure 1.3 The kinesin superfamily
A. The phylogenetic tree of the Kinesin superfamily organized into families from kinesin-1 to kinesin-14B. B. The structural representation of kinesins within the superfamily and their domains. The kinesins are categorized as either N-, M-, or C-domains depending on the placement of their motor domain (N-KIFs, M-KIFs, and C-KIFs). Basic domains of KIFs include the motor domain, the coiled-coil domain, the pleckstrin homology (PH) domain, the cytoskeleton-associated protein glycine rich (CAP-Gly) domain, the phox homology (PX) domain, and the WD40 repeat domain. (Hirokawa et al., 2010)

Cytoplasmic dynein is responsible for retrograde axonal transport (Schnapp & Reese, 1989). Dynein, a microtubule-based transport protein, travels in the retrograde direction towards the cell body from the axon and towards the minus-end of microtubules. Although there are 45 distinct kinesins and 15 axonemal dyneins, only one gene exists for cytoplasmic dynein (Pfister et al., 2006; Hom et al., 2011). With only one dynein, its range of cargos is wide, including viruses, cytoskeletal elements, membrane-bound organelles, and lysosomes (Vallee et al., 2004). Dynein functions as a dimer, however, it has a much larger motor domain than kinesins, with multiple sites for ATP-binding (Kon et al., 2004). Despite being a major molecular motor, dynein cannot move itself toward the axon terminal due to the discrete microtubule orientation within axons. Therefore, approximately 80 percent of newly synthesized dynein shuttles down the axon via slow transport. The small fraction of fast-moving dynein in the anterograde direction attaches to organelles and undergoes transport by kinesins (Encalada et al., 2011; Hendricks et al., 2010). Even though only one dynein exists, cargo binding specificity is still possible through interaction with unique accessory chains in its tail as well as with adaptor proteins like dynactin (Allan 2011; Carter et al., 2016). Dynactin, a protein complex enriched in neurons, facilitates fast retrograde axonal transport and functions as a link between dynein and its organelles (Waterman-Storer et al., 1997). Although the presence of a single dynein suggests simplicity, intricacy exists in the regulation and structure of this motor protein.

1.3. Netrin-1

In the 19th century, Santiago Ramón y Cajal hypothesized that chemical guidance cues might guide axon pathfinding, based on observations of the directionality of spinal commissural axon growth towards the ventral midline of the embryonic spinal cord. One of the first proteins identified fitting this model is the secreted protein netrin-1. Netrin-1, encoded by the gene NTN1, plays a role in various cellular functions such as axon pathfinding, cell migration, and synaptogenesis (Boyer et al., 2018). Netrins, part of the laminin superfamily, are highly conserved secreted proteins. The first netrin, UNC-6, appeared in *C. elegans* (Ishii et al., 1992), and shortly after, two homologous proteins surfaced in embryonic chick brains, named netrins after the Sanskrit word “netr,”

meaning “to guide.” In the embryonic neural tube, floor plate cells secrete netrin-1 to guide axon outgrowth. *In vitro* studies confirmed netrin-1's role as a guidance cue, demonstrating its long-range chemotropic activity in axon guidance (Kennedy et al., 1994). Netrin-1 function also has short range signalling effects, with oligodendrocytes in the adult central nervous system requiring netrin-1 to regulate contacts with neighboring axons (Manitt et al., 2001). Researchers discovered three different secreted netrins (Netrins 1, 3, and 4) in mammals, along with two membrane-bound netrins (Netrins G1 and G2). All netrins have a mass of approximately 70 kDa and share two amino-terminal domains (V and VI), homologous to domains V and VI found in laminins (Figure 1.4). Although orthologues of netrin-2 only exist in chickens and zebrafish (Park et al., 2008), netrins 1, 3, 4, G1, and G2 are all present in mammals (Rajasekharan et al., 2009), with netrins 1-4 having similar amino acid sequences and chemoattractant functions (Serafini et al., 1994). Netrins G1 and G2, however, are tethered to the plasma membrane and have been implicated in synapse formation and function and play a role in nervous system development distinct from netrins 1-4 (Rajasekharan & Kennedy 2009; Nakashiba et al., 2000). The netrin family is diverse in form and function, and netrin-1 is necessary for the proper development and maintenance of the nervous system.

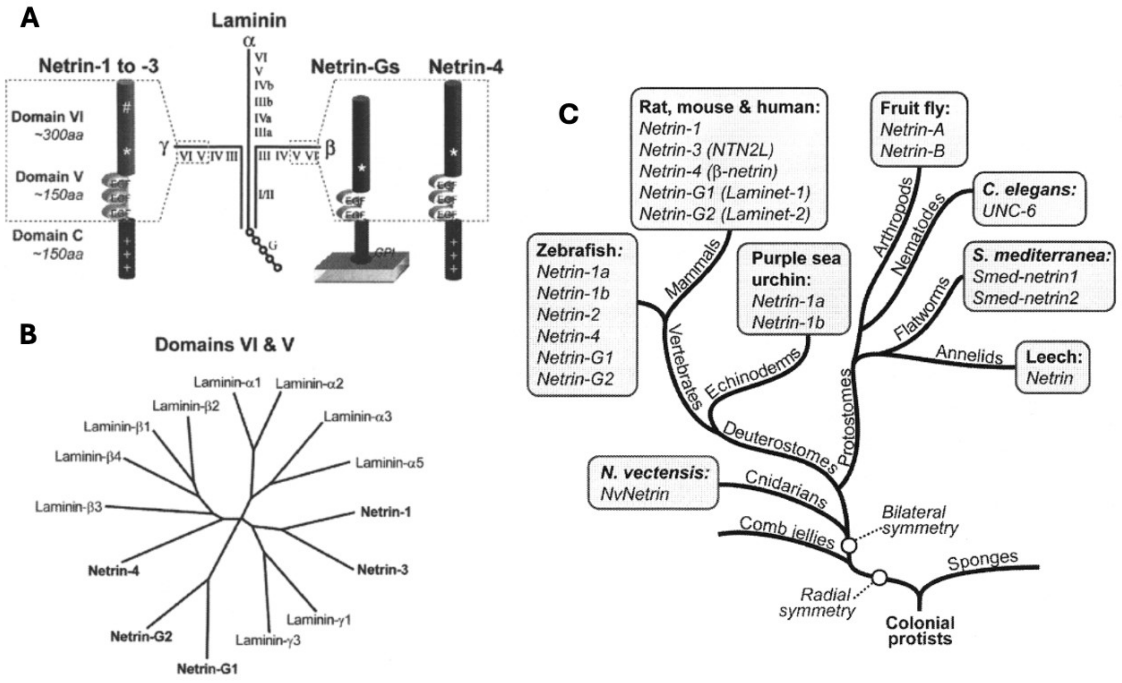

Figure 1.4 The netrin family.
A. Netrin structure and domains. All netrins contain V and VI domains which correspond to the amino terminal domains of laminins. B. Netrins and laminins phylogenetically mapped based on the sequencing of domains VI and V. Part of the laminin family, there are 5 unique netrins. Netrins -1, -3, and -4 are soluble while netrins G1 and G2 are membrane-bound. C. Evolutionary tree diagram of netrin homologs. Netrins are present in all animals with bilateral symmetry (Moore et al., 2007)

As a guidance molecule, netrin-1 has a dual role as both a chemoattractant and chemorepellent. Netrin-1 mediated chemoattraction is achieved through interaction with the receptor Deleted in Colorectal Cancer (DCC). In mice, a DCC gene knockout results in the loss of spinal ventral commissure, similarly to netrin-1 loss of function (Leggere et al., 2016). The neural growth cone lies at the end of an axon and drives axon outgrowth via chemotaxis. Through chemotaxis, growth cones detect and follow chemical gradients (Mortimer et al., 2008). Growth cones are highly motile both extending and retracting depending on extracellular and intracellular cues. DCC, localized to growth cones, enables the chemoattractant growth of axons towards netrin-1 (Torre et al., 1997). DCC is a single-pass transmembrane domain with a secondary role in apoptotic regulation (Arakawa 2004, Goldschnieder & Mehlen, 2010). In the absence of extracellular netrin-1, DCC-expressing neurons induce apoptosis through activating caspase-3. This behaviour

is thought to be tumour suppressive as DCC in mice triggers tumour apoptosis and because approximately 70 percent of colorectal cancers correspond to a DCC allelic deletion (Mehlen & Fearon 2004) Although the DCC/netrin-1 interaction was traditionally viewed as chemoattractant DCC has bifunctionality in guidance. In the presence of another receptor, UNC5, netrin-1 interacts with DCC as a repellant. (Finci et al., 2015). Experiments with cultured mouse spinal cord neurons show that UNC5 only exhibited repulsion when co-expressed with DCC (Rigato et al., 2011). Other receptors also interact with netrin-1, such as with α3β1 integrin to regulate interneuron migration through the cortical marginal zone during prenatal development (Stanco et al., 2009). Netrin-1 serves as a versatile guidance cue capable of engaging with a variety of receptors to execute diverse functions in the nervous system.

Netrin-1, although the most well described netrin, remains unexplored in terms of its localization and transport dynamics in vertebrate neurons. According to transcriptomics studies netrin-1 is expressed in human induced pluripotent stem cell (iPSC) derived neurons (Lindhout et al., 2020). Additionally, rodent studies have demonstrated netrin-1 releases synaptically and perisynaptically from the neuron upon high electrophysiological stimulation (Glasgow et al., 2018). In the central nervous system, netrin-1 is released by a variety of tissue types with diverse functionality in both long-range and short-range signalling. Synaptic release of netrin-1 by neurons regulates synaptic transmission and proves necessary for long-term potentiation (LTP) (Glasgow et al., 2021). The deletion of DCC also attenuates LTP and reduces dendritic spine volume (Horn et al., 2013). Although the release of netrin-1 from neurons has been described, the intracellular transport of netrin-1 to its site of release remains unknown. Due to the specialized functions of netrin-1 in establishing concentration gradients and regulating synaptic transmission, its proper localization is critical. Netrin-1 is a Golgi-derived protein synthesized in the cell body of the neuron that reaches its targeted sites of release via axonal transport. Preliminary studies have alluded to KIF1A as a potential kinesin motor protein involved in netrin-1 transport. In *C. elegans*, knockdown of the KIF1A homologue UNC-104 results in netrin-1 accumulation in the cell body, matching the pattern of other UNC-104 associated vesicles (Ogura et al., 2012). A connection between KIF1A and netrin-1 has been further established in rats following brain injury, where an

overexpression of KIF1A increased the concentration of secreted netrin-1 both *in vitro* and *in vivo* (Wang et al., 2018). These findings suggest that KIF1A is responsible for the transport of netrin-1 within neurons. Additionally, the dynamics of netrin-1 release in rodent models follow similar patterns to the release of dense core vesicles (DCV), a known KIF1A-associated vesicle (Glasgow et al., 2018; Boosport et al., 2012; Farina et al., 2015). Both DCV cargo and netrin-1 release require high frequency stimulation to achieve relatively low secretion. Although these findings suggest possible mechanisms behind netrin-1 transport in human neurons, further analysis of netrin-1 transport and localization is required.

1.4. KIF1A Structure and Function

KIF1A, a neuron-enriched motor protein belonging to the kinesin-3 family, contributes to the proper nervous system development and the survival of an organism. The kinesin-3 family is implicated in the long-distance cargo transport of organelles and proteins such as mitochondria, lysosomes, and synaptic proteins. When KIF1A is disrupted, we see a misallocation of essential KIF1A-dependent transport vesicles (Anazawa et al., 2022). KIF1A is known for its exceptional speed and travel distance and an impairment to its movement can be detrimental to an organism. KIF1A homozygous mutant mice typically die after birth (Yonekawa et al., 1998). In humans, mutations in KIF1A largely lead to KIF1A-Associated Neurological Disorder (KAND). KAND is a rare neurodegenerative disorder with a broad phenotypic spectrum including spastic paraplegia, intellectual disability, and seizures (Nair et al., 2023). Mutations contributing to KAND primarily occur in the motor domain, with symptom severity being linked to regions responsible for ATPase activity and MT binding (Boyle et al., 2021). Mutations associated with KAND disrupt the transport of KIF1A and its associated cargoes, and even slight changes in its processivity can have devastating neurodegenerative effects. The transport of proteins via molecular motors is a task that requires careful coordination. From sorting components based on neuronal polarity, to traversing the lengths of axons, there are many steps where even a small change in motor dynamics can have detrimental broad scale effects. KIF1A-dependent cargoes are involved in numerous biological processes and their correct transport is necessary for proper organismal development.

KIF1A is considered a highly processive molecular motor. This processivity results from unique characteristics within its N-terminal motor domain (Westerholmer-Parvinien et al., 2000). The motor domain contains an ATPase catalytic core as well as microtubule binding sites. High-resolution cryo-electron microscopy reveals that kinesin-3 motor domains have a higher microtubule binding affinity than other kinesins due to multiple amino acid differences over the binding interface (Atherton et al., 2014). Mutagenesis and single-molecule motility assays further confirm the effect of specific residues in the motor domain on microtubule binding affinity (Scarabelli et al., 2015). Kinesin-3 functions as a dimer, formed upon release of autoinhibition. Interactions of the motor and the cargo largely regulate the monomer-to-dimer switch. Upon cargo binding, intramolecular interactions between the neck and tail regions are disrupted, allowing dimerization (Tomishige et al., 2002). Dimerization is essential for ATP-dependent processive motility and super processivity (Hammond et al., 2009; Soppina et al., 2014). The ATPase catalytic core found within the motor domain of KIF1A powers movement. In the dimeric state, the two halves undergo ATP hydrolysis sequentially to take successive steps in a "hand-over-hand" model along microtubules (Figure 1.5; Yildiz et al., 2004;). During movement, the front head is tightly bound to the microtubule, while the back head swings forward to move the motor. The foot of the kinesin swings forward and binds to the microtubule upon release of ADP and the binding of ATP. This creates a conformational change which generates a power stroke to move the back leg forward following ATP hydrolysis. Throughout this process, the mechanics of the ATPase cycle are crucial for processivity and considered rate-limiting (Gilbert et al., 1995). Members of the kinesin-3 family are considered highly processive partly because they exhibit high ATP turnover rates (Soppina et al., 2022). The microtubule binding and motor characteristics of the kinesin-3 family give the proteins an affinity for long and fast travel, allowing them to efficiently transport cargo to distal ends of the cell.

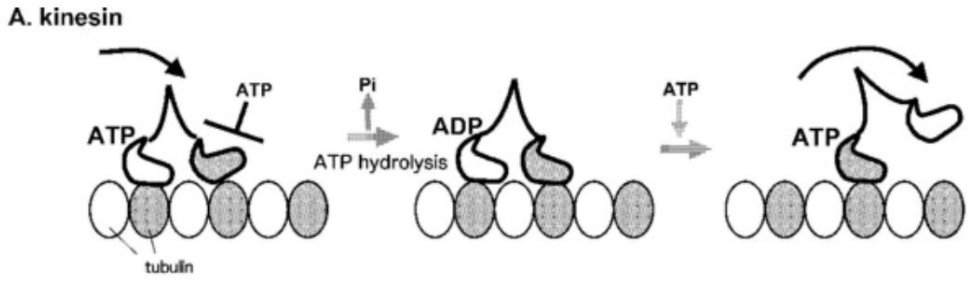

Figure 1.5 Hand-over-hand model of kinesin movement.
The front foot (grey) is first immobilized to the microtubule upon the binding of ATP. This triggers a conformational change to swing the back foot (white) forward. To achieve the movement forward, it first undergoes ATP hydrolysis. The back foot can now move forward to be immobilized to the microtubule upon binding ATP, repeating the cycle. (Taguchi 2005).

Each motor protein within the kinesin-3 family demonstrates specificity in its cargoes and resulting functional responsibilities. KIF1A is responsible for a range of vesicles including dense core vesicles (DCVs) and synaptic vesicle precursors (SVPs) (Figure 1.6; Lo et al., 2011; Hall & Hedgecock, 1991). These vesicles are necessary for synaptogenesis, neuronal function, and cellular homeostasis. DCVs are typically identified by the presence of granin family members and are necessary for proper neuronal development and function. They carry a variety of cargoes such as brain-derived neurotrophic factor (BDNF) and chromogranin (CHG) (Dieni et al., 2012). SVPs are a separate class of transport vesicles and were the first cargoes identified for KIF1A. They are involved in building and regulating synapses and contain proteins such as synaptophysin, VAMP2, and synaptic vesicle protein 2. Cargo binding to the motor is complex and the mechanism is not well characterized, however, certain domains and factors are known to contribute to this process (Figure 1.6). The pleckstrin homology (PH) domain is a lipid-binding domain shown to interact with specific residues on the cargo vesicular surface (Klopfenstein and Vale, 2004). Often, specificity is also achieved through adaptor proteins which can be necessary for cargo-motor interactions (Hirokawa et al., 2010). KIF1A binding to SVPs is regulated by the adaptor protein Rab3, which is a GTPase that regulates binding in a DENN/MADD dependent mechanism (Niwa et al., 2008). There are several theories regarding KIF1A-DCV binding, including facilitation by the transmembrane adaptor protein carboxypeptidase E (Park et al., 2008) or

regulation by calcium acting via calmodulin (Stucchi et al., 2018). Another layer of regulation is achieved by the vesicle capture mechanisms upon cargo delivery. Once DCVs and SVPs are in transit, proper delivery to synaptic sites is mediated by interactions with scaffolding and adaptor proteins such as Liprin-α and JNK (Stucchi et al., 2018; Bharat et al., 2017). Altogether, many mechanisms play a hand in the specificity of KIF1A cargo binding and transport.

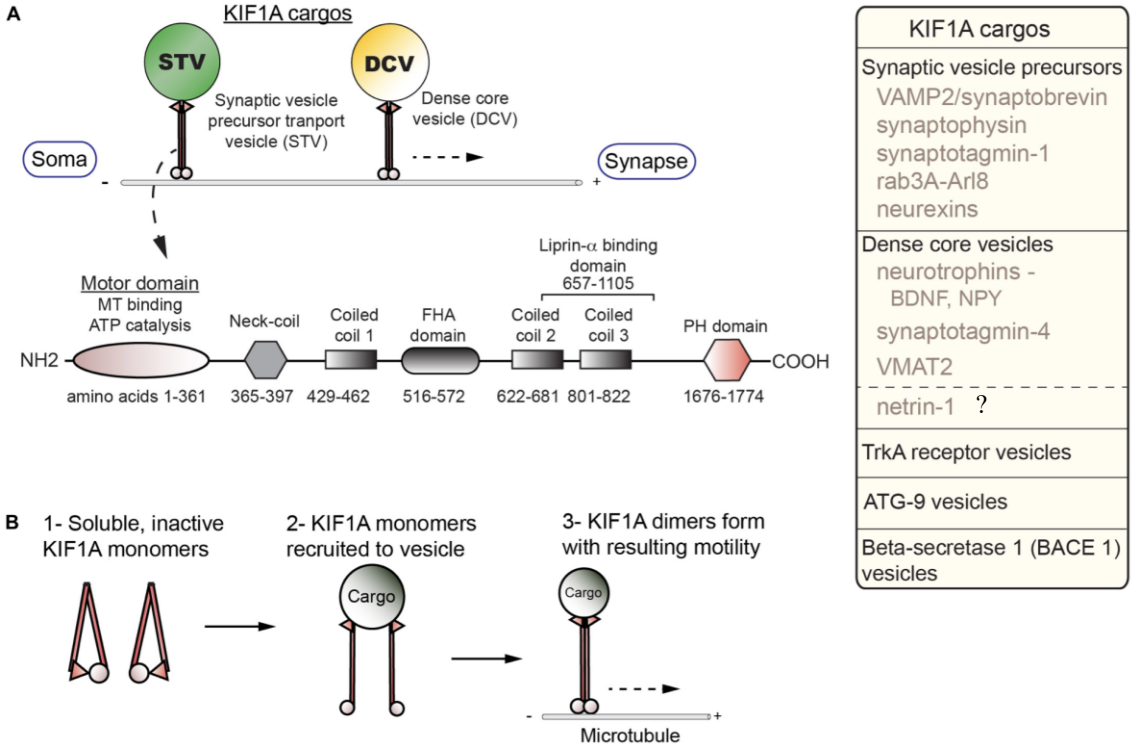

Figure 1.6 Structure, cargoes, and dimerization of KIF1A.
A. Diagram of the KIF1A mediated movement of synaptic vesicle precursors/transport vesicles (SVP/STV) and dense core vesicles (DCV) along microtubules. The domain structure of KIF1A reveals an N-terminal motor domain equipped with a microtubule (MT) binding domain and an ATP catalytic core, a neck linker domain, coiled-coil domains, a forkhead-associated (FHA) domain, and a pleckstrin homology (PH) domain at the C-terminal. KIF1A carries a variety of vesicle types, each with a unique set of cargoes. B. KIF1A exists as inactive monomers which are recruited to transport vesicles to form active dimers. (Gabrych et al., 2019)

Dense core vesicles (DCV) are neuronal organelles that transport a variety of neuropeptides and factors required for neuronal development, synaptic function, and learning and memory. Under an electron microscope, DCVs appear as vesicles filled with a dark center made of soluble proteins (Trueta et al., 2012). DCVs are known to carry a

variety of cargoes including proBDNF, BDNF, chromogranin (CHG), Neuropeptide Y (NPY), and synaptotagmin-4 (Figure 1.6; Dieni et al., 2012). DCVs are found in both neuronal and endocrine cells (Topalidou et al., 2019), and DCV cargo such as BDNF has been found in most areas of the brain such as the cortex, hippocampus, mesencephalon, and spinal cord (Bathina & Das 2015). DCVs follow a similar path of biogenesis and transport as per other secretory vesicles. They are filled with neuropeptides in the cell body and then travel to synaptic sites where their contents are released upon action-potential triggered calcium influx (Hartmann et al., 2001; Persoon et al., 2018). Like other proteins packaged into transport vesicles, DCV cargoes undergo post-translation modifications and are packaged into vesicles through the endomembrane system. During the formation of DCVs, proteins are delegated into vesicles via sorting signals such as specific amino acid sequences, phosphorylation sites, or attached carbohydrate groups (Ford et al., 2021; Dikeakos & Reudelhuber 2007). The exact mechanism behind DCV biogenesis is unknown, but they are thought to bud from the trans-Golgi network like other secretory vesicles (Schekman & Orci 1996). Evidence suggests that DCV budding requires the presence of granins such as CHG, which acts as an "on/off" switch for DCV formation (Kim et al., 2001). Following DCV biogenesis, the vesicle will interact and bind to KIF1A and cytosolic dynein to begin trafficking (Lo et al., 2011). Once the DCV has reached its destination it will undergo exocytosis, fusing with the plasma membrane to release its contents extracellularly. The intricacies of DCV fusion remain elusive, but they are known to largely use the same pathways as secretory vesicles (SV), such as with, SNAP-25, synaptobrevin-2/VAMP2, SNARE, and Munc13 and RIM (Shimojo et al., 2015; Persoon et al., 2019). Upon calcium-dependent excitation, synatobrevin-2/VAMP2, SNAP-25, and syntaxin-3 will coil together to form a SNARE complex which leads to membrane fusion (Figure 1.7). After fusion, the contents of the vesicle are exocytosed and the vesicular lipid membrane is merged to the plasma membrane. This mechanism is what facilitates neuropeptide release from DCVs and is the final stage in the journey of secretory vesicle formation and transport. Previous evidence as well as my own findings suggest that netrin-1 is transported within dense core vesicles (DCV). Since DCVs are known to transport within both axons and dendrites (Persoon et al., 2018), I expect netrin-1 to also be transported throughout the cell.

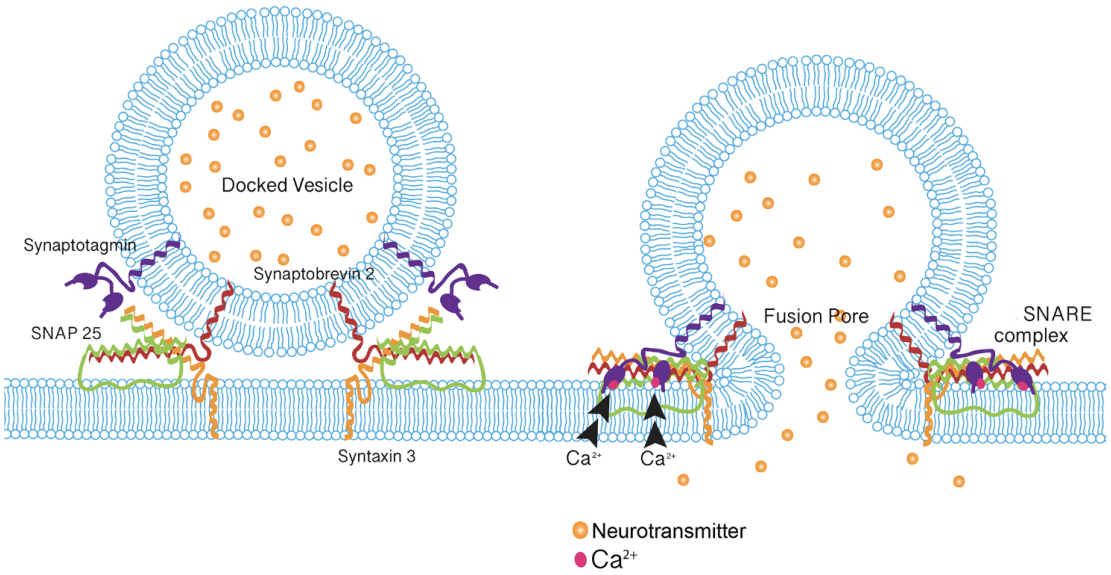

Figure 1.7 Mechanism of secretory vesicle fusion.
Small nuclear RNA-activating protein (SNAP-25), the SNARE protein syntaxin-3, and synaptobrevin-2/Vesicle associated membrane protein-2 (VAMP2) come together to form a SNARE complex to drive vesicle fusion. Upon interaction of these proteins, the docked vesicle fuses with the plasma membrane, and the contents of the secretory vesicle are exocytosed. (Thoreson & Hays 2020)

1.5. iPSC-Derived Neurons as a Model System

Induced pluripotent stem cells (iPSCs) are generated from somatic cells through treatment with specific reprogramming factors. The four factors: octamer-binding transcription factor 4 (Oct4), sex-determining region Y-box 2 (Sox2), Kruppel-like factor 4 (Klf4), and cellular Myc (c-Myc), can be introduced to induce pluripotency in a variety of somatic tissues (Takahashi & Yamanaka, 2006). The transcription factors Oct4 and Sox2 are essential for iPSC generation while Klf4 and c-Myc aid in the maintenance of pluripotency. iPSCs are typically generated through viral and DNA vectors or the direct delivery of reprogramming factors (Kim et al., 2009). After induction with reprogramming factors, the cells quickly form colonies similar to embryonic stem (ES) cells. After generating iPSCs, the cells can then be differentiated into any cell type in the body, including cardiomyocytes, hepatocytes, and neurons. There are multiple techniques for generating forebrain type neurons including via viral transduction and small molecule differentiation (Figure 1.8). Viral transduction involves overexpressing the transcription factor neurogenin-2 (NGN2), which produces a neuronal phenotype within 7 days (Zhang

et al., 2013). NGN2 rapidly converts both ES and iPSCs, to form excitatory synaptic neuronal networks. An alternative approach to producing neurons is via monolayer small molecule differentiation. This method involves more intermediate steps and requires the iPSCs to first undergo neural induction to produce neural progenitor cells (NPC) (Bell et al., 2019). NPCs are produced through the inhibition of TGF-β/BMP-dependent SMAD signalling (Figure 1.8). NPCs can then be further differentiated into neurons with the addition of factors supporting neuronal development such as laminin, BDNF, B-27 supplement, and N2 supplement (Bell et al., 2019). Within 5 days of differentiation from NPCs, the neurons become electrophysiologically active. Lindhout et al. 2020 describe iPSC-derived neurons going through typical initial neurodevelopmental stages, as previously described in rat hippocampal neurons (Dotti et al., 1998). The cells took on a neuronal morphology by day 7 (stage 2), with a decrease in proliferation and NPC markers and an increase in the neuron specific markers β3- Tubulin and MAP2. At days ≥7 (stage 3), the cells were morphologically characterized by the appearance of long emerging axons at least twice the length of the other neurites. At 14 days the cells were still developing, with extending and thinning axons and assembling axon initial segment (AIS) components. There are a variety of different methods for generating iPSC-derived neurons, and researchers continue to optimize and develop new protocols.

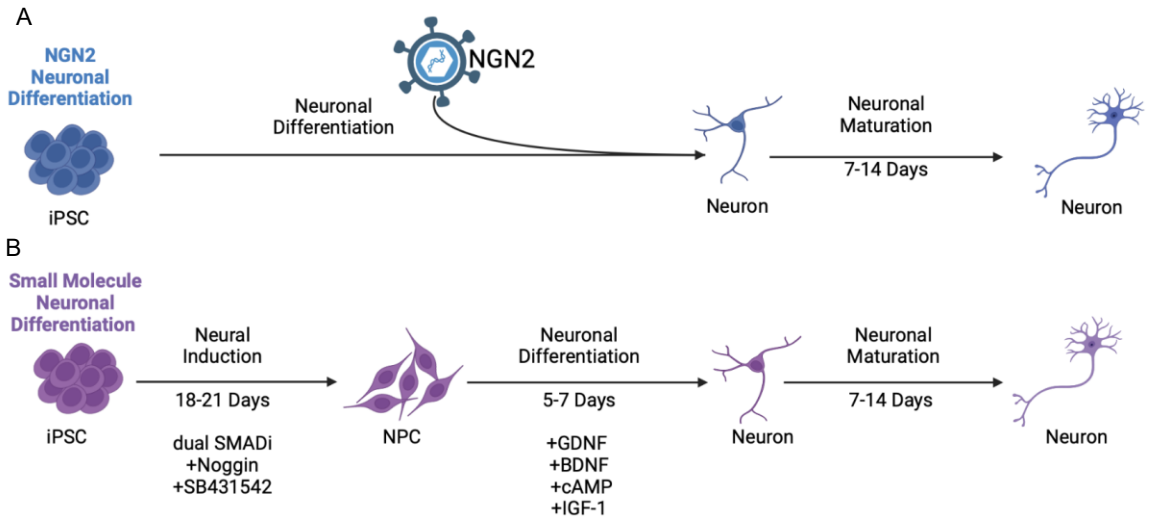

Figure 1.8 Approaches in generating iPSC-derived neurons.
There are multiple approaches to generating induced pluripotent stem cell (iPSC)-derived neurons, including via the transcription factor neurogenin-2 (NGN2) and small molecule differentiation. A. Viral transduction of NGN2 will trigger the immediate development of a neuronal morphology in iPSCs. The neurons mature after transduction over the course of 7-14 days. B. Small molecule differentiation involves the iPSCs undergoing neural induction to become NPCs via dual SMADi with the treatment of Noggin and SB431542. iPSCs are cultured with these small molecules for 18-21 days with repeated passages. NPCs will then undergo further neuronal differentiation to develop into neurons. Common small molecules used to generate a forebrain cortical neuronal phenotype include glia cell line neurotrophic factor (GDNF), brain derived neurotrophic factor (BDNF), cyclic adenosine monophosphate (cAMP), and insulin growth factor 1 (IGF-1). After 5-7 days of neuronal differentiation, the cells have differentiated into forebrain neurons and are further matured for 7-14 days. (Made in BioRender)

iPSC-derived neurons offer a bridge in modeling human systems and fill previously inaccessible niches in biological research. Human samples have long been difficult to obtain, this is especially true for brain tissue. iPSC-derived neurons being created from more easily accessible somatic cell samples removes a large hurdle in conducting neurobiological research. Although alternative species models are often employed, underlying biochemical and cellular differences may impact findings. Characterizations of iPSC-derived sensory neurons show typical protein expression and response to drug treatments compared to tissue samples (Hiranuma et al., 2024). Additionally, in developing iPSC-derived neurons, microtubule organization was consistent with those found in non-human models (Lindhout et al., 2020; Yau et al., 2016). iPSC-derived neurons are also representative of disease model systems.

Electrophysiological studies of schizophrenia patient iPSC-derived neurons show an association of electrical activity with the patient's personal schizophrenia clinical status (Cerceo Page et al., 2022). Because neurons and other cell types can be generated from patient somatic cells, this offers a unique opportunity to create cell lines that also capture the patient's unique genetic background. iPSC-derived neurons are a relatively new system with many advantages, and current studies suggest that they are reliable in representing many biological processes.

Although iPSC-derived neurons offer an efficient and promising new tool, challenges persist regarding culture consistency and quality. There is considerable variation in protocols, which significantly affects cell morphology. The first issue arises in the production of iPSCs. Heterogeneity in iPSC production can be attributed to technical artifacts, as well as subtle variations in the multi-step process (Popp et al., 2018). At this point, small variances can lead to drastic differences in the outcome of iPSC-derived neurons. Throughout the process of generating iPSC-derived neurons, conditions such as culture media composition, matrix, passage number, and cell confluency can influence developmental outcomes (Volpato & Webber 2020). Currently, there is no standard protocol in the field, and given possible variations in cell lines, it appears that culturing protocols must be somewhat self-tailored. The first decision to make is in the differentiation technique, such as by overexpressing the transcription factor NGN2 or by exposing cells to small molecule differentiation factors. The matrix used can also have broad-scale developmental effects. Within the nervous system, the extracellular matrix shapes neural development, and this holds true for cultured iPSC-derived neurons (Jain et al., 2020). Two common matrices are Matrigel (Bell et al., 2019) and a combination of poly-L-ornithine (PLO) and laminin (Zhang et al., 2013). Matrigel is produced from the Engelbreth-Holm-Swarm (EHS) mouse sarcoma and resembles the basement membranes present in many tissues, while PLO and laminin are routinely employed in primary rat hippocampal neuron cultures. Such drastic differences in the composition of the matrices can have significant impacts given their possible effects on intracellular signaling (Hastings et al., 2019). Therefore, while iPSC-derived neurons open doors in experimentation, establishing a reliable protocol is a necessary first step.

1.6. Project Overview

The primary goal of my thesis was to characterize netrin-1 trafficking in developing iPSC-derived neurons. iPSC-derived neurons are a promising system that allows us to study biological processes in a human model. One of the many biological processes that have yet to be observed in human neurons is the intracellular trafficking of netrin-1. Netrin-1 is implicated in the development and maintenance of the central nervous system and is expressed in a variety of tissue types, including neurons. In rat neurons, netrin-1 has been observed to be released synaptically, and in *C. elegans*, netrin-1 has co-localized with UNC-104/KIF1A cargoes. What has yet to be characterized is how netrin-1 is localized and transported to its potential sites of release in human neurons. Therefore, I assessed the transport dynamics of netrin-1 in iPSC-derived neurons. Additionally, I characterized our iPSC-derived neurons and described the effects of varying culture conditions.

My two primary aims are:

1. Characterizing and developing the iPSC-derived neuron culturing

   Given the variability in iPSC-derived neuron culturing protocols and the possible developmental effects, different conditions need to be tested and characterized. Therefore, I will be comparing the effects of NGN2-based differentiation with small molecule differentiation. I will also compare the effect of the substrates Matrigel and PLO/Laminin on neuronal development to ascertain which produces the most consistent cultures. After settling on methods in differentiation, I will evaluate the culture's neuronal identity via immunocytochemistry.

2. Assess the localization and trafficking of netrin-1 in human iPSC-derived neurons

   Netrin-1, an essential protein in nervous system function and development, is expressed in human neurons and released in rat neurons in a similar pattern to DCVs. However, the intracellular trafficking of netrin-1 in neurons has never been observed. Given the previous association between netrin-1 and KIF1A, I will be using live-cell imaging to assess their co-transport. Additionally, I will assess netrin-1 transport dynamics such as velocity and run length, as well as its association with known KIF1A cargo to then determine its resident transport vesicle.

Chapter 2. Materials and Methods

2.1. iPSC and NPC culturing

iPSCs used for neurogenin-2 (NGN2) differentiation came from a commercial line obtained from Coriell (#GM27938) generated through the expression of the transcription factor OCT4. This line is a wildtype clone isolated from a female patient with mosaicism with a KIF1A mutation (R203S). iPSCs were cultured on Matrigel (Corning) coated 6-well tissue culture dishes in mTeSR plus medium (STEMCELL Technologies). Matrigel coating involved diluting Matrigel on ice to a 1:100 in a solution of Dulbecco's Modified Eagle Medium (DMEM) and Ham's F12 medium (1:1) with added Hepes (15 mM). Each well received 1 ml of Matrigel, and then was incubated at 37°C for one hour and then at room temperature for another hour. Excess Matrigel was removed before the addition of iPSCs. iPSCs were passaged 1-2 times a week before the colonies became too confluent. To passage the iPSC cultures, ReLeSR (STEMCELL Technologies) was added to the culture dish and immediately aspirated. ReLeSR, an enzyme-free reagent, dislodges cells as aggregates to maintain their colonial organization. After incubating at 37°C and 5% CO_2 for 3-5 minutes with the remaining ReLeSR, 1 ml of mTeSR Plus culture medium was added to each well. The cells were dislodged by tapping the sides of the dish for 30-60 seconds. Cells were then harvested using a serological pipette, and 3-5 drops of harvested cell culture media were added to each well of a new tissue culture dish. Before the addition of the harvested cells, culture dishes were pre-coated with Matrigel and 2mls of mTeSR plus medium was added to each well. iPSCs were passaged a maximum of 10 times before being discarded, and medium exchanges (2 ml/well) occurred every 1-2 days. All cell cultures were incubated at 37°C and 5% CO_2.

The NPCs used for the small molecule differentiation approach were a separate line from the iPSCs (Coriell; #GM27938) used for NGN2 differentiation. Dr. Y Zhu (Simon Fraser University) prepared these NPCs from iPSCs reprogrammed from peripheral blood mononuclear cells of a healthy male donor using the Erythroid Progenitor Reprogramming Kit (STEMCELL Technologies). NPCs were generated via

dual SMADi. NPCs were cultured in Matrigel-coated 6-well tissue culture dishes with Neural Progenitor Medium (STEMCELL Technologies) and passaged every 1-2 weeks before reaching full confluency. To passage NPCs, cells were incubated with ACCUTASE (STEMCELL Technologies) at 37°C for 5 minutes. After incubation, cells were gently pipetted up and down with a P1000 to dislodge them and ensure a single-cell suspension. Culture medium composed of DMEM/F12 (1:1) and Hepes (15mM) was added, and cells were harvested into a conical tube and centrifuged at 300g for 5 minutes. After removing the supernatant containing ACCUTASE and culture medium, cells were resuspended in Neural Progenitor Medium. Cells were then diluted 4-6 times from their harvest density and plated onto new Matrigel-coated dishes. Complete media exchanges with Neural Progenitor Medium occurred every 1-2 days (2ml/well).

2.2. Neuronal differentiation and maturation

Neurons were differentiated using two different approaches, the first being small molecule differentiation, and the second using the transcription factor NGN2. At a certain point in both protocols, the cells are plated onto pre-treated glass coverslips. Two different substrates were tested to coat these coverslips. The first being Matrigel and the second being a combination poly-l-ornithine (PLO) and laminin. In this subsection, I will describe each of these protocols.

2.2.1. Small molecule differentiation

Neurons produced via small molecule differentiation generated from NPCs using the Forebrain Neuron Differentiation Kit (STEMCELL Technologies). NPCs were passaged with ACCUTASE plated onto Matrigel-coated 6-well plates at 80,000-125,000 cells/cm^2 in Forebrain Differentiation Medium, and complete medium exchanges occurred daily. Cells proliferated in the differentiation media for 5-7 days until reaching 90% confluency. Cells were then harvested using ACCUTASE and plated onto glass coverslips in neuronal medium at 100,000-125,000 cells/ml. At this point of plating the cells onto glass coverslips, they were considered 0 DIV. Neuronal medium was made with Forebrain Neuron Maturation Medium (STEMCELL Technologies), and added

mouse laminin (1 µg/ml; Thermo Scientific), BDNF (10 ng/ml; STEMCELL Technologies), NT3 (10 ng/ml; STEMCELL Technologies), and B-27/SM1 (STEMCELL Technologies). Half-medium changes occurred every 2-3 days.

2.2.2. Neurogenin-2 differentiation

To begin NGN2 differentiation, iPSCs cultured were passaged with ACCUTASE and plated onto glass coverslips at 100,000-125,000 cells/ml in mTeSR Plus medium (Figure 2.1). The cells were plated as a single cell culture, The following day, iPSCs were treated for 4 hours with lentivirus for the constitutive expression of the tetracycline transactivator fusion protein (rtTA) and the tetracycline-inducible expression of NGN2 and puromycin resistance. After 4 hours, the lentivirus was removed and replaced with neuronal medium containing doxycycline (1 µg/ml; Thermo Scientific) to induce NGN2 and puromycin resistance expression. The cells were now considered 0 DIV. 24 hours after the lentiviral treatment, the cells were treated with puromycin (1 µg/ml; Gibco) in neuronal medium overnight, to select against cells that were not transduced. The following day, the puromycin treatment medium was replaced with neuronal medium. Half-medium changes occurred every 2-3 days.

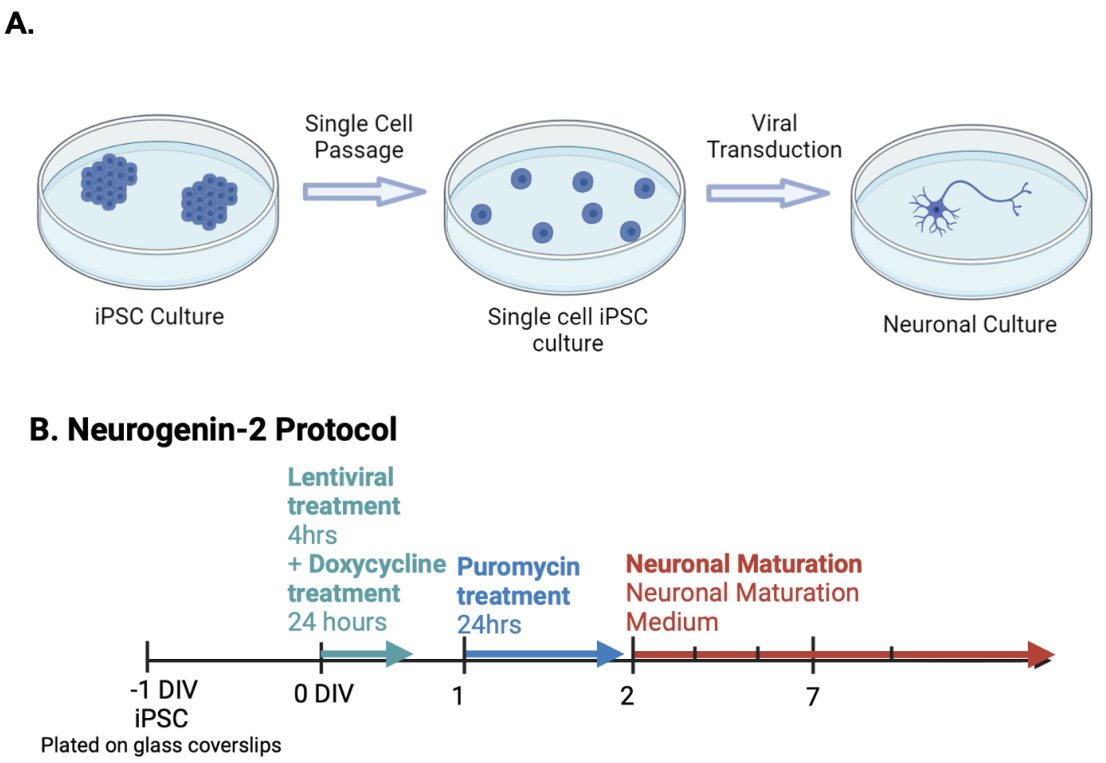

Figure 2.1 Timeline of the NGN2 treatment.
A. To prepare for NGN2- based neuronal differentiation, the iPSCs underwent single-cell passaging onto glass coverslips (-1 DIV). B. At 0 DIV, the iPSCs were treated with lentivirus and doxycycline to induce the expression of NGN2. At 1 DIV, the cells were treated with puromycin to select for transduced cells. At 2 DIV and onwards, the cells were cultured and matured in neuronal medium. (Made in BioRender)

The expression of NGN2 and puromycin resistance is driven by the TetO promoter, which requires two elements: the tetracycline transactivator fusion protein (rtTA) and tetracycline/doxycycline (Baron & Bujard 2000). Therefore, along with the expression of NGN2 for neuronal differentiation, the expression of rtTA is necessary. In the presence of tetracycline/doxycycline, the rtTA protein binds to the TetO promoter, inducing transcription of NGN2 and puromycin resistance (Figure 2.2; Zhang et al., 2013). At 0 DIV, iPSCs are treated with doxycycline and transduced with two transgenes; one encoding rtTA and the other encoding NGN2 and puromycin resistance. After transduction, the expression of rtTA will commence immediately, and the combination of rtTA and doxycycline will drive NGN2 and puromycin resistance expression. Expression will continue for 24 hours until the doxycycline treatment medium is changed for neuronal medium.

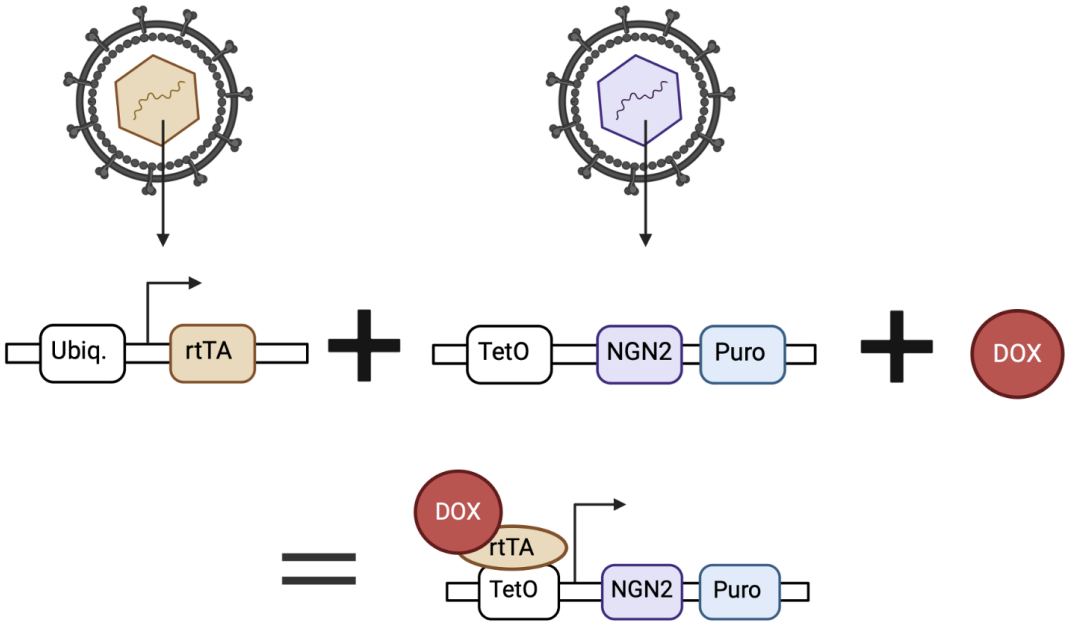

Figure 2.2 Tetracycline inducible NGN2 expression system.
The TetO system requires three parts: ubiquitously expressed tetracycline transactivator fusion protein (rtTA), the Tet-responsive transgene, and tetracycline/doxycycline (DOX). In this case, the Tet-responsive transgene expresses both neurogenin-2 (NGN2) and puromycin resistance (Puro). (Made in BioRender)

Lentiviruses were generated in HEK293T cells using the Lenti-X Packaging Single Shot Kit (Takara Bio) with separate transfections of two plasmids (pLV-hNGN2-Puro and FudeltaGW-rtTA) (Figure 2.3). After transfection, lentiviruses were harvested twice from the cell culture at 48 hours and 72 hours and then pooled together. The lentiviruses are then centrifuged and concentrated using the Lenti-X Concentrator (Takara Bio). The concentrated lentiviruses are centrifuged again, resuspended in neuronal medium, and stored at -80°C. When used for transduction, the lentivirus was diluted five to 10 times in mTeSR Plus medium. The optimal concentration of lentivirus was determined through experimentation to minimize toxicity to the cells.

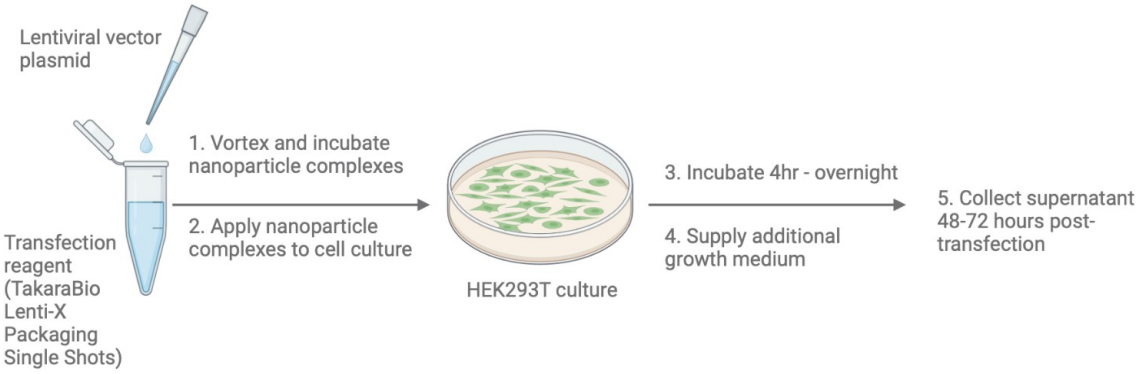

Figure 2.3 Lenti-X packaging single-shot protocol.
Workflow for the lentivirus packaging kit from Takara bio. First the viral packaging vector is added to the nanoparticles and then used to transfect HEK293T cells. After 48-72 hours, the HEK293T cells will express the vector and produce lentiviruses which will be released into the supernatant. (Made in BioRender)

2.2.3. Matrigel coating of glass coverslips

Glass coverslips were initially prepared with an overnight nitric acid wash. The following day, the coverslips were repeatedly rinsed with 18MΩ water and sterilized at 200°C for 4 hours. The coverslips were then placed into sterile 12-well tissue culture dishes for Matrigel coating and cell plating. Matrigel was thawed on ice and diluted 1:100 into DMEM/F12 (1:1) with added Hepes (15mM). Matrigel was added to each well containing glass coverslips and incubated at 37°C for 1 hour, then at room temperature for 1 hour. The excess Matrigel was removed, and cells were plated directly onto the coverslips without washing.

2.2.4. Poly-l-ornithine and laminin coating of glass coverslips

Before PLO and laminin plating, coverslips were prepared via acid washing as described above. PLO was diluted to 50 µg/ml in borate buffer (0.1M; pH 8.5), plated onto the coverslips, and incubated at 4°C overnight. After removing the PLO through repeated washing with phosphate-buffered saline (PBS), laminin was diluted to 5 µg/ml in PBS and plated onto the coverslips. The laminin was incubated for 2 hours at 37°C. Before cell plating, the laminin was removed, and the coverslips were repeatedly washed with PBS.

2.3. Plasmid generation

E. coli expressing pEF1α-Netrin-1-mRuby3 (VectorBuilder; Appendix; Figure A.7), KIF1A-NeonGreen (Appendix; Figure A.8), CHG-GFP (Gifted by Dr. Laurent Taupenot), pLV-TetO-hNGN2-Puro (Addgene; Appendix; Figure A.9), and FudeltaGW-rtTA (Addgene; Appendix; Figure A.10). were initially grown overnight on agar and Luria broth (LB) plates supplemented with appropriate antibiotics. Individual colonies were then selected and transferred to separate sterile round-bottom tubes containing 2 ml of liquid LB with antibiotics. The tubes were incubated for 2 hours in a 37°C shaker, after which the contents were transferred to sterile Erlenmeyer flasks containing 55 ml of liquid LB with antibiotics. The bacteria were then shaken and further incubated at 37°C for 12-16 hours. Plasmids were subsequently extracted using the QIAprep Plasmid MidiPrep Kit (Qiagen), and their concentrations were determined using a Nanodrop spectrophotometer. Plasmid identity was confirmed through restriction enzyme digestion using HindIII, NotI, EcoRI, and BamH1 (New England Biolabs), followed by agarose gel electrophoresis.

2.4. Transfections

Transfections were performed using the EndoFectinMAX Transfection Kit (GeneCopoeia). 1 µg of plasmid DNA was diluted in 50 µl of serum-free Optimem (ThermoFisher). For double transfections, 0.5 µg of each plasmid was diluted in Optimem. Separately, EndoFectinMAX reagent was diluted in Optimem; 2 µl of transfection reagent was added to 50 µl of Optimem. The samples were vortexed and incubated for 5 minutes at room temperature. After 5 minutes, the 50 µl of diluted DNA was added to the diluted transfection reagent. The mixture was vortexed and incubated at room temperature for 15-20 minutes. Before adding the transfection reagent and DNA to the cell cultures, neuronal medium was removed from the cells, transferred to a sterile 50 ml tube, and replaced with 0.9 ml of serum-free Optimem. After the incubation period, the transfection reagent and DNA mixture was added dropwise to the cell cultures. The tissue culture plate containing the cells was gently rocked back and forth to distribute the reagent, and the cells were incubated in a 5% CO2 and 37°C incubator for 2 hours.

Following the incubation, the Optimem containing the transfection reagent and DNA was removed from the cells and replaced with the previously collected neuronal medium. The cells were then imaged 24-48 hours post-transfection to assess transgene expression.

2.5. Immunocytochemistry

Cells were prepared for immunocytochemistry (ICC) with fixation. They were fixed in a 4% PFA solution and incubated at 37°C for 15-20 minutes. After fixation, cells were washed twice with PBS and once with tri-buffered saline (TBS) to quench. Subsequently, they were treated with 0.2% Triton in PBS for 3 minutes at room temperature. The cells were then washed three times with PBS and blocked for 45 minutes with a 5% BSA/0.5% fish skin gelatin blocking medium. Primary antibodies were diluted in the blocking medium as follows: Chicken anti-netrin-1 (1:200; Novus), Rabbit anti-KIF1A (1:500; Abcam), Guinea pig anti-β3-Tubulin (1:500; Synaptic Systems), Rabbit anti-Chromogranin A (1:500; Sigma). Cells were incubated with the primary antibodies overnight at 4°C in a humidity chamber. The next day, cells were washed three times with PBS and incubated with diluted secondary antibodies for 2 hours at room temperature: anti-chicken 488 (1:1000; Sigma), anti-rabbit 555 (1:1000; Sigma), and anti-guinea pig cy5 (1:500; Synaptic Systems). After incubation, cells were washed three times with PBS and once with 18MΩ water. Finally, cells were mounted onto microscope slides using ProLong Diamond Antifade Mountant (ThermoFisher), and the slides were placed in the dark to cure for 24 hours. Edges were sealed with nail polish, and samples were imaged using fluorescent microscopy.

2.6. Live cell imaging and Fluorescent microscopy

Live-cell imaging was conducted in a heated chamber using wide-field fluorescent microscopy (DMI 6000B, Leica) equipped with a Hamamatsu Orca-ER-1394 CCD camera. Neurons were mounted on glass coverslips in BrainPhys Imaging Optimized Media (STEMCELL Technologies) pre-warmed to 37°C. The chamber was maintained at 37°C, with additional warming around the lens. Imaging was performed using a 63X/1.4 NA objective with immersion oil, Videos were captured at 4

frames/second for 90-120 frames. Neurons were identified based on cell morphology. Single-color videos were acquired via stream acquisition, while double-transfected neurons were imaged via near-simultaneous two-color live imaging. Immunohistochemical images were acquired using both wide-field microscopy (DMI 6000B, Leica) and Airyscan microscopy (LSM800 Airyscan, Zeiss).

2.7. Image analysis

Co-localization analysis was done via Zeiss Zen Blue imaging analysis software. The images underwent deconvolution via Aryscan image processing. Axonal regions were selected for analysis based on morphological characteristics and traced within the Zeiss Zen Blue software. The co-localization analysis was done via segmentation to identify punctate localization of fluorescent signal. After segmentation, each puncta was analyzed for the intensity and presence of signal in both fluorescent channels. True signal was considered that which exceeded three times the average intensity present in the background. The puncta were then sorted as either positive for the presence of one or both fluorescent markers.

2.8. Video analysis

Single colour live cell imaging videos were analyzed using MetaMorph software to generate kymographs. Kymograph distances were calibrated to a 630x magnification (1 pixel = 0.160508 μm). Transport events in kymographs were manually traced and processed using custom software (Kwinter and Silverman 2009) to generate parameters including velocity, direction, and run length. Co-transport analyses were done by hand to count the number of double and single transport events from generated kymographs. All data was assembled and organized into Excel before importing into GraphPad Prism for analysis and graphing. Velocity and run length data are represented as the mean (M) $\pm$ standard deviation (SD) and all videos were taken at 4 frames/second.

Chapter 3. Characterizing and Developing iPSC-derived Neuron Culturing

The first goal of my thesis was to optimize and characterize our iPSC-derived neuron cultures. The use of iPSC-derived neurons to model human systems is relatively new, and a reliable, generally-agreed-upon standard has yet to be established. There are a multitude of different protocols in the field, with variability observed across labs (Volpato et al., 2018; Wu et al., 2007). Therefore, developing reliable iPSC-derived neurons involves a somewhat trial-and-error approach and differentiation protocols must be tailored to achieve desired results. I compared two widely used protocols to generate neurons: expression of the transcription factor neurogenin-2 (NGN2) and small molecule differentiation. I also assessed the effects of different coating matrices on culture quality. The goal of this process was to generate reproducible neuronal cultures that exhibit typical features of biochemical and morphological polarity.

3.1. Comparison of differentiation protocols

3.1.1. Small molecule versus neurogenin-2 based differentiation

Within the brain, the differentiation of neurons is a complex process modulated by many factors. Various cell types have the ability to develop into neurons depending on the implementation of various inducers and cellular events (An et al., 2022). Differentiation factors employed during neurogenesis such as NGN2 have been identified for their neural inductive effects and potential in iPSC-derived neuron culturing (Zhang et al., 2013). Alternatively, a small molecule differentiation treatment of cultures triggers certain biochemical pathways that guide the culture's development to the desired fate (Yap et al., 2015). Both methods have been implemented and have their respective advantages and disadvantages, but a clear preference in the field has yet to be established. Currently, both methods are used to create representative human models to study biological processes and neurodegenerative disorders. Therefore, I individually assessed differentiation methods to determine which produces optimal cultures for my experimentation.

Two different cell lines were used in the comparison of differentiation protocols. The first is an iPSC cell line obtained from Coriell (#GM27938). This line is a wildtype clone isolated from a patient with mosaicism for the KIF1A mutation C.609G>T (R203S) and was used with the NGN2 protocol to produce neurons. With immunocytochemical staining, this line was confirmed to be Oct4 positive and NESTIN negative (Appendix; Figure A.2). Oct4 is a common iPSC marker while NESTIN is expressed in neural progenitor cells (NPC). The second iPSC cell line was produced from the peripheral blood mononuclear cells of a healthy male donor using the Erythroid Progenitor Reprogramming Kit (STEMCELL Technologies) and was used for small molecule differentiation. These iPSCs were also found to be positive for Oct4, and after differentiation into NPCs by Dr Y. Zhu (Simon Fraser University), were NESTIN positive (Appendix; Figure A.1).

Small molecule differentiation generates iPSC-derived neurons that follow a more typical developmental pattern compared to NGN2 differentiation. With small molecule differentiation, iPSCs first go through an intermediate step where they are differentiated into NPCs. In the nervous system, NPCs differentiate into a variety of glia and neuronal cell types (Martinez-Cerdeno & Noctor 2018). With the Stemdiff Neural Induction Kit from STEMCELL Technologies, NPCs are differentiated from iPSCs through the inhibition of the TGF-β/BMP signalling pathway (Figure 3.1.A). The NPCs were then differentiated into neurons over the course of 5-7 days with the addition of the Stemdiff Forebrain Neuron Differentiation Kit from STEMCELL Technologies. After the differentiation process, the cells were replated onto coverslips (0 DIV) and underwent maturation (Figure 3.1).

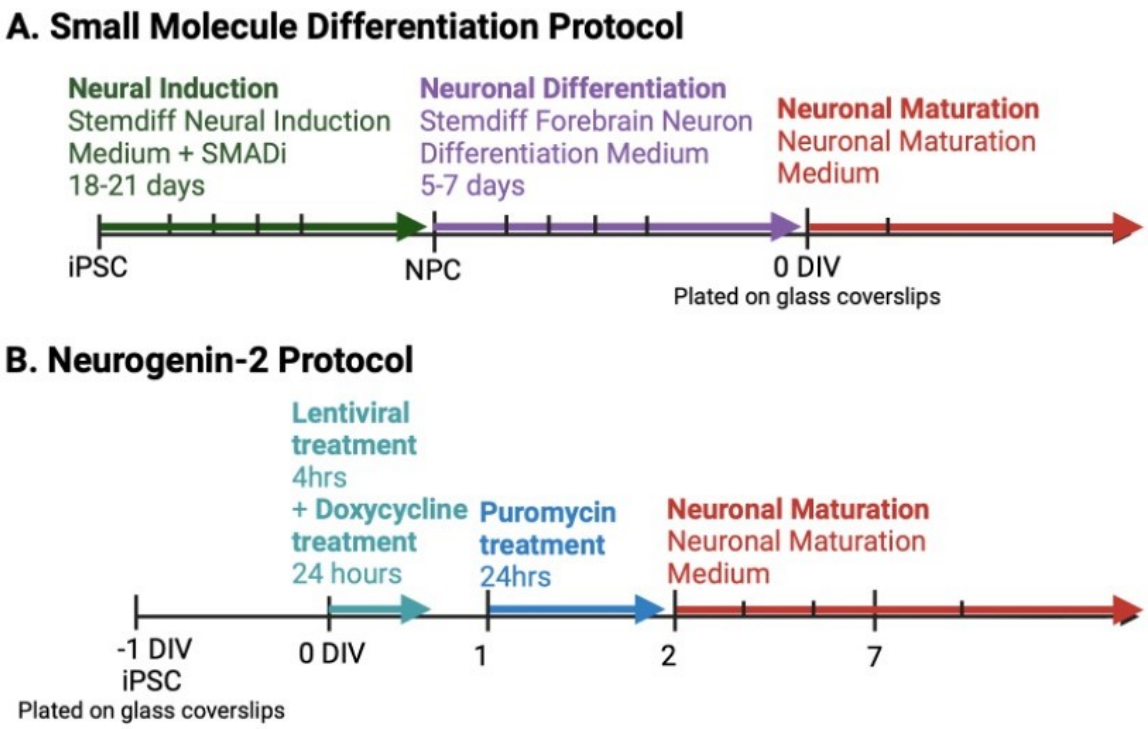

Figure 3.1 Comparison of NGN2 and small molecule differentiation protocols. A. The small molecule differentiation technique starts with the neural induction of iPSCs with the Stemdiff Neural Induction Kit (STEMCELL Technologies). After 18-21 days of culturing the iPSCs in induction medium, NPCs are generated. The NPCs are then treated with the Stemdiff Forebrain Neuron Differentiation Kit (STEMCELL Technologies) for 5-7 days to produce neurons. After this, the neurons (0 DIV) will undergo neuronal maturation. B. The neurogenin-2 (NGN2) protocol is the shorter of the two and begins with the treatment of iPSCs with lentivirus for 4 hours. Immediately after transduction, the cells are treated with doxycycline to induce NGN2 expression. 24 hours later, the culture is treated with puromycin to select against untransduced cells. After 7 days, cells take on a neuronal morphology. (Made in BioRender)

The transcription factor NGN2 is a protein encoded by the NEUROG2 gene that induces a neuronal phenotype in iPSCs. It plays a crucial role in neurodevelopment, controlling the differentiation of glutamatergic neurons in dorsal telencephalic progenitors (Scardigli et al., 2003). NGN2 also guides the differentiation of forebrain neurons by accelerating cortical gene transcription (Mattar et al., 2008). NGN2 is a basic helix-loop-helix transcription factor that serves as a master regulator of key genes involved in CNS development. NGN2 mutant mice show significant alteration in the expression of several downstream transcription factors necessary for neocortical specification (Schuurmans et al., 2004). Because NGN2 has been implicated in the

development of neurons, its induced expression in iPSCs was explored to directly differentiate cells. Overexpression of NGN2 in iPSCs induces a neuronal phenotype in as early as 7 days *in vitro* (DIV) (Fernandopoulle et al., 2018; Zhang et al., 2013). Besides rapidly generating neurons, NGN2 also offers the potential for purer and more consistent cultures compared to small molecule differentiation. Lentiviral transduction often achieves NGN2 overexpression, and the paired expression of antibiotic resistance allows for the efficient selection of transduced cells (Figure 3.1.B). Every batch of lentivirus produced was tested with a series of dilutions to minimize toxicity to the cells, while maintaining transduction and expression efficiency. A comparison of cell density before viral transduction (0 DIV) and after both transduction and selection (3 DIV) showed that approximately 70% of cells survive the entire process (Appendix; Figure A.3). Immunocytochemical staining at 3 DIV post transduction confirmed NGN2 expression (Appendix; Figure A.3). At 3 DIV, the cells already begin to develop neurites and express the neuronal marker β3-Tubulin (Appendix; Figure A.4). β3-Tubulin, a tubulin subunit found almost exclusively in neurons (Pathol 1989), marks the development of a population acquiring neuronal characteristics. Over the course of 7 DIV, the cells continued to develop, with increased β3-Tubulin expression and neurite lengthening.

Overtime, culture differences between the two differentiation techniques become more pronounced. During the first 7 DIV, the cultures follow a similar developmental profile, with the extension of neurites and expression of β3-Tubulin (Appendix, Figure A.4; Appendix, Figure A.5). However, at 14 DIV, stark differences in cell morphology emerge, with the NGN2 cell bodies becoming increasingly clumped and axons fasciculating (Figure 3.2). Fasciculation, the bundling of axons, indicates poor culture quality and is a significant barrier for further experimentation and imaging. Neurons were cultured in 12-well plates and each of the two differentiation protocols were replicated a total of 3 times. At 14 DIV, the pattern was consistent across all cultures, with NGN2 derived neurons exhibiting significant fasciculation and cell clumping. The small molecule-derived neurons do not exhibit the same level of fasciculation and survive in culture for up to 3 months. Therefore, because of the longevity and culture stability, we established small molecule differentiation as our preferred method going forward.

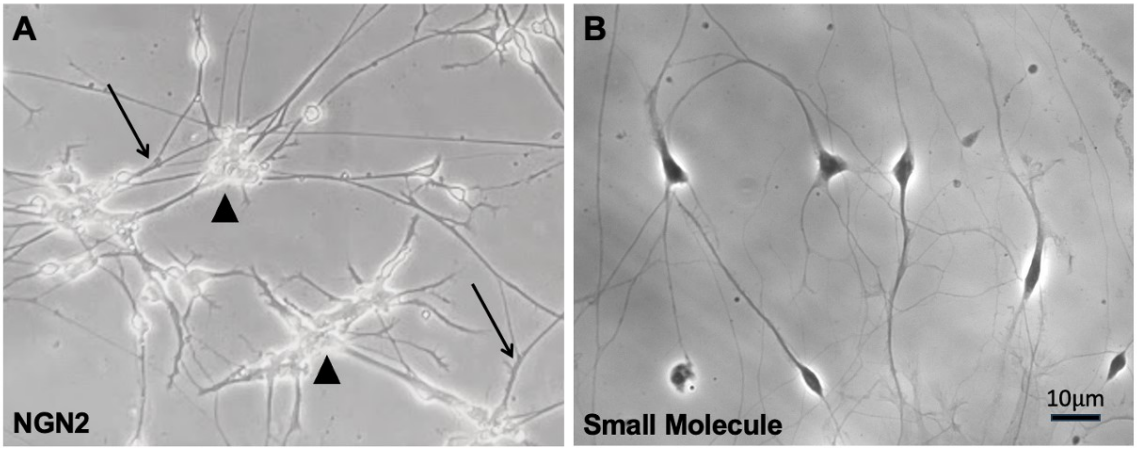

Figure 3.2 Comparison of NGN2 and small molecule differentiation in generating iPSC-derived neurons.
Cells were plated at 100,000 cells/well onto Poly-L-Ornithine and Laminin-coated glass coverslips and matured for 14 DIV. A. NGN2 derived neurons displaying significant cell body clumping (denoted by arrowheads) and fasciculated axons that begin to detach from the plate (denoted by arrows). B. Small molecule derived neurons do not yet experience fasciculation and cell body clumping issues.

3.1.2. Effect of coating protocols on culture development

After establishing the use of small molecule differentiation, I proceeded to test different substrates to assess their effect on cell survival and development. In the developing nervous system, the extracellular matrix provides structural support and serves as an inductive substrate for cellular signaling (Walma & Yamada, 2020). Currently, there is no general consensus in the field regarding the coating matrix. The choice of substrate is crucial for adhesion and potential developmental effects, especially in the case of neuron culturing. Neurons typically do not adhere easily to standard culture-treated surfaces, unlike other anchorage-dependent cell types. This is because neuronal survival depends on particular coating and chemical modifications made to the cultureware (Yu et al., 2008). Furthermore, the extracellular matrix significantly affects neurodevelopment and neuronal differentiation in culture (Liu et al., 2020). Therefore, a series of substrates were tested in neuronal plating including Poly-L-Ornithine (PLO), Poly-D-Lysine (PDL), Poly-L-Lysine (PLL), Fibronectin, Matrigel, and Geltrex (Table 1). Each substrate was tested at different concentrations and the neurons were matured for 7 DIV. After 7 DIV, the cells were assessed for initial survival and attachment following

their plating. At this stage, with the large volume of substrate combinations, only one neuronal culture was tested, with each substrate combination being replicated on 3 separate coverslips. Of the list, two substrates stood out as the best candidates; Matrigel (1:100 dilution) and Poly-L-Ornithine (50 µg/ml) with Laminin (10 µg/ml). Following plating, these two substrates and their combinations yielded the highest cell adhesion and survival. Therefore, we went forward with these two options for further testing and analysis.

Coating Matrix	Concentration
Poly-D-Lysine + Laminin	10-50 µg/ml; 5-10 µg/ml
Poly-L-Lysine + Laminin	10-50 µg/ml; 5-10 µg/ml
Poly-L-Ornithine + Laminin	10-50 µg/ml; 5-10 µg/ml
Fibronectin	1-5 µg/cm^2
Matrigel	1.5-2 µl/cm^2 (1:100 Dilution)
Geltrex	1.5-2 µl/cm^2 (1:100 Dilution)

Table 3.1 Neuronal coating matrices.
The left column (Coating Matrix) describes the different substrates and combinations used in testing to determine the optimal coating protocol for the development and maturation of iPSC-derived neurons. The right column (Concentration) describes the range of concentrations and dilution factors used in testing each substrate.

Matrigel and Poly-L-Ornithine (PLO) with Laminin are two common matrices used in iPSC-derived neuron culturing (Bell et al., 2019; Zhang et al., 2013). Matrigel is extracted from mouse EHS tumors that contain components found in many tissue basement membranes (Passanti et al., 2022). It supports the survival and differentiation of brain-derived neural stem cells (Wang et al., 2020) and the long-term survival of neurons in culture (Yan et al., 2018). PLO, a synthetic amino acid chain, is often used to coat dishes in primary neuron cultures. Besides PLO, there are many synthetic amino acid options such as Poly-L-Lysine (PLL). Although functionally similar, PLO is often used in combination with laminin and can increase the adhesion of human neurons on glass coverslips (Milky et al., 2022).

I compared Matrigel and PLO and Laminin coating effects on iPSC-derived neuron development. Cells were plated at 150,000 cells/well in a 12-well plate onto glass coverslips coated with either PLO and Laminin or Matrigel. After 14 DIV, the overall culture morphology showed a predominant secondary cell type emerge on the Matrigel-coated dishes (Figure 3.3), which proliferated extensively over time. Comparatively, PLO and Laminin-coated dishes were more homogeneous without rapid proliferation from this cell type. Three replicates of 12-well plates were done to test each substrate and this pattern was consistent across all of them. Hence, all iPSC-derived neurons will be cultured via small molecule differentiation on PLO and Laminin-coated glass coverslips (Figure 3.3).

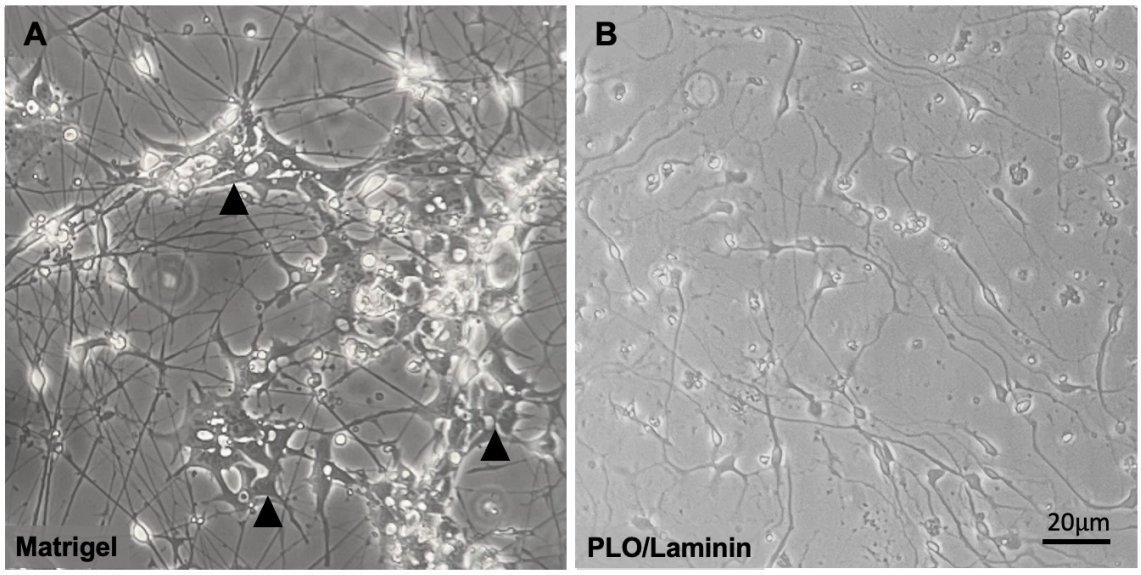

Figure 3.3 Matrigel and PLO/Laminin as matrices in generating iPSC-derived neurons.
All cells were plated at 150,000 cells/well and matured for 14 DIV. A. Matrigel cultures experienced increased cell body clumping and the proliferation of a secondary cell-type (denoted by arrowheads) that eventually overtook the cultures B. PLO and Laminin cultures did not see the proliferation of this secondary cell type, and cell body clumping was not observed.

3.2. Characterization of the iPSC-derived neuron cultures

A consideration in using iPSC-derived neurons concerns their developmental profile. To date, the characteristic stages of iPSC-derived neuronal development have not

been as well described as in primary rodent neuron cultures (Dotti et al., 1988). Morphological analyses of iPSC-derived neurons have revealed that they follow canonical early neurodevelopmental stages, with neurites extending from 3 DIV and the axon initial segment emerging at 7 DIV (Lindhout et al., 2020). For example, time-lapse analysis of axon growth shows that from 3 to 15 DIV, the length of axons of iPSC-derived neurons continues to extend (Kang et al., 2017). Proteomics and transcriptomics studies confirm this pattern, with neuronal markers increasing in expression from 3 DIV to 7 DIV (Lindhout et al., 2020). I differentiated and cultured cells according to our finalized protocol (Figure 3.1.A). After the differentiation step and plating onto coated glass coverslips, the cells were fixed at 0, 3, and 7 DIV. Our neurons developed similarly to the literature, with neurites emerging and extending early in development (Figure 3.4). By 7 DIV, the cells had adopted a neuronal morphology with extending axons (Figure 3.4.A-C). β3-Tubulin expression also increased over 7 DIV, exhibiting a typical pattern throughout the cell body and axons (Figure 3.4.D-E). Since establishing the culturing protocol, it has been repeated 10 times, with each culture following the same developmental patterns.

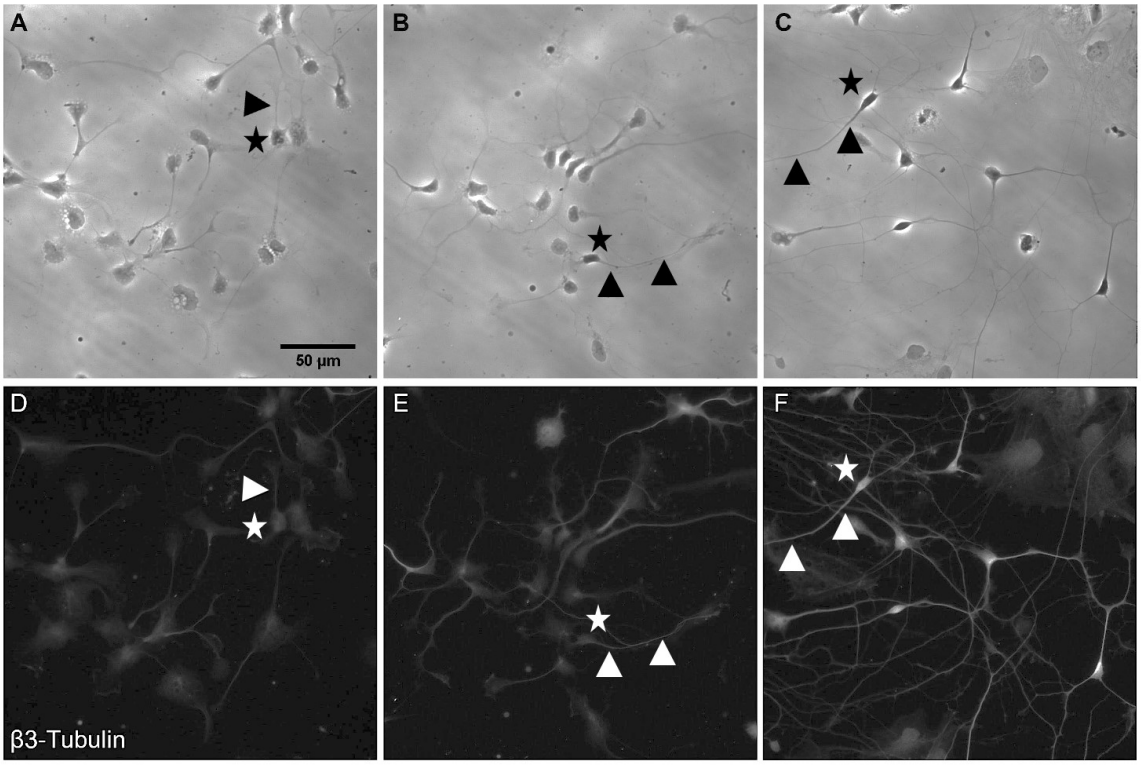

Figure 3.4 Small molecule derived iPSC-derived neurons development over 7 DIV.

A-C. Phase images of cells at 0 DIV, 3 DIV, and 7 DIV during neuronal maturation. Neurites emerge and elongate to produce axons and develop a neuronal morphology. D-F. β3-Tubulin immunocytochemical stains of the cells from panels A-C. β3-Tubulin expression is visible at 3 DIV and increases up to 7 DIV. Stars denote cell bodies and arrowheads denote elongating neurites.

Chapter 4. Assessing netrin-1 trafficking and its association with KIF1A

Netrin-1 is a secreted protein found in human neurons that is integral for the proper maintenance and formation of the nervous system. The proper function of netrin-1, however, is dependent on its proper transport and localization. Intracellular trafficking, vital for proteins to move towards their site of function, involves packaging Golgi-derived proteins into vesicles and transporting them via motor proteins along microtubules in eukaryotic cells. In human neurons, the intracellular trafficking of netrin-1 remains unknown. In *C. elegans*, netrin-1 associates with unc104/KIF1A-dependent vesicle cargoes, suggesting it may be carried by KIF1A and associated with other KIF1A-trafficked vesicles. Kinesin-dependent motor protein trafficking undergoes regulation at multiple steps to ensure proper cargo delivery. Therefore, understanding the trafficking of netrin-1 will give insight into its regulation and function. In this section I will discuss my novel findings on the transport dynamics of netrin-1 in human iPSC-derived neurons. I assessed the patterns of movement of netrin-1 along the axon, measuring velocity and run length, and determined its association with KIF1A. Furthermore, I assessed netrin-1's co-localization with and co-transport with the KIF1A-dependent cargo chromogranin (CHG).

4.1. Netrin-1 localization in iPSC-derived neurons

While netrin-1 distribution has been visualized in *C. elegans* neurons, its presence in human neurons remains to be observed. Determining netrin-1's subcellular localization is necessary for further investigation of its trafficking and secretion from neurons. For example, the organization of proteins at synapses is necessary for proper synaptic activity (Kim & Huganir 1999) and netrin-1 has been shown to regulate synaptic transmission (Glasgow et al., 2018). Because neurons are such highly polarized cells, confirming the intracellular localization of netrin-1 to specific structures, such as axons and dendrites, is necessary. Therefore, I conducted immunocytochemical staining of endogenous netrin-1. Fluorescent microscopy reveals netrin-1 presence both within the cell body and along

axons in a punctate manner (Figure 4.1.A). The vesicular pattern resembles those observed with other KIF1A cargoes such as BDNF (Lo et al., 2011). This pattern contrasts with the typical cytoskeletal staining pattern of β3-Tubulin, which is more diffuse and uniform (Figure 4.1.B). This staining was done three times in three separate cultures, and the patterning was consistent across all replicates. This marks the initial visualization of netrin-1 within human neurons and its unique patterning.

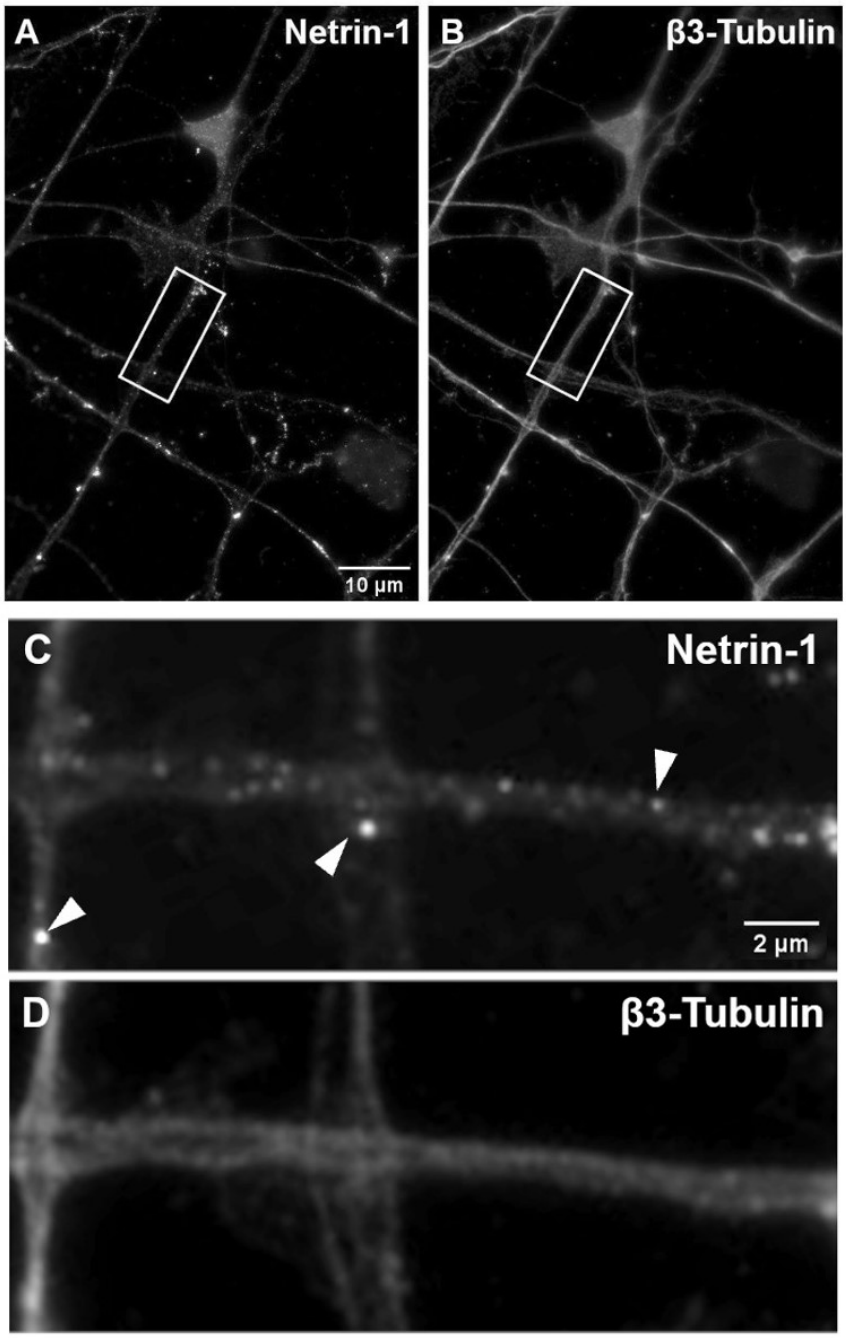

Figure 4.1 Endogenous localization of netrin-1 in human iPSC-derive neurons. A. Netrin-1 distribution in a neuron 7 DIV. B. β3-Tubulin expression in the same cell. C. Inset from panel A. Netrin-1 expression is punctate (denoted by arrowheads) and localized throughout the neuron. D. Inset from panel B. The β3-Tubulin patterning is expressed in a uniform pattern throughout the neuron.

4.2. Netrin-1 transport in iPSC-derived neurons

Live imaging of fluorescently tagged cargo enables real-time visualization and assessment of characteristics such as velocity, run length, and directionality. To evaluate netrin-1 movement in iPSC-derived neurons, I transfected cultures with netrin-1-mRuby3 using EndoFectinMAX. mRuby3 is a red-fluorescent protein and was chosen for its resistance to denaturation at pH extremes and because can be up to 10-fold brighter than more conventional fluors, such as EGFP and RFP (Kredel et al., 2009). Additionally, mRuby3 was chosen because it was found to produce higher brightness and be more photostable than its predecessors mRuby and mRuby2 (Bajar et al., 2016). The brighter and more photostable mRuby3 was necessary to minimize photobleaching for the length of the live-cell imaging process. I started with an initial assessment of netrin-1-mRuby3 localization via immunocytochemical staining with a cytoskeletal marker to determine if it resembles the pattern of endogenous netrin-1. MAP2 is a neuron-specific cytoskeletal marker enriched in dendrites. Overlap of netrin-1-mRuby3 with MAP2 reveals that it is present both in dendrites and in MAP2 negative regions, i.e., the axon (Figure 4.2). Thus, netrin-1-mRuby3 was punctate and localized throughout the cell, similarly to its endogenous distribution (Figure 4.2; Figure 4.1). The netrin-1-mRuby3 expression and MAP2 immunocytochemical staining was done in only one culture, however, this distribution of netrin-1-mRuby3 was consistent with the general pattern observed via live-cell imaging. For live-cell imaging, 21 videos (n = 21) of 21 individual cells were recorded from 5 different cultures at 14 DIV. Netrin-1-mRuby3 was expressed and trafficked throughout the cell body and all its processes, and videos were taken of transfected axonal segments with a minimum length of 20 μm (Figure 4.3.A). Videos were captured at a rate of 4 frames/second, from which kymographs depicting netrin-1 movement (y-axis) over 20 seconds (x-axis) were generated (Fig. 4.3.B-C). In total, there were 367 transport events in the anterograde direction and 330 events in the retrograde direction. Events below 2 μm traveled were excluded from the totals to eliminate possible transport events caused by diffusion (Abney et al., 1999). The mean velocity of netrin-1-mRuby3 was 1.56 ± 0.76 μm/second in the anterograde direction, and 1.70 ± 0.79 μm/second in the retrograde direction (Fig. 4.3.D, F). Compared to the observed

velocities, the total run lengths had more variation with the average length in the anterograde direction being 5.33 ±4.8μm and the retrograde direction having an average length of 6.67±6.6 μm. The velocities and run lengths of netrin-1 are consistent with previous findings of KIF1A transport and the transport of KIF1A-associated cargoes (Lo et al., 2011; Chiba et al., 2019). These findings confirm the bidirectional transport of netrin-1 and give insight into its transport characteristics.

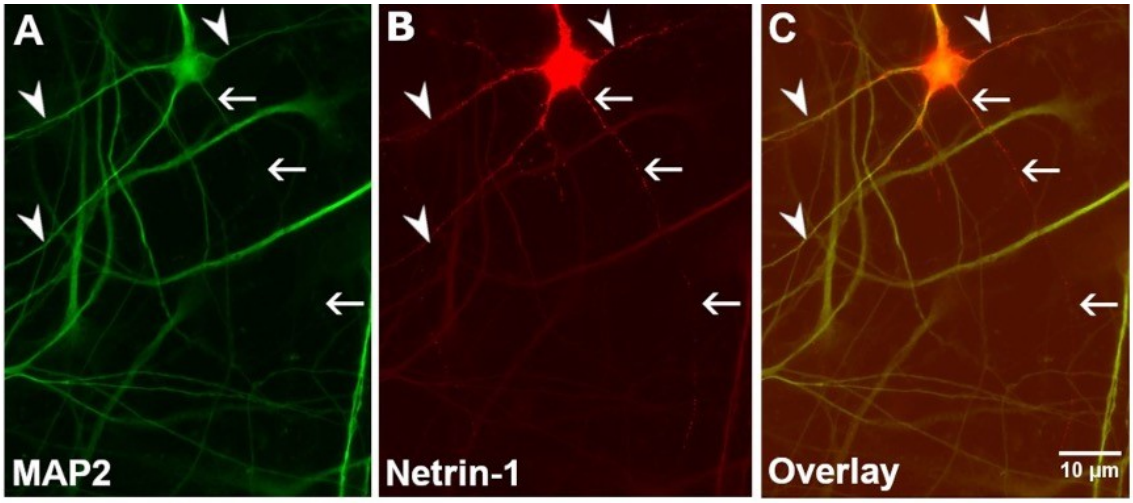

Figure 4.2 Netrin-1-mRuby3 localization in axonal and dendritic structures
A. Endogenous MAP2 expression, with MAP2 positive dendrites denoted by arrowheads, and MAP2 negative axonal structures are denoted by arrows. B. Exogenously expressed Netrin-1-mRuby3 distribution throughout the transfected neuron. C. Overlay of MAP2 and netrin-1-mRuby expression, showing that netrin-1 is localized to both positive and negative MAP2 structures; dendrites and the axon, respectively. Neurons were cultured for 30 DIV and all panels correspond to the same cell.

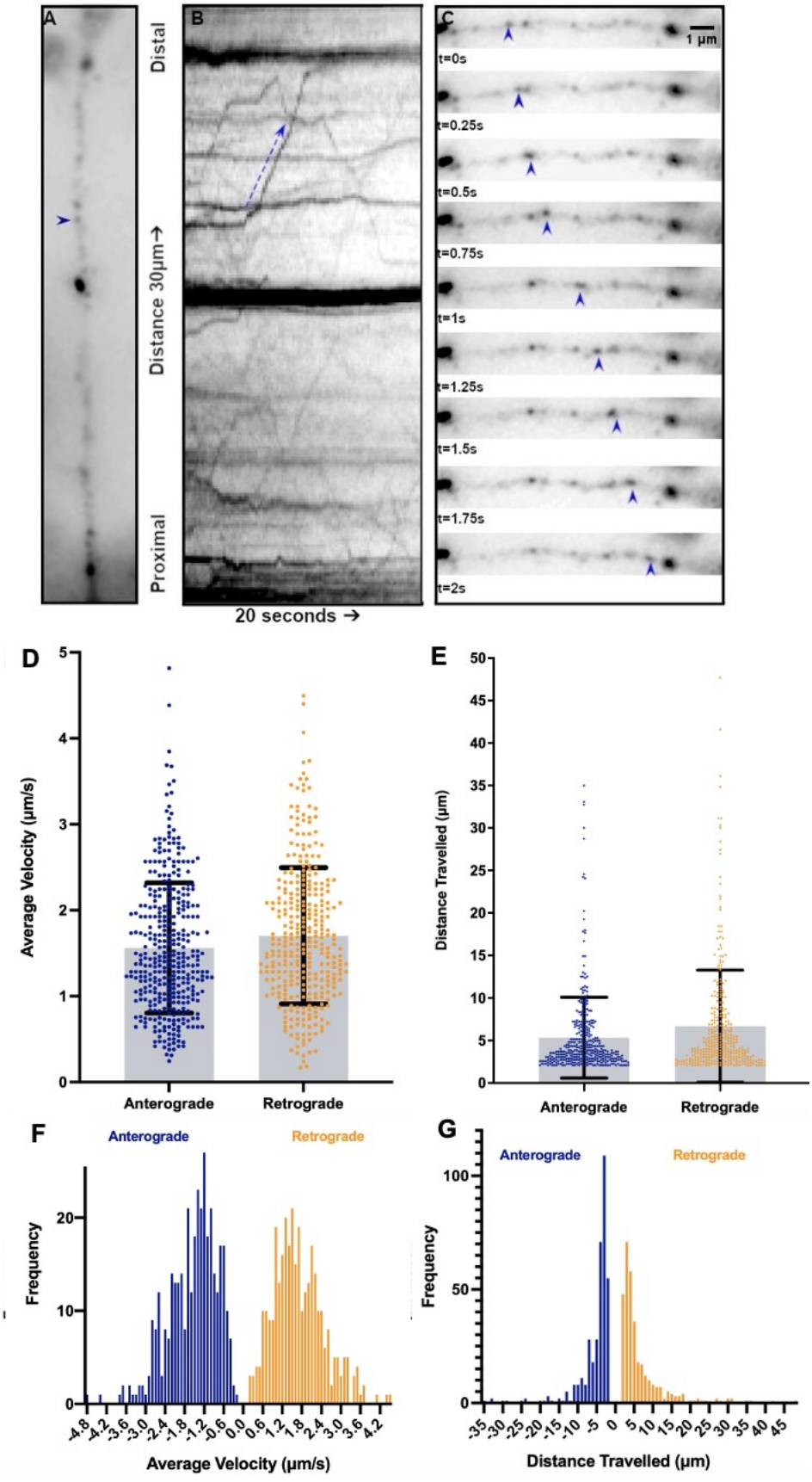
A
B
C
Distal
Distance 30µm→
Proximal
20 seconds →
1 µm
t=0s
t=0.25s
t=0.5s
t=0.75s
t=1s
t=1.25s
t=1.5s
t=1.75s
t=2s
D
Average Velocity (µm/s)
Anterograde
Retrograde
E
Distance Travelled (µm)
Anterograde
Retrograde
F
Anterograde
Retrograde
Frequency
Average Velocity (µm/s)
G
Anterograde
Retrograde
Frequency
Distance Travelled (µm)

Figure 4.3 Netrin-1 transport in iPSC-derived neurons.
A. 30 μm segment of a neuron expressing netrin-1-mRuby3. B. Kymograph produced by a 20 second video taken of trafficking in the axonal segment in panel A at 4 frames/second. Positive slopes represent anterograde movement that moves towards the distal end (away from the cell body) and negative slopes represent retrograde movement which move towards the proximal end (towards the cell body). C. Stream acquisition of a moving particle (blue arrow) traveling in the anterograde direction. D. Average velocities of netrin-1 moving in both the anterograde (Mean (M) = 1.56 μm/second; Standard deviation (SD) = 0.76; n = 21 cells from 5 independent cultures; 367 transport events) and retrograde direction (M=1.70 μm/second; SD = 0.79; n = 21 cells, 5 cultures, 330 events). E. Average run lengths of netrin-1 moving in both the anterograde (M = 5.33 μm; SD = 4.8; n = 21 cells, 5 culture, 367 events) and retrograde directions (M = 6.67 μm; SD = 6.6; n = 21 cells, 5 cultures, 330 events). F. Histogram showing the distribution of netrin-1 velocities from panel D. G. Histogram showing the distribution of netrin-1 run lengths from panel E. For all panels, anterograde events are represented in blue and retrograde events are represented in orange.

4.3. Assessing netrin-1 and KIF1A's association

Although netrin-1 is implicated in numerous developmental processes, its intracellular transport mechanism remains poorly understood. Kinesin motor proteins are responsible for the anterograde transport of many essential proteins and organelles. Despite netrin-1's co-localization with UNC-104 in *C. elegans*, its association with KIF1A in mammalian neurons has not been explored. Given netrin-1's synaptic release in rat hippocampal neurons (Glasgow et al., 2018), active intracellular transport to release sites is likely. Thus, I assessed netrin-1 and KIF1A's association to elucidate its transport mechanism in human neurons. To visualize the endogenous co-localization of netrin-1 and KIF1A, cells were fixed and immunocytochemically stained with netrin-1, KIF1A, and β3-Tubulin (Figure 4.4.A). Both the netrin-1 and KIF1A staining revealed a punctate pattern that, when overlapped, showed significant co-localization (Figure 4.4.B-D). Quantitative analysis of 3 axonal regions (n = 3) from 3 separate cells within one culture revealed that 90.1% of netrin-1 puncta were co-localized with KIF1A, while only 9.1% did not overlap with KIF1A (Figure 4.4.E) Additionally, the observed netrin-1 patterning was confirmed by imaging immunocytochemically stained cells in another fluorescent channel as a control for background signal and bleed through (Appendix; Figure A.6).

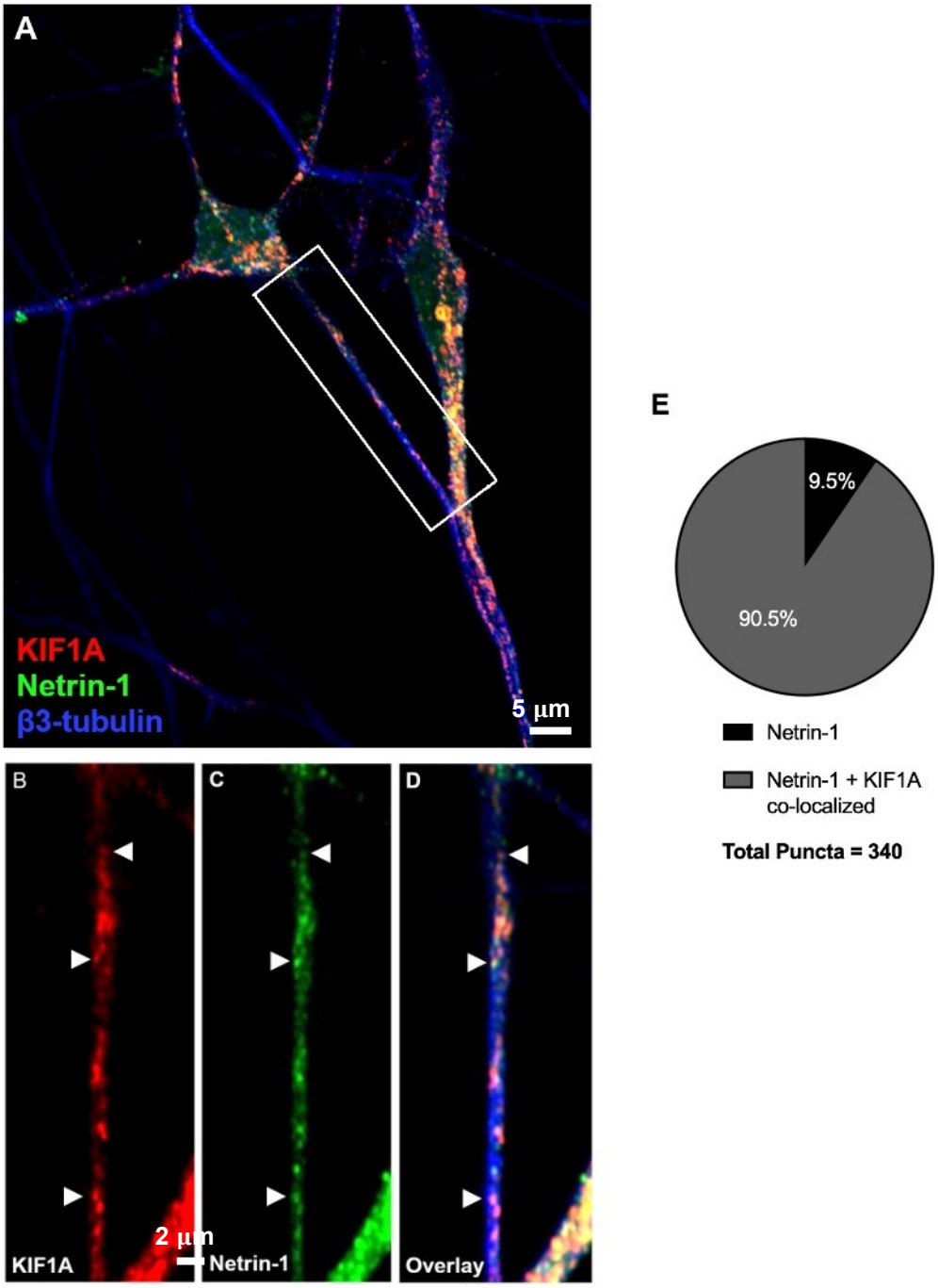

Figure 4.4 Endogenous co-localization of KIF1A and netrin.
A. Overlayed image of KIF1A (Red), netrin-1 (Green), and β3-Tubulin (Blue) staining of an iPSC-derived neuron (7 DIV). B. Enlarged image of a neuronal segment (inset in panel A) stained with KIF1A. C. Enlarged image of the same neuronal segment stained with netrin-1 (inset in panel A). D. Overlaying immunocytochemical staining with netrin-1, KIF1A, and β3-Tubulin of the same neuronal segment (inset in panel A). The white arrowheads denote co-localized puncta of netrin-1 and KIF1A. E. The percentage of netrin-1 puncta that co-localize and do not co-localize with KIF1A (n = 3 axonal segments from 3 individual cells within one culture).

Following the establishment of a relationship between netrin-1 and KIF1A, this study utilized live-cell imaging to investigate whether KIF1A serves as the active motor in transporting netrin-1. Neurons were doubly transfected with netrin-1-mRuby3 and KIF1A-NeonGreen and imaged 24-48 hours later. Near-simultaneous two-colour live imaging generated kymographs capturing the movement of both fluorescently tagged proteins (Figure 4.5). Movies were captured at 4 frames per second, and overlapping frames revealed co-transported particles (Figure 4.5.A). Kymographs were generated, traced, and particle movement was categorized as either a co-transport or a single transport event (Figure 4.5.B). Analysis was conducted on 5 co-transport videos (n = 5) obtained of axonal segments from 5 individual cells from 3 different cultures matured 7-14 DIV. KIF1A transport events outnumbered netrin-1 transport events, with KIF1A totaling 258 and netrin-1 totaling 130. Analysis revealed that in the anterograde direction, 81% of netrin-1 events co-transported with KIF1A, while 43% of KIF1A events co-transported with netrin-1 (Figure 4.5.C). In the retrograde direction, 59% of netrin-1 events co-transported with KIF1A events, and 39% of KIF1A events co-transported with netrin-1 (Figure 4.5.C).

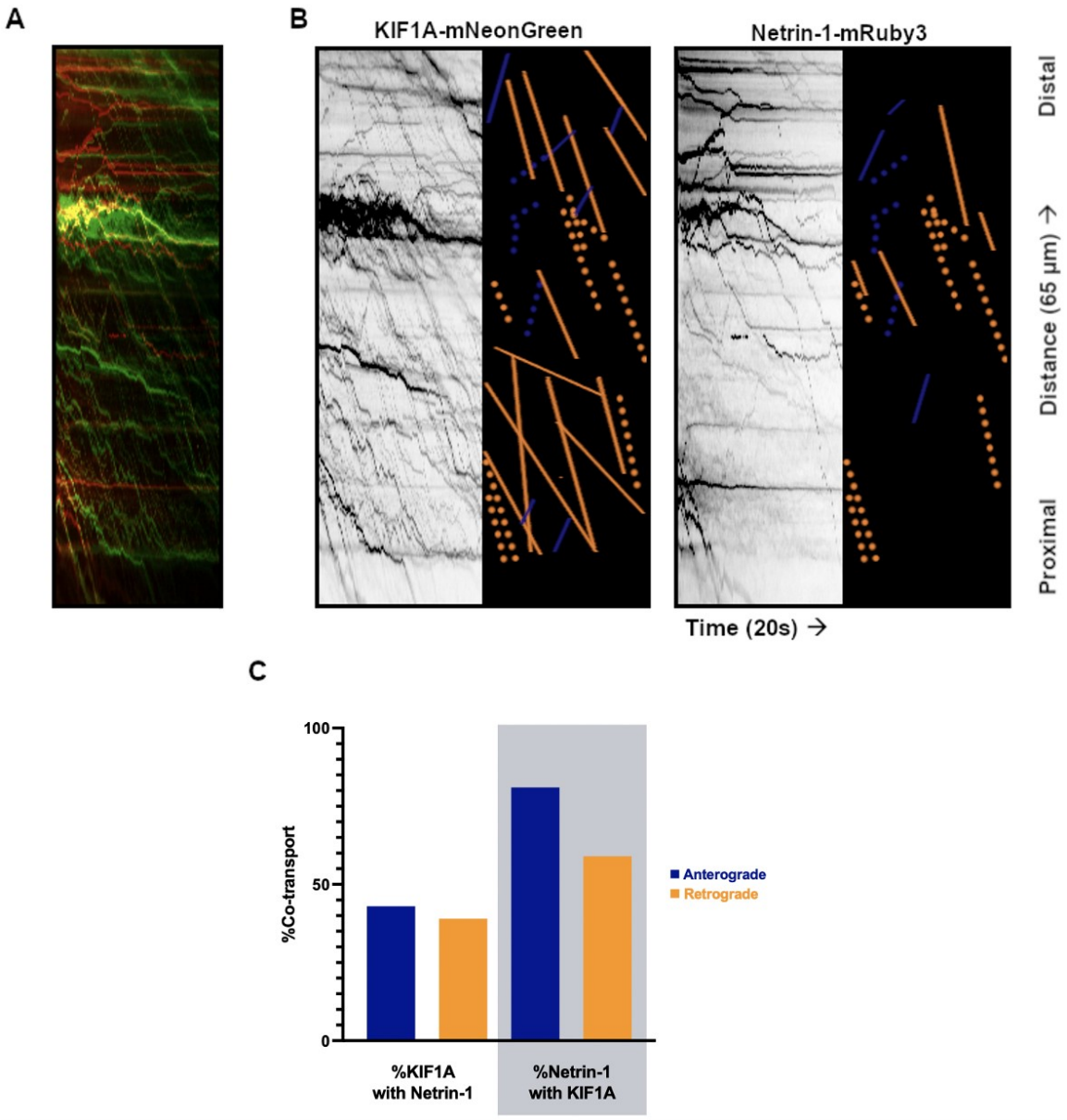

Figure 4.5 Netrin-1 and KIF1A co-transport

A. Overlapping kymographs of netrin-1-mRuby3 and KIF1A-neongreen created from videos of a single 65µm axonal segment of an iPSC-derived neuron (7 DIV) for 20 seconds (4 frames/second). B. Separate kymographs of netrin-1-mRuby3 and KIF1A-neongreen movement with examples of tracings of transport events. Blue lines represent anterograde events and orange lines represent retrograde events. Solid lines represent single transport events while dotted lines represent co-transport events. Particles move in both the distal direction (away from the cell body) and the proximal direction (towards the cell body). C. Graphical representation of the percent of co-transport between KIF1A and netrin-1 events in both the retrograde and anterograde directions (n = 5 videos of 5 different cells from 3 independent cultures).

4.4. Netrin-1 resides in dense core vesicles

Now that KIF1A has been implicated in the transport of netrin-1, I next questioned the possible vesicle housing netrin-1. KIF1A transports proteins housed in known vesicles such as DCVs and SVPs. Netrin-1's release in rat hippocampal neurons follows similar patterns as DCV release in terms of excitability and the rate of release (Glasgow et al., 2018, Boosport et al., 2012; Farina et al., 2015). Therefore, I hypothesized that netrin-1 was also packaged in DCVs carried by KIF1A. To test this hypothesis, I did a preliminary analysis of netrin-1 localization with the known resident and canonical DCV cargo chromogranin (CHG). CHG is a protein related to endocrine function and packaged in secretory vesicles (Ciesielski-Treska et al., 1998). Using immunocytochemistry, I assessed the co-localization of netrin-1 and CHG within iPSC-derived neurons. Both the netrin-1 and CHG staining revealed a punctate pattern that, when overlapped, showed near complete co-localization (Figure 4.6.A-C). Additionally, quantitative analysis of 3 axonal segments (n = 3) from 3 different cells within the same culture revealed that 84.3% of netrin-1 puncta were co-localized with CHG (Figure 4.6.D). These findings strongly suggest that netrin-1 is transported within DCVs, I therefore further assessed this association through live-imaging of these two cargos within the same neuron.

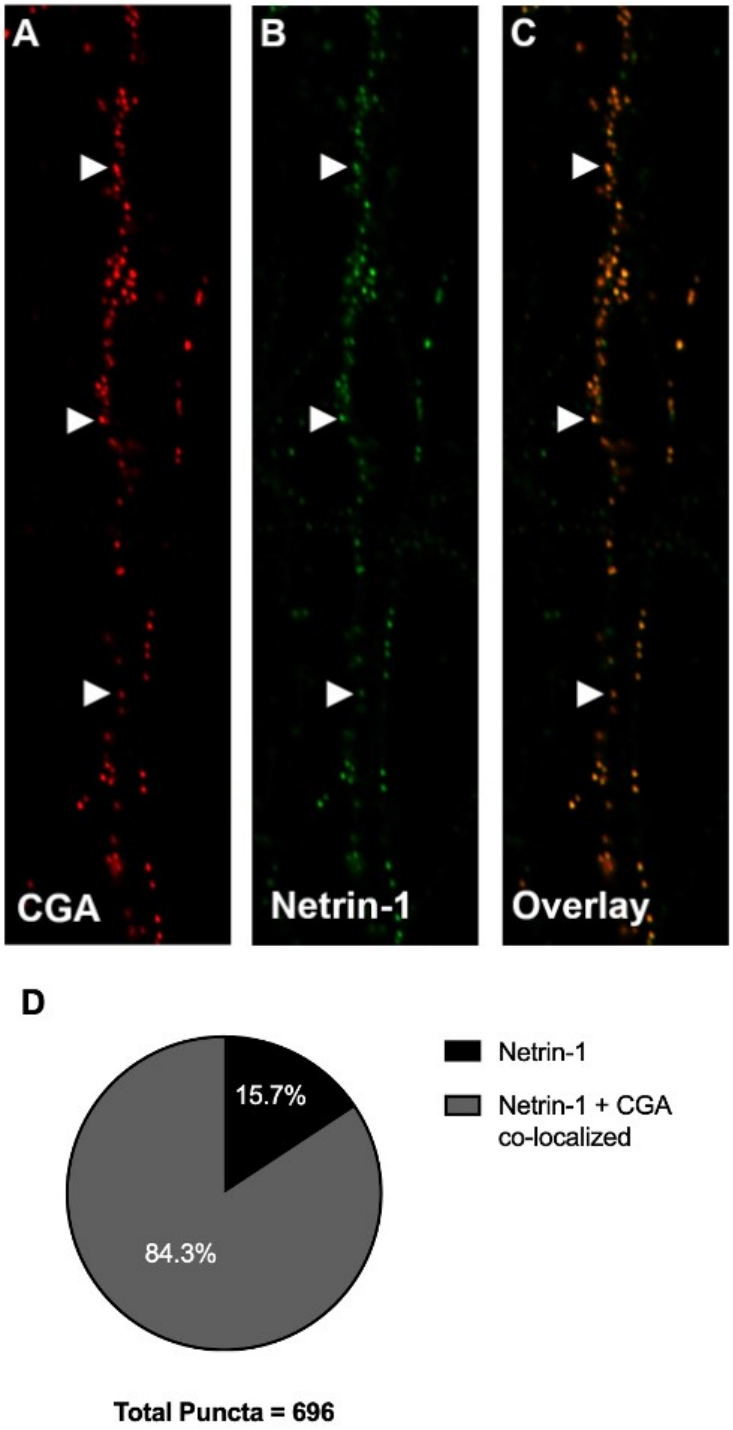

Figure 4.6 Co-localization of endogenous netrin-1 and CGA.
A. Punctate distribution of chromogranin-A (CGA) distribution in a segment of an iPSC-derived neuron (7 DIV). B. Punctate distribution of netrin-1 distribution in the same neuronal segment as panel A. C. Overlay of netrin-1 (green) and CGA (red) co-localization (orange) showing near complete overlap. Arrowheads denote co-localization. D. Percentage of netrin-1 puncta that co-localize and do not co-localize with CGA (n = 3 axonal segments from 3 individual cells within the same culture).

Neurons at 7 DIV were co-transfected with netrin-1-mRuby and CHG-GFP and 24-48 hours after transfection, the cells were imaged via near-simultaneous two-colour live imaging (Figure 4.7). In total, 5 co-transport videos were analyzed (n = 5) of axonal segments of 5 different cells from 3 different cultures. CHG transport events outnumbered netrin-1 transport events, with CHG totaling 344 and netrin-1 totaling 283. Subsequent co-transport analysis revealed that in the anterograde direction, 96% of Netrin-1 events co-transported with CHG movement events, while 75% of CHG transport events overlapped with netrin-1 events (Fig 4.7.B). In the retrograde direction, 82% of netrin-1 events overlapped with CHG events, and 72% of CHG events overlapped with netrin-1 events (Figure 4.7). These high rates of co-transport are consistent with the high overlap observed in the endogenous staining. Because netrin-1 co-transports with CHG, it is likely that netrin-1 is housed in DCVs.

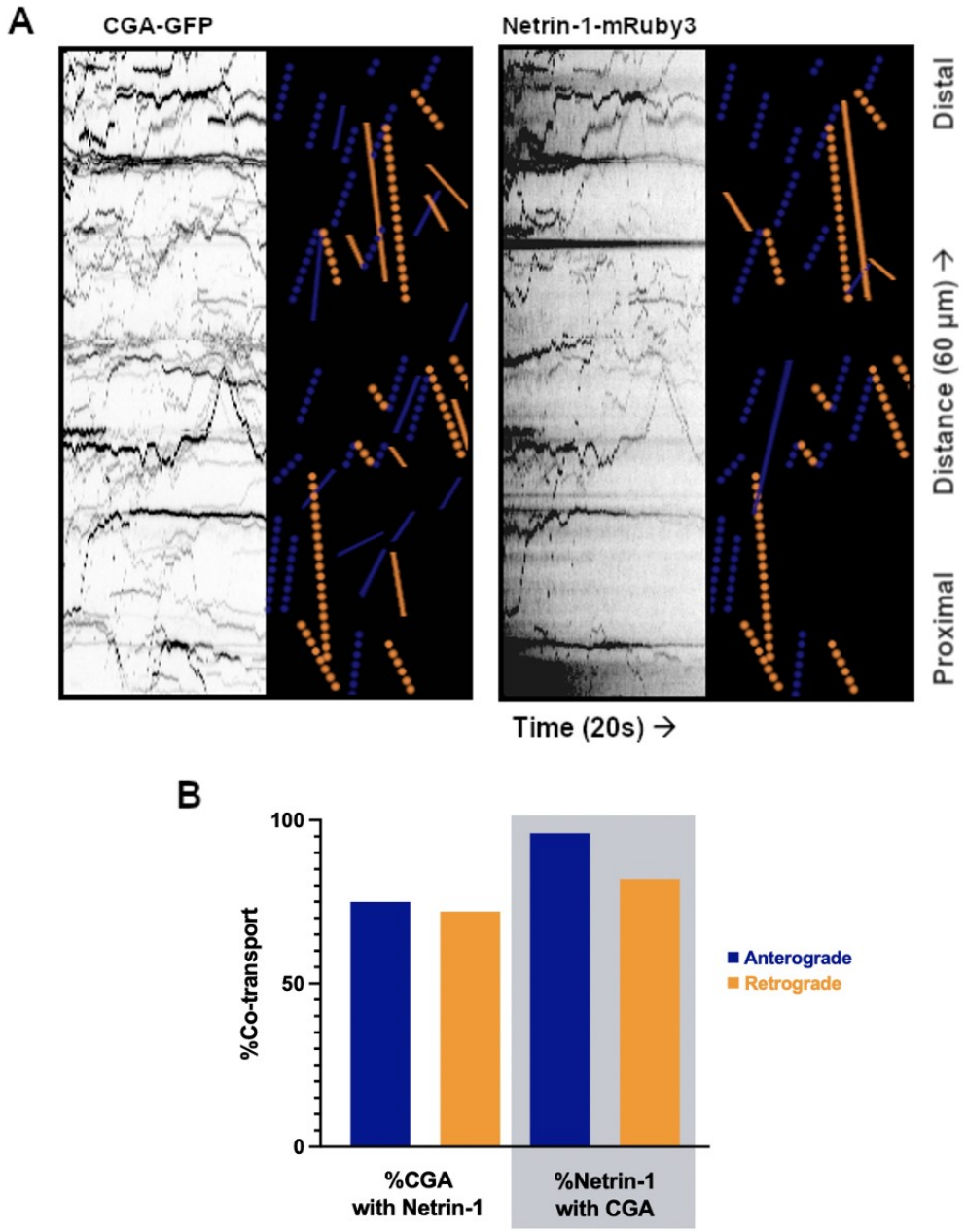

Figure 4.7 Netrin and Chromogranin co-transport
Kymographs were created from a video of a 60µm axonal segment of an iPSC-derived neuron (7 DIV) for 20 seconds (4 frames/second). A. Separate kymographs of netrin-1-mRuby3 and chromogranin-A (CGA)-GFP movement with examples of tracings of transport events. Blue lines represent anterograde events and orange lines represent retrograde events. Solid lines represent single transport events while dotted lines represent co-transport events. Kymographs show movement towards the distal end (away from the cell body) and towards the proximal end (towards the cell body) over time C. Graphical representation of the percentage of co-transport between CGA and netrin-1 transport events in both the retrograde and anterograde directions (n = 5 videos of 5 different cells from 3 independent cultures).

Chapter 5. Discussion

5.1. Summary

Netrin-1 is a protein of interest due to its diverse functions in the central nervous system, including guiding axonal outgrowth, maintaining glial-neuronal contacts, and promoting LTP. These biological processes are essential for the survival and health of many organisms, and netrin-1 loss-of-function is detrimental for CNS development and function (Cline et al., 2023). Netrin-1 is found in all deuterostomes and highly conserved among mammals (Figure 1.4). Although proteomics and transcriptomics studies reveal that it is present in human iPSC-derived neurons (Lindhout et al., 2020), its cellular location, function, and mechanisms of action in human neurons have not been studied. Moreover, the intracellular transport of netrin-1 remains unknown in human neurons and other animal models. Transport is necessary for the function of Golgi-derived proteins for delivery to their site of action and for potential post-translational modifications that occur in transit. To understand netrin-1 intracellular transport, determining the motor protein that translocates netrin-1 vesicles and the vesicle population for which netrin-1 resides is necessary. This information is relevant for understanding netrin-1's biological function and potential therapeutic effects in transport disorders like KAND.

The primary goal of my thesis was to study the intracellular transport of netrin-1 in human neurons. The first step in accomplishing this was to develop iPSC-derived neuron cultures to establish a human model for trafficking netrin-1. After testing two differentiation methods and various substrates, we determined that the optimal protocol for producing iPSC-derived neuron cultures involved small molecule differentiation and coating cultureware with PLO and Laminin. Following a year of development and testing of these methods, I proceeded to experiments aimed at studying netrin-1 transport and localization in human neurons. I confirmed the presence of netrin-1 in human neurons through immunocytochemical staining and fluorescent live-imaging of exogenous netrin-1 (netrin-1-mRuby3). Subsequently, I demonstrated that netrin-1 undergoes bidirectional transport in the axons of human neurons. Furthermore, endogenous netrin-1 co-localizes with KIF1A (Figure 4.4) and exogenously expressed netrin-1 is trafficked by KIF1A

(Figure 4.5). Upon discovering netrin-1's association with KIF1A, I confirmed its co-localization and co-transport with the KIF1A-dependent cargo Chromogranin (CHG) (Figure 4.6; Figure 4.7).

5.2. iPSC-derived neuron culturing

Compared to NGN2 derivation, small molecule-derived neurons produce cultures with more typical morphology and greater longevity *in vitro*. Neurons undergoing small molecule differentiation typically do not fasciculate and adopt a more characteristic neuronal morphology after 14 DIV (Figure 3.2; Kaneko & Sankai 2014). They follow developmental stages more similar to *in vivo* development, transitioning from iPSCs to NPCs before maturing into neurons. Alternatively, NGN2-based differentiation involves the transient expression of NGN2 in iPSCs (Zhang et al., 2013). Although NGN2 implementation is efficient, its transient expression via lentiviral transduction does not exactly follow the natural NGN2 expression pattern in progenitor cells. In the developing nervous system, NGN2 undergoes carefully coordinated upregulation and downregulation to promote proneuronal pathways throughout multiple stages of differentiation (Hume et al., 2022). These differences could possibly explain why NGN2-derived neurons are morphologically underdeveloped compared to small molecule-derived neurons, which more closely resemble cultured primary neurons (Figure 3.2; Nehme et al., 2018; Zhang et al., 2013). Methods may exist to mediate this difference, such as expressing NGN2 in NPCs, generating stably expressing cell lines to reduce heterogeneity caused by lentiviral transductions, or co-culturing with astrocytes. Although neither small molecule nor NGN2 differentiation can fully replicate the complexity of *in vivo* developmental factors and events, small molecule differentiation appears to be the preferred method (Figure 3.2; Figure 3.3).

Substrates provide specific structural and biochemical cues that may greatly affect culture development. Culturing iPSC-derived neurons on Matrigel produces more heterogeneous cultures (Figure 3.3). After several weeks in culture, non-neuronal cell types on Matrigel-coated cultures emerge and proliferate quickly. Because the composition of Matrigel is largely heterogeneous and undefined, cultures will interact

with multiple signalling factors and ligands such as Nidogens, type IV collagen, and heparan sulfate proteoglycans (Huang et al., 2020; Wrighton et al., 2014). Although Matrigel supports the differentiation of pluripotent cells into neurons (Uemura et al., 2010), it also promotes differentiation toward diverse cell fates such as cardiomyocytes and osteocytes (Burridge et al., 2014; Eslaminejad & Elham 2010). One alternative substrate option for neuron culturing is the combination of PLO and Laminin. This method is commonly used and known to enhance neuronal differentiation (Ge et al., 2015; Xiong et al., 2023). In my experiment, PLO and laminin were effective in reducing the presence of non-neuronal cell types (Figure 3.3). The differences in the development of these two culture types may be explained by the distinct signaling pathways triggered by different substrates.

The optimization of neuronal cultures is crucial for future experiments in mature neurons. Overtime, most cell cultures will become less viable with age, and neurons are especially vulnerable *in vitro* being postmitotic and highly sensitive to their environments (Baricevic et al., 2023; Millet & Gillete 2012). The monolayer culturing of neurons is a commonly used approach that provides a homogenous culture environment and allows for the imaging of individual cells. While monolayer cultures are less representative of *in vivo* conditions compared to 3-dimensional models or organoids, they are essential for my transfection and imaging experiments. One challenge with monolayer iPSC-derived neuron culturing is the tendency for cell bodies to clump and axons to fasciculate, particularly when the neurons are not thriving. This issue can be exacerbated by improper substrate choice and differentiation protocols, as observed with the NGN2 protocol and Matrigel (Figure 3.2; Figure 3.3). After identifying that cells perform more robustly with small molecule differentiation and PLO and Laminin substrates, they progressed through typical developmental stages (Figure 3.4; Banker 2018), with improved morphology and survival for subsequent imaging-based experiments. By 3 DIV, neurites began to develop and continued to elongate through 7-14 DIV. The neuronal marker β3-Tubulin showed increased expression over time and was uniformly localized within the cells (Figure 3.4). This developmental pattern is typical of previously described iPSC-derived neuron cultures (Lindhout et al., 2020). In conclusion, optimizing iPSC-derived neuron cultures

is essential for conducting reliable imaging experiments, and PLO and Laminin provided the optimal substrate for neuronal development.

5.3. Netrin-1 transport in human neurons

Bidirectionality is a hallmark of motor-based transport, and potentially necessary for proper DCV cargo processing. Netrin-1's bidirectional movement mirrors the behavior of other KIF1A transport (Figure 4.3; Lo et al., 2011; Lee et al., 2004; Maeder et al., 2013). While the exact reasons behind the bidirectional nature of organelle transport remain unclear, some evidence suggests this process is crucial for proper cargo processing. For instance, BDNF undergoes proteolytic cleavage from pro-BDNF within DCVs (Wang et al., 2021). Not only are BDNF and pro-BDNF both packaged into DCVs, evidence suggests that proteolytic cleavage of pro-BDNF occurs during transport (Nagappan et al., 2009; Dieni et al., 2012; Kowianski et al., 2018). Therefore, it is hypothesized that the bidirectional nature of intracellular transport allows time for the processing of cargo like pro-BDNF. Other KIF1A cargoes such as synapsin I also undergo similar post-Golgi modifications with disruptions in their processing contributing to synaptic disruption (Lanxia et al., 2022). While the intracellular post-Golgi modifications of netrin-1 have not been well characterized, evidence suggests that through development and maturation of the CNS, there may be changes in netrin-1 modifications such as with proteolysis and glycosylation (Manitt et al., 2001). Other DCV cargo have also been shown to experience age-dependent modifications such as the proteolytic cleavage of Synapsin I (Lanxia et al., 2022). Further study of intracellular netrin-1 processing is necessary to determine if bidirectional transport contributes to these mechanisms, however, this offers a potentially important layer of regulation in netrin-1 trafficking.

In addition to protein processing, bidirectional transport may be necessary for the proper delivery of cargo. Intracellular transport takes place in a crowded cytoplasm, with a complex microtubule network scoured with proteins and organelles that act as obstacles. The recruitment of antagonistic motors, such as kinesins and dynein, allows for bidirectional transport and to circumvent crowding and obstacles. Molecular motors

avoid obstacles with methods such as side-stepping along the microtubule lattice and rotating around cargoes (Mitra et al., 2019; Ferro et al., 2019), which require the recruitment of both kinesins and dynein (Hancock, 2014; Kaplan et al., 2018; Ferro et al., 2019). In addition to maneuvering around roadblocks, bidirectional transport may act as a proofreading mechanism. Like many biochemical processes in the cell, cargo capture is not guaranteed even if the motor-cargo complex is able to reach the destination. Therefore, bidirectional transport may compensate for this error rate by allowing for the cargo to pass the site of capture multiple times. As described in Ferro et al., 2019, this concept comes from other observations of saltatory motion in nature such as polymerase backstepping and error correction. The cytoplasmic environment is complex and the capture of DCVs and KIF1A is coordinated by many factors. Therefore, the somewhat random directionality and movement of cargo may work to circumvent the stochastic nature to cargo delivery.

In addition to its bidirectional nature, the velocity and run lengths of netrin-1 vesicles align with microtubule motor-based transport. The intracellular velocity and run lengths of a vesicle provide insight into its mode of travel. “Slow” axonal transport occurs at less than 0.1 μm/sec, while “fast” transport happens at over 0.5 μm/sec and is often powered by members of the kinesin-3 family, like KIF1A (Guedes-Dias et al., 2019). Netrin-1 transport velocity matches the characteristics of other known kinesin-dependent vesicle transport, particularly that of DCVs (Figure 4.3; Lo et al., 2011; Maeder et al., 2013; Chiba et al., 2019). The run lengths also exceed that of slow transport and are consistent with kinesin-based transport (Zaniewski et al., 2018). These findings are also consistent with the transport characteristics of other neuropeptides like neuropeptide Y and BDNF (Lo et al., 2011; Nassal et al., 2022). In the case of proteins like netrin-1, reliable and fast transport to release sites via kinesin molecular motors is essential to maintain function.

Netrin-1’s co-localization and co-transport with KIF1A suggests that KIF1A is a candidate motor responsible for Netrin-1 transport. After finding that netrin-1 likely relies on kinesin motor-based transport, determining the specific kinesin involved was necessary given the breadth and diversity of the kinesin superfamily (Figure 1.3). An

assessment of the endogenous co-localization of netrin-1 and KIF1A confirmed their association (Figure 4.4). The co-localization of KIF1A and netrin-1 mirror patterns seen with other KIF1A dependent cargoes such as neuropeptide Y and BDNF (Hummel & Hoogenraad 2021; Lo et al., 2011). Moreover, netrin-1 co-localization with UNC-104/KIF1A cargo has been confirmed in *C. elegans* (Ogura et al., 2012). Given that transport is a dynamic process, live cell analysis was next required to demonstrate netrin-1 and KIF1A's association. Using fluorescently tagged markers, I confirmed the co-transport of Netrin-1 and KIF1A (Figure 4.5). Furthermore, my observations of Netrin-1 transport velocity and run lengths are consistent with previous KIF1A transport analyses (Figure 4.3; Lo et al., 2011; Zaniewski et al., 2020). Given that the sorting of proteins to vesicles and motors follows tight regulation, these findings suggest that KIF1A is the primary motor responsible for netrin-1 transport. KIF1A's association with cargo relies on various processes such as adaptor protein interactions and calcium and calmodulin regulation (Hummel & Hoogenraad 2021; Stucchi et al., 2018). However, even though these mechanisms regulate cargo-motor specificity, a secondary kinesin type may also still contribute. Studies suggest that other kinesins such as KIF5 may work in tandem with KIF1A to transport vesicles (Gumy et al., 2017). Although the transport of a single vesicle type via multiple motors may be somewhat redundant, it is thought to act as a safeguard to balance KIF dysfunction (Ali & Yang 2020). In the case of netrin-1, which plays a diverse set of roles, multiple kinesins may be necessary to circumvent transport issues and maintain physiological activity. These findings not only underscore the significant role of KIF1A in netrin-1 transport but also open avenues for further investigation into its precise mechanisms.

Netrin-1's co-localization and co-transport with chromogranin (CHG) suggests that DCVs are the primary vesicle type responsible for housing netrin-1. CHG, a well-characterized resident protein of DCVs and transported by KIF1A, shows distinct endogenous overlap with Netrin-1 in ICC analysis, indicating that Netrin-1 resides in the same vesicle type (Figure 4.6). Moreover, CHG is excluded from other vesicle types such as SVPs (Graeme-Cook 2009) and plays a crucial role in DCV biogenesis (Pasqua et al., 2015). In addition to immunocytochemical analysis, live imaging demonstrates that Netrin-1 nearly completely co-transports with CHG (Figure 4.7). This overlap

significantly exceeds that of previously observed DCV cargoes such as Neuropeptide Y and synaptotagmin-4 which show only a 10% co-localization (Stucchi et al., 2018). Therefore, Netrin-1 co-transporting with CHG suggests that it is also primarily delegated to DCVs. The co-transport of exogenously expressed netrin-1 with CHG further supports its trafficking by KIF1A. DCVs primarily traffic via KIF1A (Lo et al., 2011), and loading onto KIF1A is regulated by calcium and calmodulin (Stucchi et al., 2018; Figure 5.1). Additionally, studies characterizing netrin-1 behaviour show the protein aligns with DCV function and physiological impact. DCVs originate from the endomembrane system, house neuropeptides, and release at synaptic sites upon high-frequency stimulation (Boosport et al., 2012; Farina et al., 2015). This release pattern mirrors that of netrin-1, which also requires high electrophysiological stimulation for secretion (Glasgow et al., 2018). DCVs are responsible for the transport of proteins like BDNF, neuropeptide Y, and synapotagmin-4, which participate in synapse formation and plasticity (Gabrych et al., 2019). To facilitate the function of these proteins, DCVs are delegated to synaptic sites. Not only has netrin-1 been observed to be released at synapses, it also underlies synaptic plasticity and is necessary for activity-dependent LTP (Glasgow et al., 2024). Therefore, the co-transport of netrin-1 and CHG within DCVs may account for netrin-1 synaptic release and regulation.

Netrin-1's localization via DCVs and KIF1A is a necessary preliminary step to its potential chemotropic and synaptic functions. Because netrin-1 is a secreted chemotropic cue, it requires supply to distal sites, necessitating active transport via motor proteins and the recruitment to release sites. DCVs reside predominantly in dendritic spines and presynaptic regions, containing various neuropeptides and neurotransmitters (Chiba et al., 2023; Tao et al., 2018). UNC104/KIF1A facilitates this DCV localization to synapses and the formation of synaptic buttons (Zhan et al., 2004; Pack-Chung et al., 2007). Netrin-1, a chemotactic cue, is secreted at synaptic sites and interacts with DCC at both pre- and post- synaptic sites (Glasgow et al., 2018; Glasgow et al., 2021). Because of its association to DCVs, netrin-1 is recruited to these synaptic sites through DCV and KIF1A capture mechanisms. KIF1A-driven DCVs are captured at dendritic spines through interactions with scaffolding proteins like liprin-α and TANC2 (Stucchi et al., 2018; Figure 5.1). Liprin-α is also necessary for presynaptic assembly and the capture of

KIF1A-dependent cargo (Marco de la Cruz et al., 2024). Other mechanisms have also been identified to contribute to DCV recruitment to synapses such as with JNK destabilization and synapsin mediation (Bharat et al., 2017; Yu et al., 2021). Once captured, the release of DCV is also carefully mediated through coordinated fusion mechanisms. DCVs fuse with the plasma membrane upon action-potential triggered calcium influx (Hartmann et al., 2001; Persoon et al., 2018). DCVs fuse in both axons and dendrites (Mastuda et al., 2009; Dean et al., 2009), with approximately 80% of fusion events occurring at the axon (Persoon et al., 2018). Despite prolonged electrophysiological stimulation, only up to 6% of DCVs are released (Persoon et al., 2018). This may be explained by the unique behaviour of DCVs. Compared to other vesicle types like synaptic vesicles, they are more mobile and potentially less likely to interact with regulatory proteins to trigger fusion. In mammalian neurons, various proteins such as dynamins, SNAP-25, and VAMP2 regulate DCV fusion (Moro et al., 2021; Van de Bospoort et al., 2012). With DCV fusion, its contents, including netrin-1 are released extracellularly. Netrin-1 can diffuse up to 250 μm, however, in the adult CNS the majority of secreted netrin-1 is bound to a component of the cell surface of the secreting or neighbouring cells (Manitt et al., 2001). This is concurrent with netrin-1 function as both a long-range and short-range cue. Netrin-1 can diffuse and act as long-range guidance cue (Boyer et al., 2018) while also having a paracrine effect with LTP and synaptogenesis (Glasgow et al., 2024; Goldman et al., 2013). Therefore, netrin-1 plays a crucial developmental and functional role in the nervous system facilitated by the transport and packaging into DCVs.

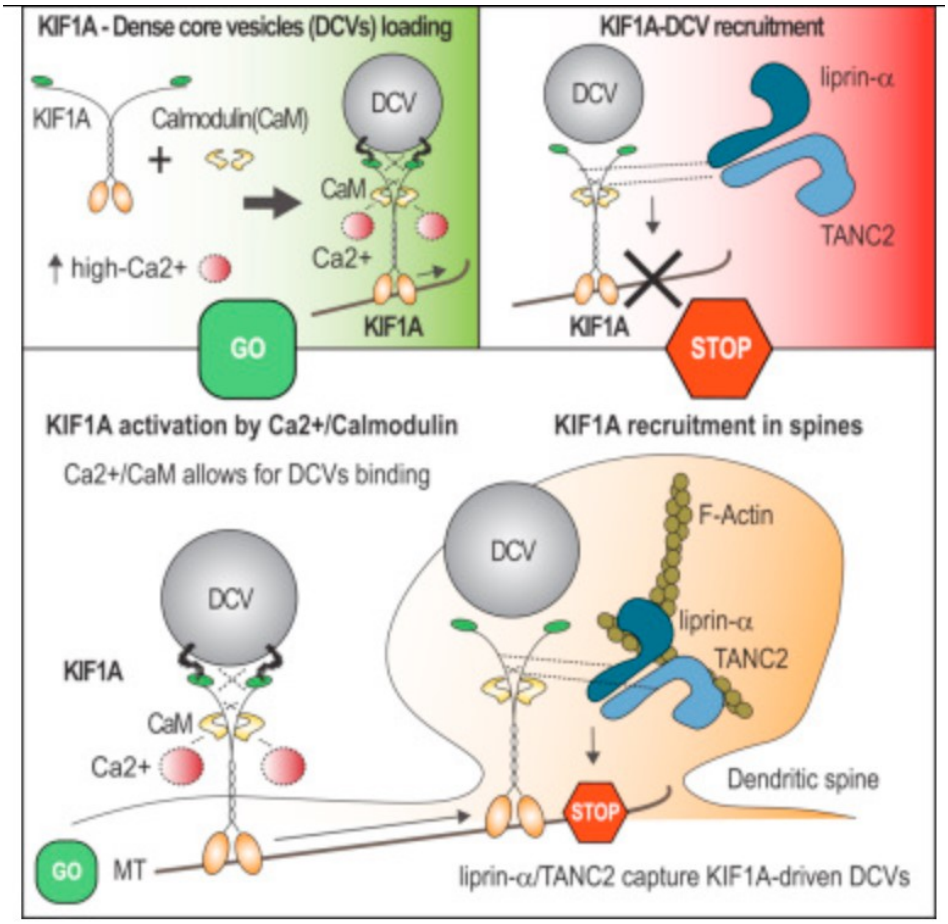

Figure 5.1 Regulation of DCV loading and recruitment
Representation of the regulation of dense core vesicle (DCV) loading to KIF1A in the presence of calcium (Ca2+) and calmodulin (CaM). Then, the motor-cargo complex is formed and reaches dendritic spines where liprin-α and tetratricopeptide repeat, ankyrin repeat and coiled-coil containing 2 (TANC2) recruit the KIF1A driven DCV to delivery sites (Stucchi et al., 2018).

5.4. Limitations

Reproducibility across cell lines and laboratories has been challenging in generating iPSC-derived neurons. The absence of biological replicates in my study limits possible assessments of variability (Dolmetsch & Geschwind, 2013). Variability may stem from several factors, such as incomplete reprogramming of iPSCs (Hu et al., 2010) and donor-to-donor heterogeneity in their genetic background. Molecular and functional analyses of iPSC-derived neurons have highlighted the impact of donor and culture variability on neuronal development (Schwartzentruber et al., 2017). While intracellular motor-based transport is generally conserved, other aspects of an individual's genetic

background can influence its function. Transport is regulated at multiple levels, including microtubule dynamics, motor recruitment, and cargo packaging (Lawrence et al., 2023). Although my thesis included technical replicates, the use of only one cell line to study netrin-1 transport precluded biological replicates. Unfortunately, repeating experiments across multiple cell lines within the timeframe of my degree was impractical due to the workload involved. Moreover, using multiple cell lines presents challenges because different lines exhibit varying capabilities in neuronal development (Knock & Julian, 2021). Large-scale variation analyses suggest that studying variants with substantial effects may require assessments across at least 20 different individual cell lines (Schwartzentruber et al., 2017). Therefore, while employing multiple cell lines could bolster the results, the associated workload posed a significant obstacle in this study.

Advancements in iPSC-derived neuron culturing continue to evolve to better represent human models, but technical challenges remain a barrier. In the human brain, neural stem cells receive spatiotemporal cues crucial for their development and function (Maldonado-Sato et al., 2014). Organoids and 3-dimensional iPSC-derived neuron cultures are gaining popularity because they better replicate architectural features of the human brain compared to monolayer cultures, mimicking CNS spatial organization and cell-ECM interactions (Yim et al., 2016). However, they introduce greater complexity due to varied culturing parameters such as with substrate stiffness, porosity, and pore size, which can influence cellular behavior (Zhang et al., 2014; Wang et al., 2010). While these methods offer many advantages, they add complexity in addressing the specific aims of my thesis. Currently, 2-dimensional monolayer cultures are optimal for live-cell transport analysis. Adopting a 3-dimensional model for iPSC-derived neuron development could be a promising direction, yet it would necessitate drastic changes to our current live-imaging. Conventional microscopy is limited with low light penetrance and small working distances, therefore moving towards techniques such as multiscale light-sheet microscopy (De Medeiros et al., 2022) is necessary for organoid imaging. Therefore, while incorporating a 3-dimensional model for iPSC-derived neurons holds potential benefits, it will require additional labor in adapting to our current experiments.

Netrin-1 traffics within DCVs via KIF1A, yet the involvement of other motor proteins and vesicle types in netrin-1 transport cannot be definitively ruled out. Dual-color live-imaging analysis indicated that significant portions of netrin-1 is transported by KIF1A. However, the portion of single netrin-1 transport events suggests that some netrin-1 did not co-transport with KIF1A (Figure 4.5). Similar levels of co-transport have been observed between other cargoes and KIF1A (Lo et al., 2011). It's plausible that the single netrin-1 transport events could still involve KIF1A, but may not have been detectable due to technical limitations. Firstly, it's likely that endogenous untagged KIF1A contributes to some of the netrin-1 movement. Typically, multiple motors are recruited to transport vesicles, and there could be a ratio of exogenous to endogenous KIF1A required for observable cargo movement. Secondly, since the number of kinesins attached to a cargo varies, it is possible that there were too few attached to be detectable in the single netrin-1 transport events. Thirdly, despite imaging in two dimensions, the axon's three-dimensional structure with its depth and complexity could influence the orientation of the motor-cargo complex during imaging. These factors may explain the discrepancies observed in netrin-1 transport. Additionally, considering the regulatory complexity of kinesin-motor complex assembly, it's possible that another kinesin could be involved in netrin-1 transport. Multiple kinesins are known to transport specific organelles and proteins (Hirokawa et al., 2009). Therefore, further investigation is necessary to conclusively determine if netrin-1 is exclusively trafficked by KIF1A. These limitations also apply to understanding DCV co-transport with netrin-1. Further research into the co-transport of netrin-1 with other vesicle markers is essential to comprehensively unravel netrin-1 transport mechanisms.

5.5. Future Directions

iPSC-derived neuron culturing could benefit significantly from integrating new techniques. One promising avenue I have yet to explore is combining small molecule differentiation with the NGN2 approach, which has proven successful in generating other types of neuronal models (Limone et al., 2022). Introducing NGN2 expression during the development of small molecule-derived neurons and selecting via puromycin resistance may enhance the homogeneity and reproducibility of the cultures. Moreover,

transitioning from traditional monolayer culturing to alternative methods could further enhance culture quality. For instance, the embryoid body method involves generating 3-dimensional cultures that simulate early embryo development (Liyang et al., 2014). Alternatively, I could incorporate a co-culture system with astrocytes (Hwang et al., 2022). Astrocytes are support cells in the central nervous system that maintain the extracellular environment and can contribute to *in vitro* neuronal differentiation. Although microtubule-based transport is generally conserved and unlikely affected by changes in culture method, adopting these alternative techniques has the potential to extend culture longevity and make improvements for experimentation.

I observed netrin-1 co-localization with endogenous KIF1A and CHG, however, additional investigation can bolster the evidence towards their co-localization and co-transport. Proximity ligation assays (PLA) are commonly used to assess the subcellular localization of endogenous proteins (Hegazy et al., 2020). The two endogenous proteins are first treated with primary antibodies, then enzyme-linked secondary antibodies are added and will lead to a fluorescent signal when the proteins are less than 40nm apart. DCVs are typically between 75-100nm in size, therefore, if the co-localization of cargoes such as netrin-1 and CGA is detected via PLA, then it can be assumed that they reside in the same vesicle. The addition of another biochemical assay such as by purifying DCVs and then probing for co-localization could also bolster findings (Kreutzberger et al., 2019). These assays can be repeated to assess netrin-1's association with a variety of DCV cargo. Additionally, PLA can be used as a negative control to assess netrin-1 co-localization with non-DCV or non-KIF1A cargoes such as Piccolo and Bassoon, two cargoes carried by KIF5 in piccolo and bassoon transport vesicles (Fejtova et al., 2009).

Further confirmation of netrin-1's dependence on KIF1A requires functional analysis. An shRNA knockdown of KIF1A would directly assess its necessity in netrin-1 transport and elucidate the potential utilization of other motor proteins. RNA interference (RNAi) has already been used to reduce KIF1A expression and assess its role in cargo transport (Lo et al., 2011). Following knockdown, characterization of netrin-1's localization and transport will reveal if KIF1A is the sole motor responsible for netrin-1 transport. If netrin-1 transport persists, it can be assumed that another motor protein is

responsible and can then be identified with further experimentation. Additionally, a KIF1A rescue experiment should act as a control and restore netrin-1 transport. As an alternative to RNAi, a CRISPR knockout can be used to silence KIF1A and assess the effects on netrin-1 transport. Parallel to RNAi and CRISPR knockouts, unc-104/KIF1A mutants offer insights into netrin-1 transport. Previous studies with unc-104 and KIF1A mutants reveal cargo misallocation (Anazawa et al., 2022; Chiba et al., 2019; Ogura et al., 2012). Analyzing netrin-1 distribution in unc-104/KIF1A mutants, followed by rescue experiments, can confirm netrin-1's transport by KIF1A and reveal transport disruption effects on essential protein localization.

In the process of vesicular transport, protein sorting hinges on sorting signals. Two models propose how cargoes sort to DCVs. The first, the “sorting by entry” model, sees cargoes enter nascent DCVs as they bud off the trans-Golgi network. The second, the “sorting by exit” model, removes unintended cargoes from DCVs as they mature (Cattin-Ortola et al., 2019). Both models contribute to DCV development and likely use sorting signals and proteins for cargo recruitment and retention. Sorting signals are often peptide chains that interact with sorting proteins to direct cargo to specific structures. For netrin-1, it may contain a sorting signal responsible for its DCV allocation. Other DCV cargoes rely on sorting signals for proper recruitment (Dikeakos & Reudelhuber 2007; Zhang et al., 2010). For example, proinsulin contains numerous domains involved in sorting to DCVs, such as a carboxypeptidase E binding domain and two protease cleavage sites (Cool & Loh 1998; Steiner et al., 1996). As netrin-1's case remains unstudied, sequence analysis could reveal known sorting domains which could then be confirmed experimentally.

5.6. Conclusion

These are novel characterizations of intracellular neuronal netrin-1 transport, offering the first insights into this process. I demonstrated the presence and punctate distribution of netrin-1 in human neurons, laying the groundwork for transport analyses. Then, I characterized the transport of exogenously expressed netrin-1, determined its velocity and run length, and demonstrated its "fast" bidirectional nature. I then identified

KIF1A and DCVs as the motor protein and transport vesicle responsible for netrin-1 transport. Netrin-1 dysfunction has been implicated in neurodegenerative diseases like Alzheimer's and Parkinson's disease. Netrin-1 also has neuroprotective effects and is necessary for memory and synaptic plasticity (Cai et al., 2024; Glasgow et al., 2021). Findings on netrin-1 trafficking are significant because intracellular transport plays a crucial role in regulating the function of proteins and organelles. In neurons, active intracellular transport is especially vital due to their unique morphology. Secreted netrin-1 requires precise transport to fulfill its functions. Therefore, understanding netrin-1 transport provides important context for its biological role.

Moreover, knowledge of netrin-1 transport is valuable in the context of transport and neurodegenerative disorders. By identifying netrin-1 as a KIF1A-dependent cargo, it has become relevant to KIF1A-associated neurological disorder (KAND). KAND patients have neurological and developmental issues and experience symptoms such as learning disability, spastic paraplegia, and seizures (Nair et al., 2023). Netrin-1 dysfunction has also been shown to have neurodevelopmental and neurodegenerative effects (Cai et al., 2024). Given that KAND disrupts KIF1A function, the improper localization and transport of KIF1A-dependent cargoes contribute to KAND symptoms. Because netrin-1 has now been identified as a KIF1A cargo, the improper delivery of netrin-1 may be a contributing factor to KAND phenotypes. Therefore, understanding netrin-1 transport mechanisms may contribute to the understanding of the disease and may suggest future therapeutic strategies.

References

Abraham, Z., Hawley, E., Hayosh, D., Webster-Wood, V. A., & Akkus, O. (2018). Kinesin and Dynein Mechanics: Measurement Methods and Research Applications. *Journal of Biomechanical Engineering*, *140*(2), 0208051–02080511. https://doi.org/10.1115/1.4037886

Ali, I., & Yang, W. C. (2020). The functions of kinesin and kinesin-related proteins in eukaryotes. *Cell adhesion & migration*, *14*(1), 139–152. https://doi.org/10.1080/19336918.2020.1810939

Ali, M. Y., Krementsova, E. B., Kennedy, G. G., Mahaffy, R., Pollard, T. D., Trybus, K. M., & Warshaw, D. M. (2007). Myosin Va maneuvers through actin intersections and diffuses along microtubules. *Proceedings of the National Academy of Sciences of the United States of America*, *104*(11), 4332–4336. https://doi.org/10.1073/pnas.0611471104

Allan, V. J. (2011). Cytoplasmic dynein. *Biochemical Society Transactions*, *39*(5), 1169–1178. Scopus. https://doi.org/10.1042/BST0391169

An, J., Chen, B., Tian, D., Guo, Y., Yan, Y., & Yang, H. (2022). Regulation of Neurogenesis and Neuronal Differentiation by Natural Compounds. *Current Stem Cell Research & Therapy*, *17*(8), 756–771. https://doi.org/10.2174/1574888X16666210907141447

Anazawa, Y., Kita, T., Iguchi, R., Hayashi, K., & Niwa, S. (2022). De novo mutations in KIF1A-associated neuronal disorder (KAND) dominant-negatively inhibit motor activity and axonal transport of synaptic vesicle precursors. *Proceedings of the National Academy of Sciences of the United States of America*, *119*(32). https://doi.org/10.1073/pnas.2113795119

Arakawa, H. (2004). Netrin-1 and its receptors in tumorigenesis. *Nature Reviews. Cancer*, *4*(12), 978–987. https://doi.org/10.1038/nrc1504

Avila, J., León-Espinosa, G., García, E., García-Escudero, V., Hernández, F., & DeFelipe, J. (2012). Tau Phosphorylation by GSK3 in Different Conditions. *International Journal of Alzheimer's Disease*, *2012*, 578373. https://doi.org/10.1155/2012/578373

Baas, P. W., Deitch, J. S., Black, M. M., & Banker, G. A. (1988). Polarity orientation of microtubules in hippocampal neurons: Uniformity in the axon and nonuniformity in the dendrite. *Proceedings of the National Academy of Sciences of the United States of America*, *85*(21), 8335–8339.

Banker, G. (2018). The Development of Neuronal Polarity: A Retrospective View. *Journal of Neuroscience*, *38*(8), 1867–1873. https://doi.org/10.1523/JNEUROSCI.1372-16.2018

Bathina, S., & Das, U. N. (2015). Brain-derived neurotrophic factor and its clinical implications. Archives of Medical Science : AMS, 11(6), 1164–1178. https://doi.org/10.5114/aoms.2015.56342

Bell, S., Hettige, N. C., Silveira, H., Peng, H., Wu, H., Jefri, M., Antonyan, L., Zhang, Y., Zhang, X., & Ernst, C. (2019a). Differentiation of Human Induced Pluripotent Stem Cells (iPSCs) into an Effective Model of Forebrain Neural Progenitor Cells and Mature Neurons. *Bio-Protocol*, *9*(5), e3188. https://doi.org/10.21769/BioProtoc.3188

Bharat, V., Siebrecht, M., Burk, K., Ahmed, S., Reissner, C., Kohansal-Nodehi, M., Steubler, V., Zweckstetter, M., Ting, J. T., & Dean, C. (2017). Capture of Dense Core Vesicles at Synapses by JNK-Dependent Phosphorylation of Synaptotagmin-4. *Cell Reports*, *21*(8), 2118–2133. https://doi.org/10.1016/j.celrep.2017.10.084

Boyle, L., Rao, L., Kaur, S., Fan, X., Mebane, C., Hamm, L., Thornton, A., Ahrendsen, J. T., Anderson, M. P., Christodoulou, J., Gennerich, A., Shen, Y., & Chung, W. K. (2021). Genotype and defects in microtubule-based motility correlate with clinical severity in KIF1A-associated neurological disorder. *HGG Advances*, *2*(2). https://doi.org/10.1016/j.xhgg.2021.100026

Bryantseva, S. A., & Zhapparova, O. N. (2012). Bidirectional transport of organelles: Unity and struggle of opposing motors. *Cell Biology International*, *36*(1), 1–6. https://doi.org/10.1042/CBI20110413

Burridge, P. W., Matsa, E., Shukla, P., Lin, Z. C., Churko, J. M., Ebert, A. D., Lan, F., Diecke, S., Huber, B., Mordwinkin, N. M., Plews, J. R., Abilez, O. J., Cui, B., Gold, J. D., & Wu, J. C. (2014). Chemically Defined and Small Molecule-Based Generation of Human Cardiomyocytes. *Nature Methods*, *11*(8), 855–860. https://doi.org/10.1038/nmeth.2999

Caccamo, D. V., Herman, M. M., Frankfurter, A., Katsetos, C. D., Collins, V. P., & Rubinstein, L. J. (1989). An immunohistochemical study of neuropeptides and neuronal cytoskeletal proteins in the neuroepithelial component of a spontaneous murine ovarian teratoma. Primitive neuroepithelium displays immunoreactivity for neuropeptides and neuron-associated beta-tubulin isotype. *The American journal of pathology, 135(5), 801–813.*

Cai. M., Zheng, Q., Chen, Y., Siyuan, L., Zhu, H., Bing, B. (2024). Insights from the neural guidance factor netrin-1 into neurodegeneration and other diseases. *Frontiers in Molecular Neuroscience,* 17. https://doi.org/10.3389/fnmol.2024.1379726

Carter, A. P., Diamant, A. G., & Urnavicius, L. (2016). How dynein and dynactin transport cargos: A structural perspective. *Current Opinion in Structural Biology*, *37*, 62–70. https://doi.org/10.1016/j.sbi.2015.12.003

Cattin-Ortolá, J., Topalidou, I., Lau, H.-T., Hummer, B., Asensio, C. S., Ong, S.-E., & Ailion, M. (2019). CCDC186 controls dense-core vesicle cargo sorting by exit. *bioRxiv.* https://doi.org/10.1101/616458

Centeno, E. G. Z., Cimarosti, H., Bithell A., (2018). 2D versus 3D human induced pluripotent stem cell-derived cultures for neurodegenerative disease modelling. *Molecular Degeneration.* 13(1), 27. https://www.ncbi.nlm.nih.gov/pmc/articles/PMC5964712/#CR71

Chandler, C. H., Chari, S., Tack, D., & Dworkin, I. (2014). Causes and Consequences of Genetic Background Effects Illuminated by Integrative Genomic Analysis. *Genetics*, 196(4), 1321–1336. https://doi.org/10.1534/genetics.113.159426

Chiba, K., Kita, T., Anazawa, Y., & Niwa, S. (2023). Insight into the regulation of axonal transport from the study of KIF1A-associated neurological disorder. *Journal of Cell Science*, *136*(5). https://doi.org/10.1242/jcs.260742

Chou, H., Mao, X., & Ying, M. (2023). Development of transcription factor-based strategies for neuronal differentiation from pluripotent stem cells. In E. D. Buttermore (Ed.), *Phenotyping of Human iPSC-derived Neurons* (pp. 73–96). Academic Press. https://doi.org/10.1016/B978-0-12-822277-5.00003-1

Ciesielski-Treska, J., Ulrich, G., Taupenot, L., Chasserot-Golaz, S., Corti, A., Aunis, D., & Bader, M. F. (1998). Chromogranin A induces a neurotoxic phenotype in brain microglial cells. *The Journal of Biological Chemistry*, 273(23), 14339–14346. https://doi.org/10.1074/jbc.273.23.14339

Combs, B., Mueller, R.L., Morfini, G., Brady, S.T., Kanaan, N.M. (2019). Tau and Axonal Transport Misregulation in Tauopathies. In Takashima, A., Wolozin, B., Buee, L. (Eds.) *Tau Biology. Advances in Experimental Medicine and Biology*, vol 1184. Springer, Singapore. https://doi.org/10.1007/978-981-32-9358-8_7

Conde, C., & Cáceres, A. (2009). Microtubule assembly, organization and dynamics in axons and dendrites. Nature Reviews. Neuroscience, 10(5), 319–332. https://doi.org/10.1038/nrn2631

Cushion, T. D., Leca, I., & Keays, D. A. (2023). MAPping tubulin mutations. *Frontiers in Cell and Developmental Biology*, 11, 1136699. https://doi.org/10.3389/fcell.2023.1136699

De la Torre, J. R., Höpker, V. H., Ming, G. L., Poo, M. M., Tessier-Lavigne, M., Hemmati-Brivanlou, A., & Holt, C. E. (1997). Turning of retinal growth cones in a netrin-1 gradient mediated by the netrin receptor DCC. *Neuron*, 19(6), 1211–1224. https://doi.org/10.1016/s0896-6273(00)80413-4

Dean, C., Liu, H., Dunning, F. M., Chang, P. Y., Jackson, M. B., & Chapman, E. R. (2009). Synaptotagmin-IV modulates synaptic function and long-term potentiation by regulating BDNF release. *Nature Neuroscience*, 12(6), 767–776. https://doi.org/10.1038/nn.2315

Dieni, S., Matsumoto, T., Dekkers, M., Rauskolb, S., Ionescu, M. S., Deogracias, R., Gundelfinger, E. D., Kojima, M., Nestel, S., Frotscher, M., & Barde, Y. A. (2012). BDNF and its pro-peptide are stored in presynaptic dense core vesicles in brain neurons. *The Journal of Cell Biology,* 196(6), 775–788. https://doi.org/10.1083/jcb.201201038

Dikeakos, J. D., & Reudelhuber, T. L. (2007). Sending proteins to dense core secretory granules: Still a lot to sort out. *The Journal of Cell Biology*, *177*(2), 191–196. https://doi.org/10.1083/jcb.200701024

Dolmetsch, R., & Geschwind, D. H. (2011). The human brain in a dish: The promise of iPSC-derived neurons. *Cell*, *145*(6), 831–834. https://doi.org/10.1016/j.cell.2011.05.034

Dotti, C., Sullivan, C., & Banker, G. (1988). The establishment of polarity by hippocampal neurons in culture. *The Journal of Neuroscience*, *8*(4), 1454–1468. https://doi.org/10.1523/JNEUROSCI.08-04-01454.1988

D'Souza, A. I., Grover, R., Monzon, G. A., Santen, L., & Diez, S. (2023). Vesicles driven by dynein and kinesin exhibit directional reversals without regulators. *Nature Communications*, *14*(1), 7532. https://doi.org/10.1038/s41467-023-42605-8

Duke, T. (2002). Push or pull? Teams of motor proteins have it both ways. *PNAS Commentary*, 99(10), 6521-6523. https://www.pnas.org/doi/full/10.1073/pnas.112200199

Emperador, Melero, J., Nadadhur, A. G., Schut, D., Weering, J. V., Heine, V. M., Toonen, R. F., & Verhage, M. (2017). Differential Maturation of the Two Regulated Secretory Pathways in Human iPSC-Derived Neurons. *Stem Cell Reports*, *8*(3), 659–672. https://doi.org/10.1016/j.stemcr.2017.01.019

Encalada, S. E., Szpankowski, L., Xia, C., & Goldstein, L. S. B. (2011). Stable kinesin and dynein assemblies drive the axonal transport of mammalian prion protein vesicles. *Cell*, *144*(4), 551–565. https://doi.org/10.1016/j.cell.2011.01.021

Endow, S. A. (1999). Determinants of molecular motor directionality. *Nature Cell Biology*, *1*(6), 163-167. https://doi.org/10.1038/14113

Baghaban Eslaminejad, M., Bagheri, F., & Zomorodian, E. (2010). Matrigel Enhances in vitro Bone Differentiation of Human Marrow-derived Mesenchymal Stem Cells. *Iranian Journal of Basic Medical Sciences*, *13*(1), 187-194. doi: 10.22038/ijbms.2010.5062

Farina, M., van de Bospoort, R., He, E., Persoon, C. M., van Weering, J. R., Broeke, J. H., Verhage, M., & Toonen, R. F. (2015). CAPS-1 promotes fusion competence of stationary dense-core vesicles in presynaptic terminals of mammalian neurons. *eLife*, 4, e05438. https://doi.org/10.7554/eLife.05438

Fernandopulle, M. S., Prestil, R., Grunseich, C., Wang, C., Gan, L., & Ward, M. E. (2018). Transcription Factor-Mediated Differentiation of Human iPSCs into Neurons. *Current Protocols in Cell Biology*, 79(1), e51. https://doi.org/10.1002/cpcb.51

Finci, L., Zhang, Y., Meijers, R., & Wang, J.-H. (2015). Signaling mechanism of the netrin-1 receptor DCC in axon guidance. *Progress in Biophysics and Molecular Biology*, 118(3), 153–160. https://doi.org/10.1016/j.pbiomolbio.2015.04.001

Gabrych, D. R., Lau, V. Z., Niwa, S., & Silverman, M. A. (2019). Going Too Far Is the Same as Falling Short: Kinesin-3 Family Members in Hereditary Spastic Paraplegia. *Frontiers in Cellular Neuroscience*, 13, 419. https://doi.org/10.3389/fncel.2019.00419

Gagliano, J., Walb, M., Blaker, B., Macosko, J. C., & Holzwarth, G. (2010). Kinesin velocity increases with the number of motors pulling against viscoelastic drag. *European Biophysics Journal: EBJ*, 39(5), 801–813. https://doi.org/10.1007/s00249-009-0560-8

Ge, H., Tan, L., Wu, P., Yin, Y., Liu, X., Meng, H., Cui, G., Wu, N., Lin, J., Hu, R., & Feng, H. (2015). Poly-L-ornithine promotes preferred differentiation of neural stem/progenitor cells via ERK signalling pathway. *Scientific Reports*, 5(1), 15535. https://doi.org/10.1038/srep15535

Geng, A., Qiu, R., Murai, K., Liu, J., Wu, X., Zhang, H., Farhoodi, H., Duong, N., Jiang, M., Yee, J., Tsark, W., & Lu, Q. (2018). KIF20A/MKLP2 regulates the division modes of neural progenitor cells during cortical development. Nature Communications, 9(1), 2707. https://doi.org/10.1038/s41467-018-05152-1

Gennerich, A., & Vale, R. D. (2009). Walking the walk: How kinesin and dynein coordinate their steps. *Current Opinion in Cell Biology*, 21(1), 59–67. https://doi.org/10.1016/j.ceb.2008.12.002

Gilbert, S. P., Webb, M. R., Brune, M., & Johnson, K. A. (1995). Pathway of processive ATP hydrolysis by kinesin. *Nature*, 373, 671–676. https://doi.org/10.1038/373671a0

Glasgow, S. D., Fisher, T. A. J., Wong, E. W., Lançon, K., Feighan, K. M., Beamish, I. V., Gibon, J., Séguéla, P., Ruthazer, E. S., & Kennedy, T. E. (2024). Acetylcholine synergizes with netrin-1 to drive persistent firing in the entorhinal cortex. *Cell Reports*, 43(2). https://doi.org/10.1016/j.celrep.2024.113812

Glasgow, S. D., Labrecque, S., Beamish, I. V., Aufmkolk, S., Gibon, J., Han, D., Harris, S. N., Dufresne, P., Wiseman, P. W., McKinney, R. A., Séguéla, P., De Koninck, P., Ruthazer, E. S., & Kennedy, T. E. (2018). Activity-Dependent Netrin-1 Secretion Drives Synaptic Insertion of GluA1-Containing AMPA Receptors in the Hippocampus. *Cell Reports*, 25(1), 168-182.e6. https://doi.org/10.1016/j.celrep.2018.09.028

Glasgow, S. D., Ruthazer, E. S., & Kennedy, T. E. (2021). Guiding synaptic plasticity: Novel roles for netrin-1 in synaptic plasticity and memory formation in the adult brain. *The Journal of physiology*, *599*(2), 493–505. https://doi.org/10.1113/JP278704

Glomb, O., Swaim, G., LLancao, P. M., Lovejoy, C., Sutradhar, S., Park, J., Wu, Y., Cason, S. E., Holzbaur, E. L. F., Hammarlund, M., Howard, J., Ferguson, S. M., Gramlich, M. W., & Yogev, S. (2023). A kinesin-1 adaptor complex controls bimodal slow axonal transport of spectrin in Caenorhabditis elegans. *Developmental Cell*, 58(19), 1847-1863. https://doi.org/10.1016/j.devcel.2023.08.031

Goldman, J. S., Ashour, M. A., Magdesian, M. H., Tritsch, N. X., Harris, S. N., Christofi, N., Chemali, R., Stern, Y. E., Thompson-Steckel, G., Gris, P., Glasgow, S. D., Grutter, P., Bouchard, J.-F., Ruthazer, E. S., Stellwagen, D., & Kennedy, T. E. (2013). Netrin-1 Promotes Excitatory Synaptogenesis between Cortical Neurons by Initiating Synapse Assembly. *Journal of Neuroscience*, 33(44), 17278–17289. https://doi.org/10.1523/JNEUROSCI.1085-13.2013

Goldschneider, D., & Mehlen, P. (2010). Dependence receptors: A new paradigm in cell signaling and cancer therapy. *Oncogene*, 29(13), 1865–1882. https://doi.org/10.1038/onc.2010.13

Goodson, H. V., & Jonasson, E. M. (2018). Microtubules and Microtubule-Associated Proteins. *Cold Spring Harbor Perspectives in Biology*, 10(6) https://doi.org/10.1101/cshperspect.a022608

Graeme-cook, F. (2009). Neuroendocrine Tumors of the GI Tract and Appendix. In R. D. Odze & J. R. Goldblum (Eds.), *Surgical Pathology of the GI Tract, Liver, Biliary Tract, and Pancreas* (pp. 653–680). W.B. Saunders. https://doi.org/10.1016/B978-141604059-0.50028-X

Gumy, L. F., Katrukha, E. A., Grigoriev, I., Jaarsma, D., Kapitein, L. C., Akhmanova, A., & Hoogenraad, C. C. (2017). MAP2 Defines a Pre-axonal Filtering Zone to Regulate KIF1- versus KIF5-Dependent Cargo Transport in Sensory Neurons. *Neuron*, *94*(2), 347–362.e7. https://doi.org/10.1016/j.neuron.2017.03.046

Hagiwara, H., Yorifuji, H., Sato-Yoshitake, R., & Hirokawa, N. (1994). Competition between motor molecules (kinesin and cytoplasmic dynein) and fibrous microtubule-associated proteins in binding to microtubules. *Journal of Biological Chemistry*, 269(5), 3581–3589. https://doi.org/10.1016/S0021-9258(17)41903-X

Hall, D. H., & Hedgecock, E. M. (1991). Kinesin-related gene unc-104 is required for axonal transport of synaptic vesicles in C. elegans. *Cell*, 65(5), 837–847. https://doi.org/10.1016/0092-8674(91)90391-b

Hammond, J. W., Blasius, T. L., Soppina, V., Cai, D., & Verhey, K. J. (2010). Autoinhibition of the kinesin-2 motor KIF17 via dual intramolecular mechanisms. *The Journal of Cell Biology*, 189(6), 1013–1025. https://doi.org/10.1083/jcb.201001057

Hammond, J. W., Cai, D., Blasius, T. L., Li, Z., Jiang, Y., Jih, G. T., Meyhofer, E., & Verhey, K. J. (2009). Mammalian Kinesin-3 motors are dimeric in vivo and move by processive motility upon release of autoinhibition. *PLoS Biology*, 7(3), 72. https://doi.org/10.1371/journal.pbio.1000072

Hancock, W. O. (2014a). Bidirectional cargo transport: Moving beyond tug-of-war. *Nature Reviews. Molecular Cell Biology*, 15(9), 615–628. https://doi.org/10.1038/nrm3853

Harada, A., Teng, J., Takei, Y., Oguchi, K., & Hirokawa, N. (2002). MAP2 is required for dendrite elongation, PKA anchoring in dendrites, and proper PKA signal transduction. *The Journal of Cell Biology*, 158(3), 541–549. https://doi.org/10.1083/jcb.200110134

Hartmann, M., Heumann, R., & Lessmann, V. (2001). Synaptic secretion of BDNF after high-frequency stimulation of glutamatergic synapses. *The EMBO Journal*, 20(21), 5887–5897. https://doi.org/10.1093/emboj/20.21.5887

Hastings, J. F., Skhinas, J. N., Fey, D., Croucher, D. R., & Cox, T. R. (2019). The extracellular matrix as a key regulator of intracellular signalling networks. *British Journal of Pharmacology*, 176(1), 82–92. https://doi.org/10.1111/bph.14195

Hendricks, A. G., Perlson, E., Ross, J. L., Schroeder, H. W., Tokito, M., & Holzbaur, E. L. F. (2010). Motor coordination via a tug-of-war mechanism drives bidirectional vesicle transport. *Current Biology,* 20(8), 697–702. https://doi.org/10.1016/j.cub.2010.02.058

Hiranuma, M., Okuda, Y., Fujii, Y., Richard, J.-P., & Watanabe, T. (2024). Characterization of human iPSC-derived sensory neurons and their functional assessment using multi electrode array. *Scientific Reports*, 14(1), 6011. https://doi.org/10.1038/s41598-024-55602-8

Hirokawa, N., Niwa, S., & Tanaka, Y. (2010). Molecular motors in neurons: Transport mechanisms and roles in brain function, development, and disease. *Neuron*, 68(4), 610–638. https://doi.org/10.1016/j.neuron.2010.09.039

Hirokawa, N., Noda, Y., Tanaka, Y., & Niwa, S. (2009). Kinesin superfamily motor proteins and intracellular transport. *Nature Reviews Molecular Cell Biology*, 10(10), 682–696. https://doi.org/10.1038/nrm2774

Hirokawa, N., & Tanaka, Y. (2015). Kinesin superfamily proteins (KIFs): Various functions and their relevance for important phenomena in life and diseases. *Experimental Cell Research*, 334(1), 16–25. https://doi.org/10.1016/j.yexcr.2015.02.016

Hom, E. F. Y., Witman, G. B., Harris, E. H., Dutcher, S. K., Kamiya, R., Mitchell, D. R., Pazour, G. J., Porter, M. E., Sale, W. S., Wirschell, M., Yagi, T., & King, S. M. (2011). A Unified Taxonomy for Ciliary Dyneins. *Cytoskeleton,* 68(10), 555–565. https://doi.org/10.1002/cm.20533

Horn, K. E., Glasgow, S. D., Gobert, D., Bull, S. J., Luk, T., Girgis, J., Tremblay, M. E., McEachern, D., Bouchard, J. F., Haber, M., Hamel, E., Krimpenfort, P., Murai, K. K., Berns, A., Doucet, G., Chapman, C. A., Ruthazer, E. S., & Kennedy, T. E. (2013). DCC expression by neurons regulates synaptic plasticity in the adult brain. *Cell reports,* 3(1), 173–185. *https://doi.org/10.1016/j.celrep.2012.12.005*

Hsu, C.-C., Moncaleano, J. D., & Wagner, O. I. (2011). Sub-cellular distribution of UNC-104(KIF1A) upon binding to adaptors as UNC-16(JIP3), DNC-1(DCTN1/Glued) and SYD-2(Liprin-α) in C. elegans neurons. *Neuroscience*, 176, 39–52. https://doi.org/10.1016/j.neuroscience.2010.12.044

Hu, B.-Y., Weick, J. P., Yu, J., Ma, L.-X., Zhang, X. Q., Thomson, J. A., & Zhang, S. C. (2010). Neural differentiation of human induced pluripotent stem cells follows developmental principles but with variable potency. *Proceedings of the National Academy of Sciences of the United States of America*, 107(9), 4335–4340. https://doi.org/10.1073/pnas.0910012107

Huang, J., Jiang, Y., Ren, Y., Liu, Y., Wu, X., Li, Z., & Ren, J. (2020). Biomaterials and biosensors in intestinal organoid culture, a progress review. *Journal of Biomedical Materials Research Part A*, 108(7), 1501–1508. https://doi.org/10.1002/jbm.a.36921

Hulme, A. J., Maksour, S., St-Clair Glover, M., Miellet, S., & Dottori, M. (2021). Making neurons, made easy: The use of Neurogenin-2 in neuronal differentiation. *Stem Cell Reports*, 17(1), 14–34. https://doi.org/10.1016/j.stemcr.2021.11.015

Hummel, J. J. A., & Hoogenraad, C. C. (2021). Specific KIF1A-adaptor interactions control selective cargo recognition. *The Journal of Cell Biology*, 220(10). https://doi.org/10.1083/jcb.202105011

Jain, D., Mattiassi, S., Goh, E. L., & Yim, E. K. F. (2019). Extracellular matrix and biomimetic engineering microenvironment for neuronal differentiation. *Neural Regeneration Research*, 15(4), 573–585. https://doi.org/10.4103/1673-5374.266907

Jiang, X., Ogawa, T., Yonezawa, K., Shimizu, N., Ichinose, S., Uchihashi, T., Nagaike, W., Moriya, T., Adachi, N., Kawasaki, M., Dohmae, N., Senda, T., & Hirokawa, N. (2023). The two-step cargo recognition mechanism of heterotrimeric kinesin. EMBO Reports, 24(11), e56864. https://doi.org/10.15252/embr.202356864

Jordan, M. A., & Wilson, L. (2004). Microtubules as a target for anticancer drugs. *Nature Reviews. Cancer*, *4*(4), 253–265. https://doi.org/10.1038/nrc1317

Kanai, Y., Okada, Y., Tanaka, Y., Harada, A., Terada, S., Hirokawa, S., (2000). KIF5C, a Novel Neuronal Kinesin Enriched in Motor Neurons. Journal of Neuroscience, 20(17), 6374-6384. https://www.jneurosci.org/content/20/17/6374

Kang S., Chen X., Gong S., Yu P., Yau S., Su Z., Libing Z., Yu J., Pan G,. Shi L. (2017). Characteristic analyses of a neural differentiation model from iPSC-derived neuron according to morphology, physiology, and global gene expression pattern. *Scientific Reports*. https://doi.org/10.1038/s41598-017-12452-x

Kaplan, L., Ierokomos, A., Chowdary, P., Bryant, Z., & Cui, B. (2018). Rotation of endosomes demonstrates coordination of molecular motors during axonal transport. *Science Advances*, 4(3). https://doi.org/10.1126/sciadv.1602170

Karasmanis, E. P., Phan, C.-T., Angelis, D., Kesisova, I. A., Hoogenraad, C. C., McKenney, R. J., & Spiliotis, E. T. (2018). Polarity of Neuronal Membrane Traffic Requires Sorting of Kinesin Motor Cargo during Entry into Dendrites by a Microtubule-Associated Septin. Developmental Cell, 46(2), 204-218.e7. https://doi.org/10.1016/j.devcel.2018.06.013

Keefe, A. J. (2022). *Axonal transport of lysosomes in glucocerebrosidase-deficient iPSC-derived neurons*. Simon Fraser University. https://summit.sfu.ca/item/34964

Kelliher, M. T., Yue, Y., Ng, A., Kamiyama, D., Huang, B., Verhey, K. J., & Wildonger, J. (2018). Autoinhibition of kinesin-1 is essential to the dendrite-specific localization of Golgi outposts. *The Journal of Cell Biology*, 217(7), 2531–2547. https://doi.org/10.1083/jcb.201708096

Kim, D., Kim, C.-H., Moon, J.-I., Chung, Y.-G., Chang, M.-Y., Han, B.-S., Ko, S., Yang, E., Cha, K. Y., Lanza, R., & Kim, K.-S. (2009). Generation of Human Induced Pluripotent Stem Cells by Direct Delivery of Reprogramming Proteins. *Cell Stem Cell*, 4(6), 472–476. https://doi.org/10.1016/j.stem.2009.05.005

Kim, J. H., & Huganir, R. L. (1999). Organization and regulation of proteins at synapses. *Current Opinion in Cell Biology*, 11(2), 248–254. https://doi.org/10.1016/s0955-0674(99)80033-7

Kim, T., Tao-Cheng, J.-H., Eiden, L. E., & Loh, Y. P. (2001). Chromogranin A, an "On/Off" Switch Controlling Dense-Core Secretory Granule Biogenesis. *Cell*, 106(4), 499–509. https://doi.org/10.1016/S0092-8674(01)00459-7

Klopfenstein, D. R., & Vale, R. D. (2004). The lipid binding pleckstrin homology domain in UNC-104 kinesin is necessary for synaptic vesicle transport in Caenorhabditis elegans. *Molecular Biology of the Cell*, 15(8), 3729–3739. https://doi.org/10.1091/mbc.e04-04-0326

Kon, T., Nishiura, M., Ohkura, R., Toyoshima, Y. Y., & Sutoh, K. (2004). Distinct functions of nucleotide-binding/hydrolysis sites in the four AAA modules of cytoplasmic dynein. *Biochemistry*, 43(35), 11266–11274. https://doi.org/10.1021/bi048985a

Kredel, S., Oswald, F., Nienhaus, K., Deuschle, K., Röcker, C., Wolff, M., Heilker, R., Nienhaus, G. U., & Wiedenmann, J. (2009). mRuby, a Bright Monomeric Red Fluorescent Protein for Labeling of Subcellular Structures. PLoS ONE, 4(2), e4391. https://doi.org/10.1371/journal.pone.0004391

Lanxia, M., Zou, L., Xiong, M., Chen, J., Zhang, X., Yu, T., Li, Y., Liu, C., Chen, G., Wang, Z., Ye, K., & Zhang, Z. (2022). A synapsin I cleavage fragment contributes to synaptic dysfunction in Alzheimer's disease. *Aging Cell*, 21. https://doi.org/10.1111/acel.13619

Lasek, R. J., Garner, J. A., Brady, S. T. (1984). Axonal transport of the cytoplasmic matrix. *Journal of Cell Biology,* 99(1), 212–221.

Leduc, C., Padberg-Gehle, K., Varga, V., Helbing, D., Diez, S., & Howard, J. (2012). Molecular crowding creates traffic jams of kinesin motors on microtubules. *Proceedings of the National Academy of Sciences*, 109(16), 6100–6105. https://doi.org/10.1073/pnas.1107281109

Lee, M. C. S., Miller, E. A., Goldberg, J., Orci, L., & Schekman, R. (2004). Bi-directional protein transport between the ER and Golgi. *Annual Review of Cell and Developmental Biology*, 20, 87–123. https://doi.org/10.1146/annurev.cellbio.20.010403.105307

Liewald, D., Miller, R., Logothetis, N., Wagner, H.-J., & Schüz, A. (2014). Distribution of axon diameters in cortical white matter: An electron-microscopic study on three human brains and a macaque. *Biological Cybernetics*, 108(5), 541–557. https://doi.org/10.1007/s00422-014-0626-2

Limone, F., Mitchell, J. M., Juan, I. G. S., Smith, J. L. M., Raghunathan, K., Couto, A., Ghosh, S. D., Meyer, D., Mello, C. J., Nemesh, J., Smith, B. M., McCarroll, S., Pietiläinen, O., Nehme, R., & Eggan, K. (2022). Efficient generation of lower induced Motor Neurons by coupling Ngn2 expression with developmental cues. *bioRxiv.* https://doi.org/10.1101/2022.01.12.476020

Lin, Z., Li, Y., Hang, Y., Wang, C., Liu, B., Li, J., Yin, L., Jiang, X., Du, X., Qiao, Z., Zhu, F., Zhang, Z., Zhang, Q., & Zhou, Z. (2022). Tuning the Size of Large Dense-Core Vesicles and Quantal Neurotransmitter Release via Secretogranin II Liquid–Liquid Phase Separation. *Advanced Science*, 9(27), 2202263. https://doi.org/10.1002/advs.202202263

Lindhout, F. W., Kooistra, R., Portegies, S., Herstel, L. J., Stucchi, R., Snoek, B. L., Altelaar, A. M., MacGillavry, H. D., Wierenga, C. J., & Hoogenraad, C. C. (2020). Quantitative mapping of transcriptome and proteome dynamics during polarization of human iPSC-derived neurons. *eLife*, 9, e58124. https://doi.org/10.7554/eLife.58124

Liu, D., Pavathuparambil Abdul Manaph, N., Al-Hawwas, M., Bobrovskaya, L., Xiong, L.-L., & Zhou, X.-F. (2020). Coating Materials for Neural Stem/Progenitor Cell Culture and Differentiation. *Stem Cells and Development*, 29(8), 463–474. https://doi.org/10.1089/scd.2019.0288

Liyang, G., Abdullah, S., Rosli, R., & Nordin, N. (2014). Neural Commitment of Embryonic Stem Cells through the Formation of Embryoid Bodies (EBs). *The Malaysian Journal of Medical Sciences: MJMS*, 21(5), 8–16.

Lo, K. Y., Kuzmin, A., Unger, S. M., Petersen, J. D., & Silverman, M. A. (2011). KIF1A is the primary anterograde motor protein required for the axonal transport of dense-core vesicles in cultured hippocampal neurons. *Neuroscience Letters*, 491(3), 168–173. https://doi.org/10.1016/j.neulet.2011.01.018

Lourenço, F. C., Galvan, V., Fombonne, J., Corset, V., Llambi, F., Müller, U., Bredesen, D. E., & Mehlen, P. (2009). Netrin-1 interacts with amyloid precursor protein and regulates amyloid-β production. *Cell Death & Differentiation*, 16(5), 655–663. https://doi.org/10.1038/cdd.2008.191

Maeder, C. I., San-Miguel, A., Wu, E. Y., Lu, H., & Shen, K. (2014). In Vivo Neuron-Wide Analysis of Synaptic Vesicle Precursor Trafficking. *Traffic*, 15(3), 273–291. https://doi.org/10.1111/tra.12142

Manitt, C., Colicos, M. A., Thompson, K. M., Rousselle, E., Peterson, A. C., & Kennedy, T. E. (2001). Widespread Expression of Netrin-1 by Neurons and Oligodendrocytes in the Adult Mammalian Spinal Cord. *The Journal of Neuroscience*, 21(11), 3911–3922. https://doi.org/10.1523/JNEUROSCI.21-11-03911.2001

Marcó de la Cruz, B., Campos, J., Molinaro, A., Xie, X., Jin, G., Wei, Z., Acuna, C., & Sterky, F. H. (2024). Liprin-α proteins are master regulators of human presynapse assembly. *Nature Neuroscience*, 27(4), 629–642. https://doi.org/10.1038/s41593-024-01592-9

Martínez-Cerdeño, V., & Noctor, S. C. (2018). Neural Progenitor Cell Terminology. *Frontiers in neuroanatomy*, *12*, 104. https://doi.org/10.3389/fnana.2018.00104

Marx, A., Hoenger, A., & Mandelkow, E. (2009). Structures of Kinesin Motor Proteins. *Cell Motility and the Cytoskeleton*, 66(11), 958–966. https://doi.org/10.1002/cm.20392

Mattar, P., Langevin, L. M., Markham, K., Klenin, N., Shivji, S., Zinyk, D., & Schuurmans, C. (2008). Basic Helix-Loop-Helix Transcription Factors Cooperate To Specify a Cortical Projection Neuron Identity. *Molecular and Cellular Biology*, 28(5), 1456–1469. https://doi.org/10.1128/MCB.01510-07

Mehlen, P., & Fearon, E. R. (2004). Role of the dependence receptor DCC in colorectal cancer pathogenesis. *Journal of Clinical Oncology: Official Journal of the American Society of Clinical Oncology*, 22(16), 3420–3428. https://doi.org/10.1200/JCO.2004.02.019

Merighi, A. (2018). Costorage of High Molecular Weight Neurotransmitters in Large Dense Core Vesicles of Mammalian Neurons. *Frontiers in Cellular Neuroscience*, 12. https://doi.org/10.3389/fncel.2018.00272

Miki, H., Setou, M., Kaneshiro, K., & Hirokawa, N. (2001). All kinesin superfamily protein, KIF, genes in mouse and human. *Proceedings of the National Academy of Sciences of the United States of America*, 98(13), 7004–7011. https://doi.org/10.1073/pnas.111145398

Milky, B., Zabolocki, M., Al-Bataineh, S. A., van den Hurk, M., Greenberg, Z., Turner, L., Mazzachi, P., Williams, A., Illeperuma, I., Adams, R., Stringer, B. W., Ormsby, R., Poonnoose, S., Smith, L. E., Krasowska, M., Whittle, J. D., Simula, A., & Bardy, C. (2022). Long-term adherence of human brain cells *in vitro* is enhanced by charged amine-based plasma polymer coatings. *Stem Cell Reports*, 17(3), 489–506. https://doi.org/10.1016/j.stemcr.2022.01.013

Millet, L. J., & Gillette, M. U. (2012). Over a century of neuron culture: from the hanging drop to microfluidic devices. *The Yale journal of biology and medicine*, *85*(4), 501–521.

Moore, S. W., Tessier-Lavigne, M., & Kennedy, T. E. (2007). Netrins and Their receptors. In D. Bagnard (Ed.), *Axon Growth and Guidance* (pp. 17–31). Springer. https://doi.org/10.1007/978-0-387-76715-4_2

Mortimer, D., Fothergill, T., Pujic, Z., Richards, L. J., & Goodhill, G. J. (2008). Growth cone chemotaxis. *Trends in Neurosciences*, 31(2), 90–98. https://doi.org/10.1016/j.tins.2007.11.008

Mukherjee, A., Brooks, S., Bernard, F., Guichet, A., Conduit, P. (2020). Microtubules originate asymmetrically at the somatic golgi and are guided via Kinesin2 to maintain polarity within neurons. eLife. from https://elifesciences.org/articles/58943

Nagappan, G., Zaitsev, E., Senatorov, V. V., Yang, J., Hempstead, B. L., & Lu, B. (2009). Control of extracellular cleavage of ProBDNF by high frequency neuronal activity. *Proceedings of the National Academy of Sciences of the United States of America*, 106(4), 1267–1272. https://doi.org/10.1073/pnas.0807322106

Nair, A., Greeny, A., Rajendran, R., Abdelgawad, M. A., Ghoneim, M. M., Raghavan, R. P., Sudevan, S. T., Mathew, B., & Kim, H. (2023). KIF1A-Associated Neurological Disorder: An Overview of a Rare Mutational Disease. *Pharmaceuticals*, 16(2), 147. https://doi.org/10.3390/ph16020147

Nakata, T., & Hirokawa, N. (2003). Microtubules provide directional cues for polarized axonal transport through interaction with kinesin motor head. *The Journal of Cell Biology*, 162(6), 1045–1055. https://doi.org/10.1083/jcb.200302175

Nakashiba, T., Ikeda, T., Nishimura, S., Tashiro, K., Honjo, T., Culotti, J. G., & Itohara, S. (2000). Netrin-G1: a novel glycosyl phosphatidylinositol-linked mammalian netrin that is functionally divergent from classical netrins. *The Journal of Neuroscience*, 20(17), 6540–6550. https://doi.org/10.1523/JNEUROSCI.20-17-06540.2000

Niwa, S., Tanaka, Y., & Hirokawa, N. (2008). KIF1Bbeta- and KIF1A-mediated axonal transport of presynaptic regulator Rab3 occurs in a GTP-dependent manner through DENN/MADD. *Nature Cell Biology*, 10(11), 1269–1279. https://doi.org/10.1038/ncb1785

Ogura, K.-i., Asakura, T. and Goshima, Y. (2012), Localization mechanisms of the axon guidance molecule UNC-6/Netrin and its receptors, UNC-5 and UNC-40, in *Caenorhabditis elegans*. *Development, Growth and Differentiation*, 54, 390-397. https://doi.org/10.1111/j.1440-169X.2012.01349.x

Okada, Y., & Hirokawa, N. (1999). A processive single-headed motor: Kinesin superfamily protein KIF1A. *Science,* 283(5405), 1152–1157. https://doi.org/10.1126/science.283.5405.1152

Pack-Chung, E., Kurshan, P. T., Dickman, D. K., & Schwarz, T. L. (2007). A Drosophila kinesin required for synaptic bouton formation and synaptic vesicle transport. *Nature Neuroscience*, 10(8), 980–989. https://doi.org/10.1038/nn1936

Page, S. C., Sripathy, S. R., Farinelli, F., Ye, Z., Wang, Y., Hiler, D. J., Pattie, E. A., Nguyen, C. V., Tippani, M., Moses, R. L., Chen, H.-Y., Tran, M. N., Eagles, N. J., Stolz, J. M., Catallini, J. L., Soudry, O. R., Dickinson, D., Berman, K. F., Apud, J. A., … Maher, B. J. (2022). Electrophysiological measures from human iPSC-derived neurons are associated with schizophrenia clinical status and predict individual cognitive performance. *Proceedings of the National Academy of Sciences*, 119(3), e2109395119. https://doi.org/10.1073/pnas.2109395119

Park, J. J., Cawley, N. X., & Loh, Y. P. (2008). A bi-directional carboxypeptidase E-driven transport mechanism controls BDNF vesicle homeostasis in hippocampal neurons. *Molecular and Cellular Neurosciences*, 39(1), 63–73. https://doi.org/10.1016/j.mcn.2008.05.016

Park, K. W., Urness, L. D., Senchuk, M. M., Colvin, C. J., Wythe, J. D., Chien, C.-B., & Li, D. Y. (2005). Identification of New Netrin Family Members in Zebrafish: Developmental Expression of netrin2 and netrin4. *Developmental Dynamics: An Official Publication of the American Association of Anatomists*, 234(3), 726–731. https://doi.org/10.1002/dvdy.20474

Pasqua, T., Mahata, S., Bandyopadhyay, G. K., Biswas, A., Perkins, G. A., Sinha-Hikim, A. P., Goldstein, D. S., Eiden, L. E., & Mahata, S. K. (2016). Impact of Chromogranin A deficiency on catecholamine storage, catecholamine granule morphology and chromaffin cell energy metabolism in vivo. *Cell and Tissue Research*, 363(3), 693–712. https://doi.org/10.1007/s00441-015-2316-3

Passaniti, A., Kleinman, H. K., & Martin, G. R. (2022). Matrigel: History/background, uses, and future applications. *Journal of Cell Communication and Signaling*, 16(4), 621–626. https://doi.org/10.1007/s12079-021-00643-1

Perea, G., Navarrete, M., & Araque, A. (2009). Tripartite synapses: Astrocytes process and control synaptic information. *Trends in Neurosciences*, 32(8), 421–431. https://doi.org/10.1016/j.tins.2009.05.001

Pfister, K. K., Shah, P. R., Hummerich, H., Russ, A., Cotton, J., Annuar, A. A., King, S. M., & Fisher, E. M. C. (2006). Genetic Analysis of the Cytoplasmic Dynein Subunit Families. *PLOS Genetics*, *2*(1), e1. https://doi.org/10.1371/journal.pgen.0020001

Popp, B., Krumbiegel, M., Grosch, J., Sommer, A., Uebe, S., Kohl, Z., Plötz, S., Farrell, M., Trautmann, U., Kraus, C., Ekici, A. B., Asadollahi, R., Regensburger, M., Günther, K., Rauch, A., Edenhofer, F., Winkler, J., Winner, B., & Reis, A. (2018). Need for high-resolution Genetic Analysis in iPSC: Results and Lessons from the ForIPS Consortium. *Scientific Reports*, 8, 17201. https://doi.org/10.1038/s41598-018-35506-0

Rajasekharan, S., & Kennedy, T. E. (2009). The netrin protein family. *Genome Biology*, 10(9), 239. https://doi.org/10.1186/gb-2009-10-9-239

Rigato, C., Buckinx, R., Le-Corronc, H., Rigo, J. M., & Legendre, P. (2011). Pattern of invasion of the embryonic mouse spinal cord by microglial cells at the time of the onset of functional neuronal networks. *Glia*, 59(4), 675–695. https://doi.org/10.1002/glia.21140

Ross J. L., Ali M. Y., Warshaw D. M. (2008). Cargo transport: Molecular motors navigate a complex cytoskeleton. *Current Opinion in Cell Biology,* 20(1), 41-47. https://doi.org/10.1016/j.ceb.2007.11.006

Saito, N., Okada, Y., Noda, Y., Kinoshita, Y., Kondo, S., Hirokawa, N. (1997). KIFC2 Is a Novel Neuron-Specific C-Terminal Type Kinesin Superfamily Motor for Dendritic Transport of Multivesicular Body-Like Organelles. *Neuron, 18*(3), 425-438. https://www.cell.com/neuron/fulltext/S0896-6273(00)81243-X

Scarabelli, G., Soppina, V., Yao, X.-Q., Atherton, J., Moores, C. A., Verhey, K. J., & Grant, B. J. (2015). Mapping the Processivity Determinants of the Kinesin-3 Motor Domain. *Biophysical Journal*, 109(8), 1537–1540. https://doi.org/10.1016/j.bpj.2015.08.027

Scardigli, R., Bäumer, N., Gruss, P., Guillemot, F., Le Roux, I. (2003). Direct and concentration-dependent regulation of the proneural gene Neurogenin2 by Pax6. *Development*, 130, 3269-3281. https://doi.org/10.1242/dev.00539

Schnapp, B. J., & Reese, T. S. (1989). Dynein is the motor for retrograde axonal transport of organelles. *Proceedings of the National Academy of Sciences of the United States of America*, 86(5), 1548–1552. https://doi.org/10.1073/pnas.86.5.1548

Schwartzentruber, J., Foskolou, S., Kilpinen, H., Rodrigues, J., Alasoo, K., Knights, A. J., Patel, M., Goncalves, A., Ferreira, R., Benn, C. L., Wilbrey, A., Bictash, M., Impey, E., Cao, L., Lainez, S., Loucif, A. J., Whiting, P. J., Gutteridge, A., & Gaffney, D. J. (2018). Molecular and functional variation in iPSC-derived sensory neurons. *Nature Genetics*, 50(1), 54–61. https://doi.org/10.1038/s41588-017-0005-8

Serafini, T., Kennedy, T. E., Galko, M. J., Mirzayan, C., Jessell, T. M., & Tessier-Lavigne, M. (1994). The netrins define a family of axon outgrowth-promoting proteins homologous to C. elegans UNC-6. *Cell*, 78(3), 409–424. https://doi.org/10.1016/0092-8674(94)90420-0

Shimojo, M., Courchet, J., Pieraut, S., Torabi-Rander, N., Sando, R., Polleux, F., & Maximov, A. (2015). SNAREs Controlling Vesicular Release of BDNF and Development of Callosal Axons. *Cell Reports*, 11(7), 1054–1066. https://doi.org/10.1016/j.celrep.2015.04.032

Soppina, P., Patel, N., Shewale, D. J., Rai, A., Sivaramakrishnan, S., Naik, P. K., & Soppina, V. (2022). Kinesin-3 motors are fine-tuned at the molecular level to endow distinct mechanical outputs. *BMC Biology*, 20, 177. https://doi.org/10.1186/s12915-022-01370-8

Steiner, D. F., Rouillé, Y., Gong, Q., Martin, S., Carroll, R., & Chan, S. J. (1996). The role of prohormone convertases in insulin biosynthesis: Evidence for inherited defects in their action in man and experimental animals. *Diabetes & Metabolism*, 22(2), 94–104.

Stenoien, D. L., & Brady, S. T. (1999). Slow Axonal Transport. In *Basic Neurochemistry: Molecular, Cellular and Medical Aspects. 6th edition*. Lippincott-Raven. https://www.ncbi.nlm.nih.gov/books/NBK28254/

Stenoien DL, Brady ST. Slow Axonal Transport. (1999). In: Siegel GJ, Agranoff BW, Albers RW, et al., (Eds.). *Basic Neurochemistry: Molecular, Cellular and Medical Aspects*. Philadelphia: Lippincott-Raven.

Strand, B. L., Gaserod, O., Kulseng, B., Espevik, T., & Skjak-Baek, G. (2002). Alginate-polylysine-alginate microcapsules: Effect of size reduction on capsule properties. *Journal of Microencapsulation*, 19(5), 615–630. https://doi.org/10.1080/02652040210144243

Stucchi, R., Plucińska, G., Hummel, J. J. A., Zahavi, E. E., Guerra San Juan, I., Klykov, O., Scheltema, R. A., Altelaar, A. F. M., & Hoogenraad, C. C. (2018). Regulation of KIF1A-Driven Dense Core Vesicle Transport: Ca2+/CaM Controls DCV Binding and Liprin-α/TANC2 Recruits DCVs to Postsynaptic Sites. *Cell Reports*, 24(3), 685–700. https://doi.org/10.1016/j.celrep.2018.06.071

Taguchi, H. (2005). Chaperonin GroEL Meets the Substrate Protein as a “Load” of the Rings. *The Journal of Biochemistry*, 137(5), 543–549. https://doi.org/10.1093/jb/mvi069

Takahashi, K., & Yamanaka, S. (2006). Induction of pluripotent stem cells from mouse embryonic and adult fibroblast cultures by defined factors. *Cell*, 126(4), 663–676. https://doi.org/10.1016/j.cell.2006.07.024

Telias, M. (2022). Neural differentiation protocols: How to choose the correct approach. *Neural Regeneration Research*, 18(6), 1273–1274. https://doi.org/10.4103/1673-5374.360171

Terada, S., Kinjo, M., Aihara, M., Takei, Y., & Hirokawa, N. (2010). Kinesin-1/Hsc70-dependent mechanism of slow axonal transport and its relation to fast axonal transport. *The EMBO Journal*, 29(4), 843–854. https://doi.org/10.1038/emboj.2009.389

Thoreson, W. B., Hays, C. L. (2020). How ribbons make ‘sense’ for vision. *The Biochemist,* 42 (5), 36–41. https://doi.org/10.1042/BIO20200064

Tomishige, M., Klopfenstein, D. R. & Vale, R. D. (2002). Conversion of Unc104/KIF1A kinesin into a processive motor after dimerization. *Science,* 297, 2263–2267. https://doi.org/10.1126/science.1073386

Trueta, C., Kuffler, D. P., & De-Miguel, F. F. (2012). Cycling of Dense Core Vesicles Involved in Somatic Exocytosis of Serotonin by Leech Neurons. Frontiers in Physiology, 3. https://doi.org/10.3389/fphys.2012.00175

Uemura, S., Kawaguchi, K., Yajima, J., Edamatsu, M., Toyoshima, Y. Y., & Ishiwata, S. (2002). Kinesin–microtubule binding depends on both nucleotide state and loading direction. *Proceedings of the National Academy of Sciences*, 99(9), 5977–5981. https://doi.org/10.1073/pnas.092546199

Uemura, M., Refaat, M.M., Shinoyama, M., Hayashi, H., Hashimoto, N. and Takahashi, J. (2010), Matrigel supports survival and neuronal differentiation of grafted embryonic stem cell-derived neural precursor cells. *Journal of Neuroscience Research*, 88, 542-551. https://doi.org/10.1002/jnr.22223

Vale, R. D., Reese, T. S., & Sheetz, M. P. (1985). Identification of a novel force-generating protein, kinesin, involved in microtubule-based motility. Cell, 42(1), 39–50. https://doi.org/10.1016/s0092-8674(85)80099-4

Vallee, R. B., Williams, J. C., Varma, D., & Barnhart, L. E. (2004). Dynein: An ancient motor protein involved in multiple modes of transport. *Journal of Neurobiology*, 58(2), 189–200. https://doi.org/10.1002/neu.10314

Van de Bospoort, R., Farina, M., Schmitz, S. K., de Jong, A., de Wit, H., Verhage, M., & Toonen, R. F. (2012). Munc13 controls the location and efficiency of dense-core vesicle release in neurons. *The Journal of Cell Biology*, 199(6), 883–891. https://doi.org/10.1083/jcb.201208024

Van der Vaart, B., van Riel, W. E., Doodhi, H., Kevenaar, J. T., Katrukha, E. A., Gumy, L., Bouchet, B. P., Grigoriev, I., Spangler, S. A., Yu, K. L., Wulf, P. S., Wu, J., Lansbergen, G., van Battum, E. Y., Pasterkamp, R. J., Mimori-Kiyosue, Y., Demmers, J., Olieric, N., Maly, I. V., … Akhmanova, A. (2013). CFEOM1-Associated Kinesin KIF21A Is a Cortical Microtubule Growth Inhibitor. Developmental Cell, 27(2), 145–160. https://doi.org/10.1016/j.devcel.2013.09.010

Vitet, H., Bruyère, J., Xu, H., Séris, C., Brocard, J., Abada, Y.-S., Delatour, B., Scaramuzzino, C., Venance, L., & Saudou, F. (2023). Huntingtin recruits KIF1A to transport synaptic vesicle precursors along the mouse axon to support synaptic transmission and motor skill learning. *eLife*, 12, e81011. https://doi.org/10.7554/eLife.81011

Volpato, V., Smith, J., Sandor, C., Ried, J. S., Baud, A., Handel, A., Newey, S. E., Wessely, F., Attar, M., Whiteley, E., Chintawar, S., Verheyen, A., Barta, T., Lako, M., Armstrong, L., Muschet, C., Artati, A., Cusulin, C., Christensen, K., … Lakics, V. (2018). Reproducibility of Molecular Phenotypes after Long-Term Differentiation to Human iPSC-Derived Neurons: A Multi-Site Omics Study. *Stem Cell Reports*, *11*(4), 897–911. https://doi.org/10.1016/j.stemcr.2018.08.013

Volpato, V., Webber, C., (2020). Addressing variability in iPSC-derived models of human disease: Guidelines to promote reproducibility. *Disease Models & Mechanisms, 13(1).* https://www.ncbi.nlm.nih.gov/pmc/articles/PMC6994963/

De Vos, K. J., & Hafezparast, M. (2017). Neurobiology of axonal transport defects in motor neuron diseases: Opportunities for translational research?. *Neurobiology of disease*, *105*, 283–299. https://doi.org/10.1016/j.nbd.2017.02.004

Wagner, O. I., Esposito, A., Kohler, B., Klopfenstein, D. R. (2009). Synaptic scaffolding protein SYD-2 clusters and activates kinesin-3 UNC-104 in C. elegans. *PNAS*, 106(46), 19605–19610. https://doi.org/10.1073/pnas.0902949106

Walma, D. A. C., & Yamada, K. M. (2020). The extracellular matrix in development. *Development,* 147(10), dev175596. https://doi.org/10.1242/dev.175596

Wang, J., Chu, R., Ni, N., & Nan, G. (2020). The effect of Matrigel as scaffold material for neural stem cell transplantation for treating spinal cord injury. *Scientific Reports*, 10(1), 2576. https://doi.org/10.1038/s41598-020-59148-3

Wang, J., Zhai, W., Yu, Z., Sun, L., Li, H., Shen, H., Li, X., Liu, C., & Chen, G. (2018). Neuroprotection Exerted by Netrin-1 and Kinesin Motor KIF1A in Secondary Brain Injury following Experimental Intracerebral Hemorrhage in Rats. *Frontiers in cellular neuroscience*, 11, 432. https://doi.org/10.3389/fncel.2017.00432

Waterman-Storer, C. M., Karki, S. B., Kuznetsov, S. A., Tabb, J. S., Weiss, D. G., Langford, G. M., & Holzbaur, E. L. F. (1997). The interaction between cytoplasmic dynein and dynactin is required for fast axonal transport. *Proceedings of the National Academy of Sciences of the United States of America*, *94*(22), 12180–12185.

Westerholm-Parvinen, A., Vernos, I., Serrano, L. (2000). Kinesin subfamily UNC104 contains a FHA domain: Boundaries and physicochemical characterization. *FEBS Letters,* 486. https://doi.org/10.1016/S0014-5793(00)02310-3

Wrighton, P. J., Klim, J. R., Hernandez, B. A., Koonce, C. H., Kamp, T. J., & Kiessling, L. L. (2014). Signals from the surface modulate differentiation of human pluripotent stem cells through glycosaminoglycans and integrins. *Proceedings of the National Academy of Sciences*, 111(51), 18126–18131. https://doi.org/10.1073/pnas.1409525111

Wu, H., Xu, J., Pang, Z. P., Ge, W., Kim, K. J., Blanchi, B., Chen, C., Sudhof, T. C., Sun, Y. E. (2007). Integrative genomic and functional analyses reveal neuronal subtype differentiation bias in human embryonic stem cell lines. *Proceedings of the National Academy of Sciences of the United States of America,* 104(34), 13821–13826. https://doi.org/10.1073/pnas.0706199104

Xiong, Y.-J., Soomro, S. H., Huang, Z.-H., Yu, P.-P., Ping, J., & Fu, H. (2022). Poly-L-ornithine blocks the inhibitory effects of fibronectin on oligodendrocyte differentiation and promotes myelin repair. *Neural Regeneration Research*, 18(4), 832–839. https://doi.org/10.4103/1673-5374.353493

Yan, W., Liu, W., Qi, J., Fang, Q., Fan, Z., Sun, G., Han, Y., Zhang, D., Xu, L., Wang, M., Li, J., Chen, F., Liu, D., Chai, R., & Wang, H. (2018). A Three-Dimensional Culture System with Matrigel Promotes Purified Spiral Ganglion Neuron Survival and Function In Vitro. *Molecular Neurobiology*, 55(3), 2070–2084. https://doi.org/10.1007/s12035-017-0471-0

Yau, K. W., Schätzle, P., Tortosa, E., Pagès, S., Holtmaat, A., Kapitein, L. C., & Hoogenraad, C. C. (2016). Dendrites In Vitro and In Vivo Contain Microtubules of Opposite Polarity and Axon Formation Correlates with Uniform Plus-End-Out Microtubule Orientation. *The Journal of Neuroscience,* 36(4), 1071–1085. https://doi.org/10.1523/JNEUROSCI.2430-15.2016

Yap, M. S., Nathan, K. R., Yeo, Y., Lim, L.W., Poh, C. L., Richards, M., Lim, W. L., Othman, I., Heng, B.C. (2015). Neural Differentiation of Human Pluripotent Stem Cells for Nontherapeutic Applications: Toxicology, Pharmacology, and In Vitro Disease Modeling. *Stem Cells International.* https://doi.org/10.1155/2015/105172

Yildiz, A., Tomishige, M., Vale R. D., Selvin P. R. (2004). Kinesin Walks Hand-Over-Hand. *Science*, 303(5658), 676-678. https://doi.org/10.1126/science.1093753

Yin, X., Mead, B. E., Safaee, H., Langer, R., Karp, J. M., & Levy, O. (2016). Stem Cell Organoid Engineering. *Cell Stem Cell*, 18(1), 25–38. https://doi.org/10.1016/j.stem.2015.12.005

Yonekawa, Y., Harada, A., Okada, Y., Funakoshi, T., Kanai, Y., Takei, Y., Terada, S., Noda, T., & Hirokawa, N. (1998). Defect in Synaptic Vesicle Precursor Transport and Neuronal Cell Death in KIF1A Motor Protein–deficient Mice. *The Journal of Cell Biology*, 141(2), 431–441.

Yu, L. M. Y., Leipzig, N. D., & Shoichet, M. S. (2008). Promoting neuron adhesion and growth. *Materials Today*, 11(5), 36–43. https://doi.org/10.1016/S1369-7021(08)70088-9

Zahn, T.R., Angleson, J.K., MacMorris, M.A., Domke, E., Hutton, J.F., Schwartz, C. and Hutton, J.C. (2004), Dense Core Vesicle Dynamics in Caenorhabditis elegans Neurons and the Role of Kinesin UNC-104. *Traffic*, 5, 544-559. *https://doi.org/10.1111/j.1600-0854.2004.00195.x*

Zaniewski, T. M., Gicking, A. M., Fricks, J., & Hancock, W. O. (2020). A kinetic dissection of the fast and superprocessive kinesin-3 KIF1A reveals a predominant one-head-bound state during its chemomechanical cycle. *The Journal of Biological Chemistry*, 295(52), 17889–17903. https://doi.org/10.1074/jbc.RA120.014961

Zhang, X., Bao, L., & Ma, G.-Q. (2010). Sorting of neuropeptides and neuropeptide receptors into secretory pathways. *Progress in Neurobiology*, 90(2), 276–283. https://doi.org/10.1016/j.pneurobio.2009.10.011

Zhang, Y., Pak, C., Han, Y., Ahlenius, H., Zhang, Z., Chanda, S., Marro, S., Patzke, C., Acuna, C., Covy, J., Xu, W., Yang, N., Danko, T., Chen, L., Wernig, M., & Südhof, T. C. (2013). Rapid Single-Step Induction of Functional Neurons from Human Pluripotent Stem Cells. *Neuron*, 78(5), 785–798. https://doi.org/10.1016/j.neuron.2013.05.029

Appendix.

Supplementary Figures

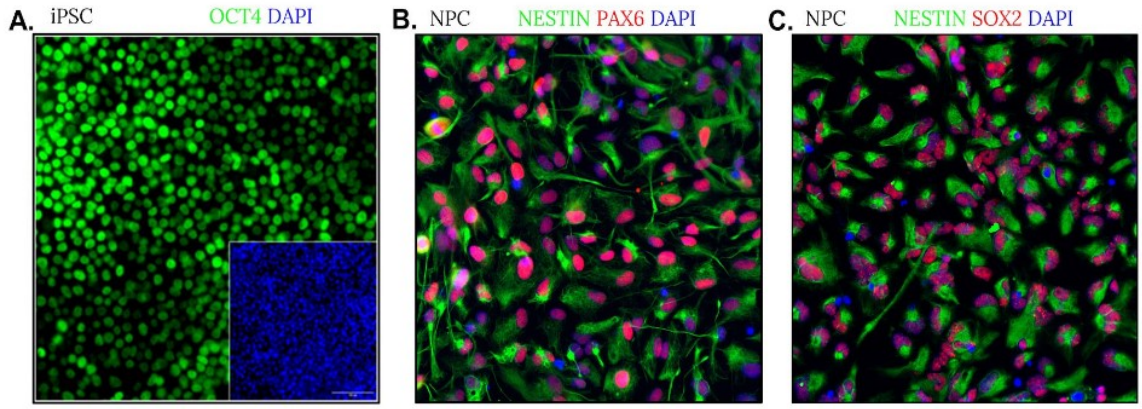

Figure A.1 iPSC and NPC characterization. Immunocytochemical stain of iPSCs and NPCs used to generate the iPSC-derived neurons via small molecule differentiation. Differentiation, immunocytochemical stain, and images generate by Dr Y. Zhu (Simon Fraser University) A. iPSCs are positive for the pluripotency marker OCT4. B-C. NPCs generated by Dr Y. Zhu are positive for the neural stem cell markers NESTIN, Pax6 and Sox2. (Keefe 2022)

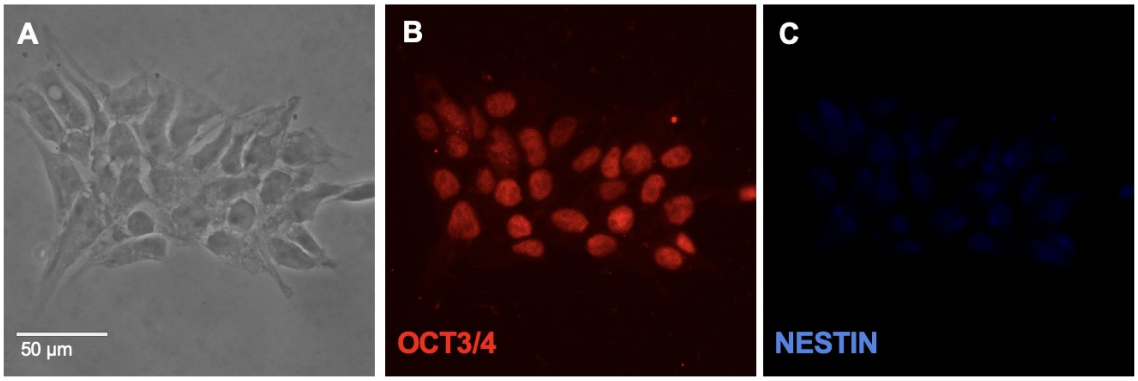

Figure A.2 OCT3/4 and NESTIN stain of iPSCs. Immunocytochemical stain of induced pluripotent stemcells (iPSC) (Corielle) used to generate iPSC-derived neurons via neurogenin-2 differentiation. A. Phase image of iPSCs. B. The iPSCs are positive for the pluripotency marker OCT3/4. C. The iPSCs are negative for the NPC marker NESTIN.

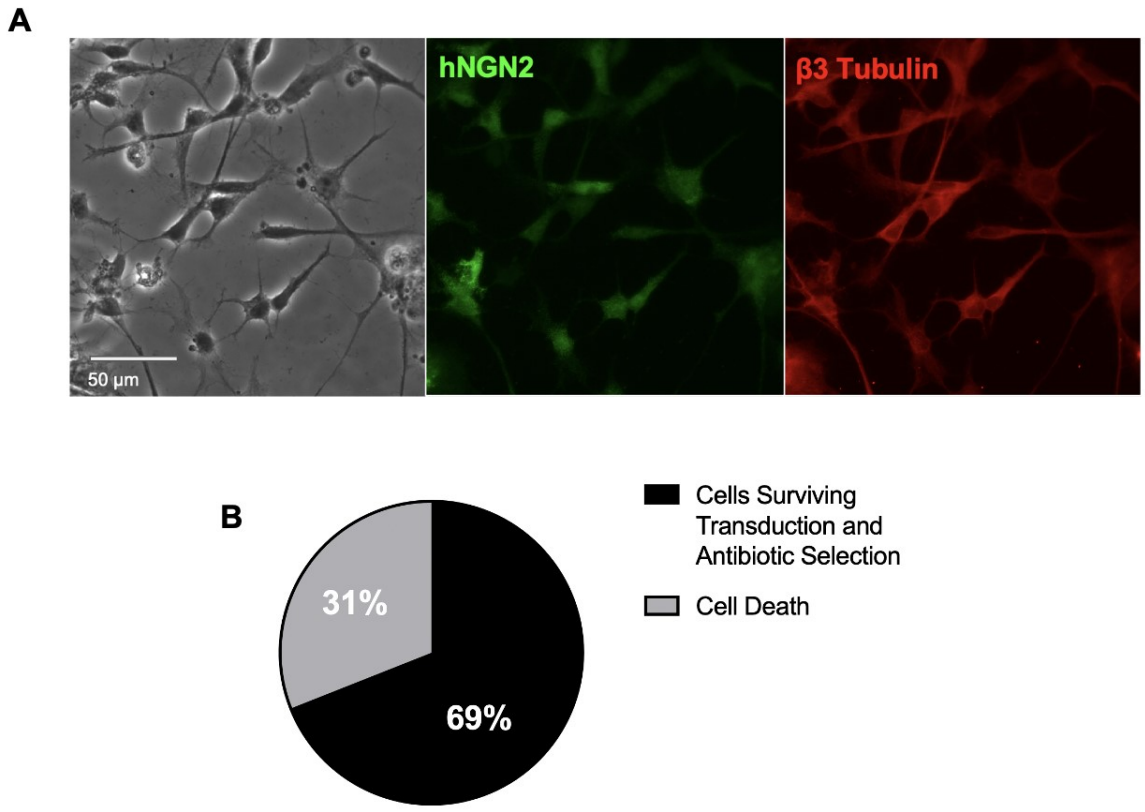

Figure A.3 Development of NGN2 induced iPSC-derived neurons. A. At 3DIV the iPSC-derived neurons are developing lengthening neurites and are shown to expressed NGN2 post lentiviral transduction. β3-Tubulin, a neuronally expressed marker is also shown to be expressed at day 3 post transduction. B. Percentage of cells surviving the transduction and antibiotic selection process of NGN2 differentiation. Cell were manually counted from phase images. (n = 3 regions of interest from 3 independent cultures)

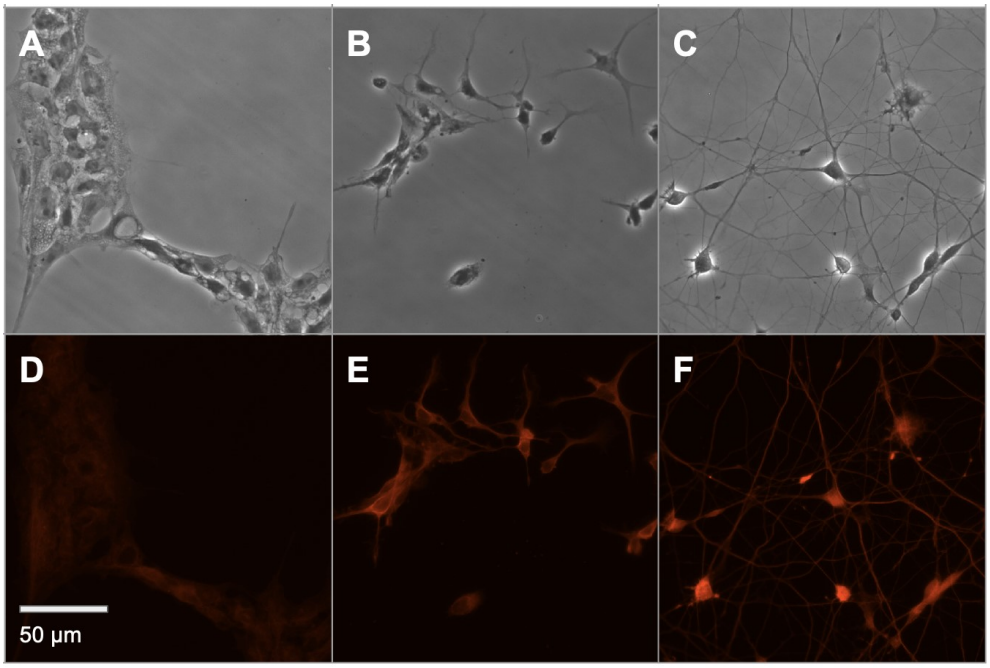

Figure A.4 Development of NGN2 induced iPSC-derived neurons over the course of 7 DIV. A-C. Phase images of cells at 0 DIV, 3 DIV, and 7 DIV. Overtime, the cells develop neurites that elongate as the cells adopt a neuronal morphology. D-F. β3-Tubulin expression at 0 DIV, 3 DIV, and 7 DIV, β3-Tubulin is expressed and already visible at 3 DIV.

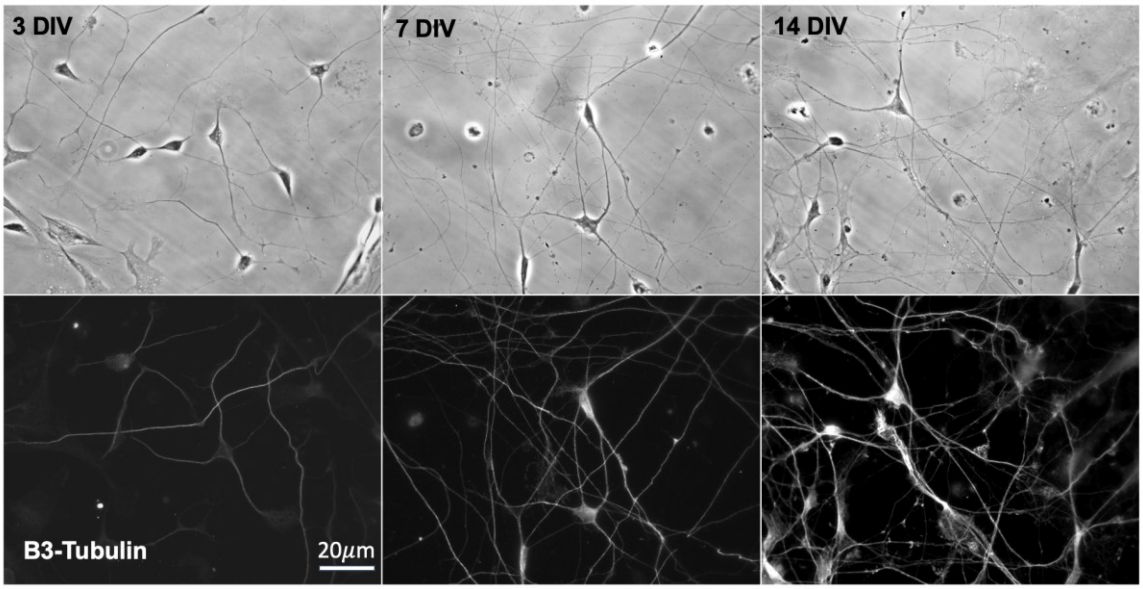

Figure A.5. Development of small molecule differentiated neurons over the course of 14 DIV. At 3 DIV, neurites are already formed and beginning to elongate and β3-Tubulin expression is visible. Over the course 14 DIV, the neuronal processes continue to lengthen and β3-Tubulin expression increases.

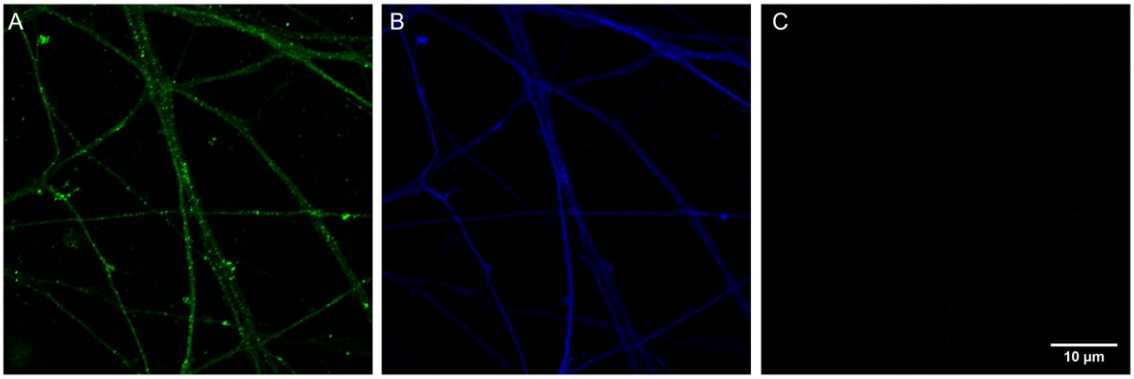

Figure A.6 Endogenous netrin-1 patterning and control. A. Endogenous netrin-1 puncta along the axons of iPSC-derived neurons. B. β3-Tubulin expression along axons of iPSC-derived neurons. C. Image of the same field taken in the red channel (A555). There is no bleed-through of signal present.

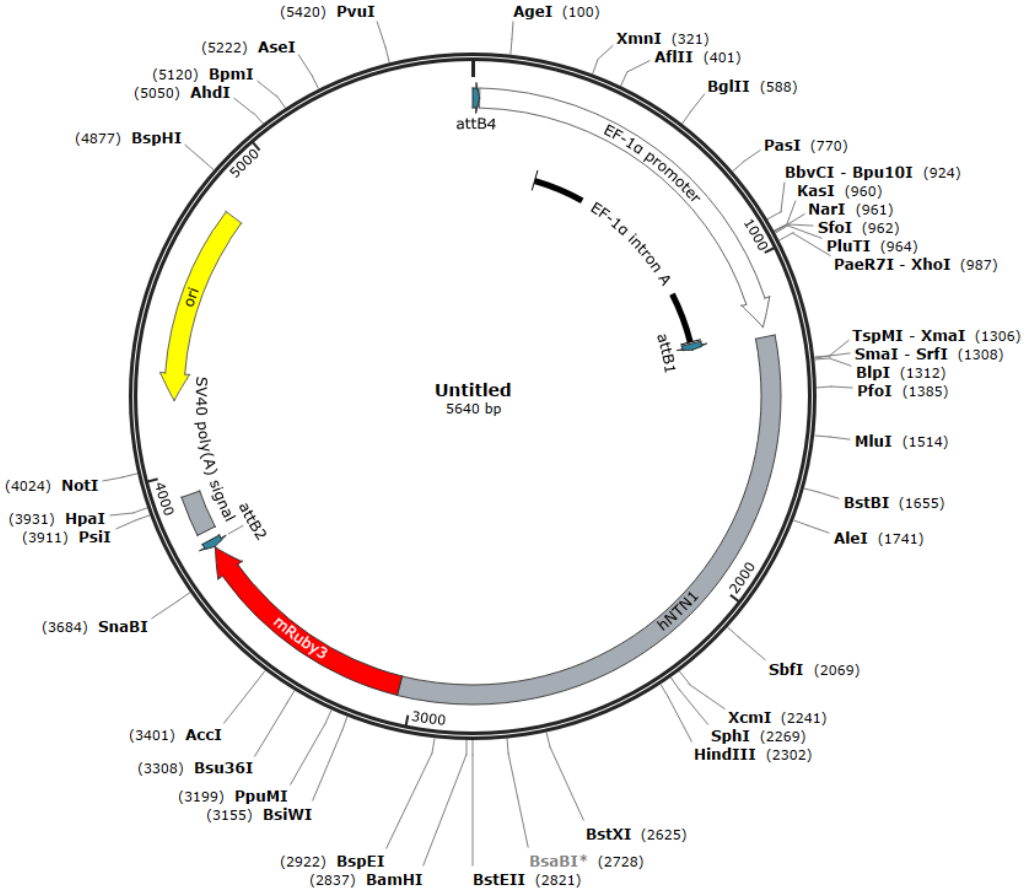

Figure A.7 pEF1A-hNetrin1-mRuby3 plasmid map. This plasmid was constructed by VectorBuilder and includes the elongation factor 1alpha (EF-1α) promoter and the human netrin-1 (NTN1), mRuby3 fluor, and ampicillin resistance genes. (Made in SnapGene)

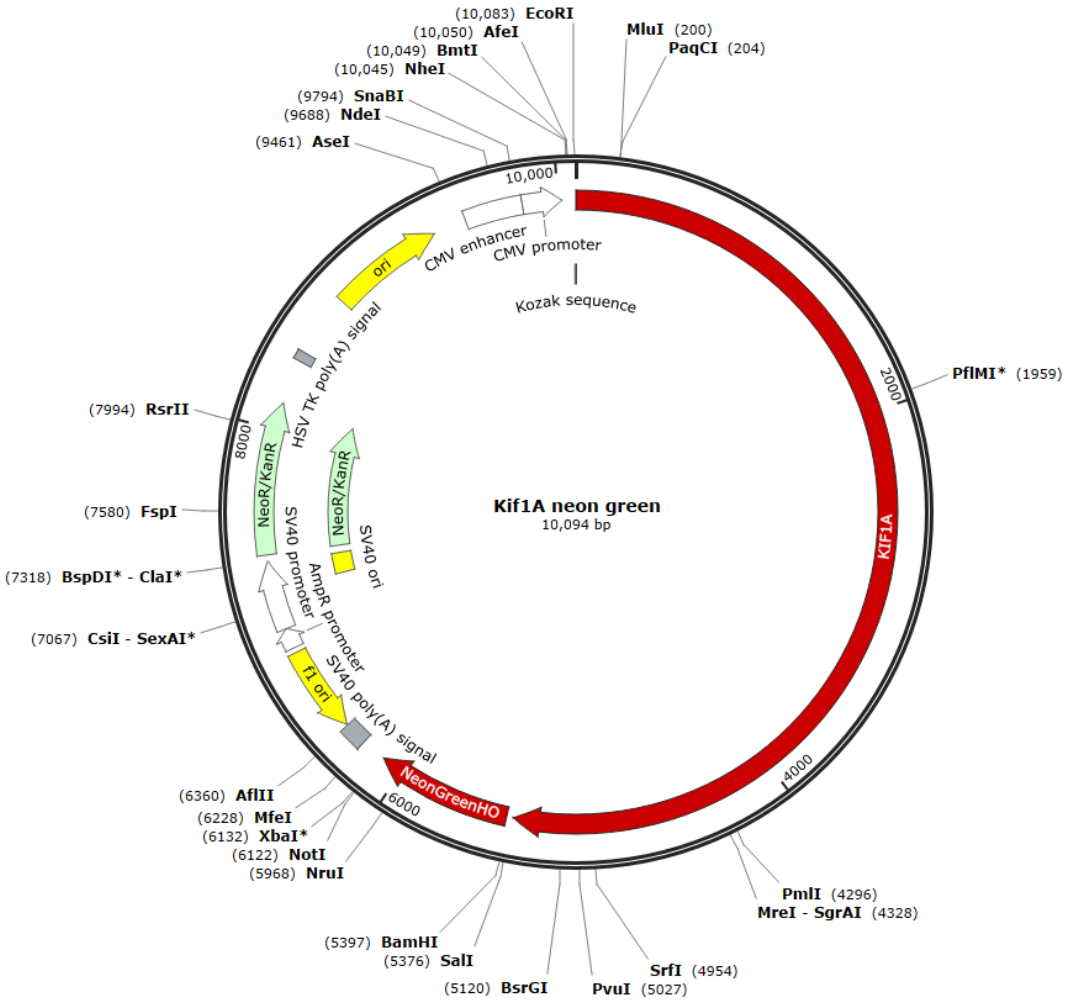

Figure A.8 KIF1A-NeonGreenHO-G plasmid map. This plasmid includes the human cytomegalovirus immediate early promoter (CMV) and the KIF1A, NeonGreen fluor, and kanamycin resistance (KanR) genes. (Made in SnapGene)

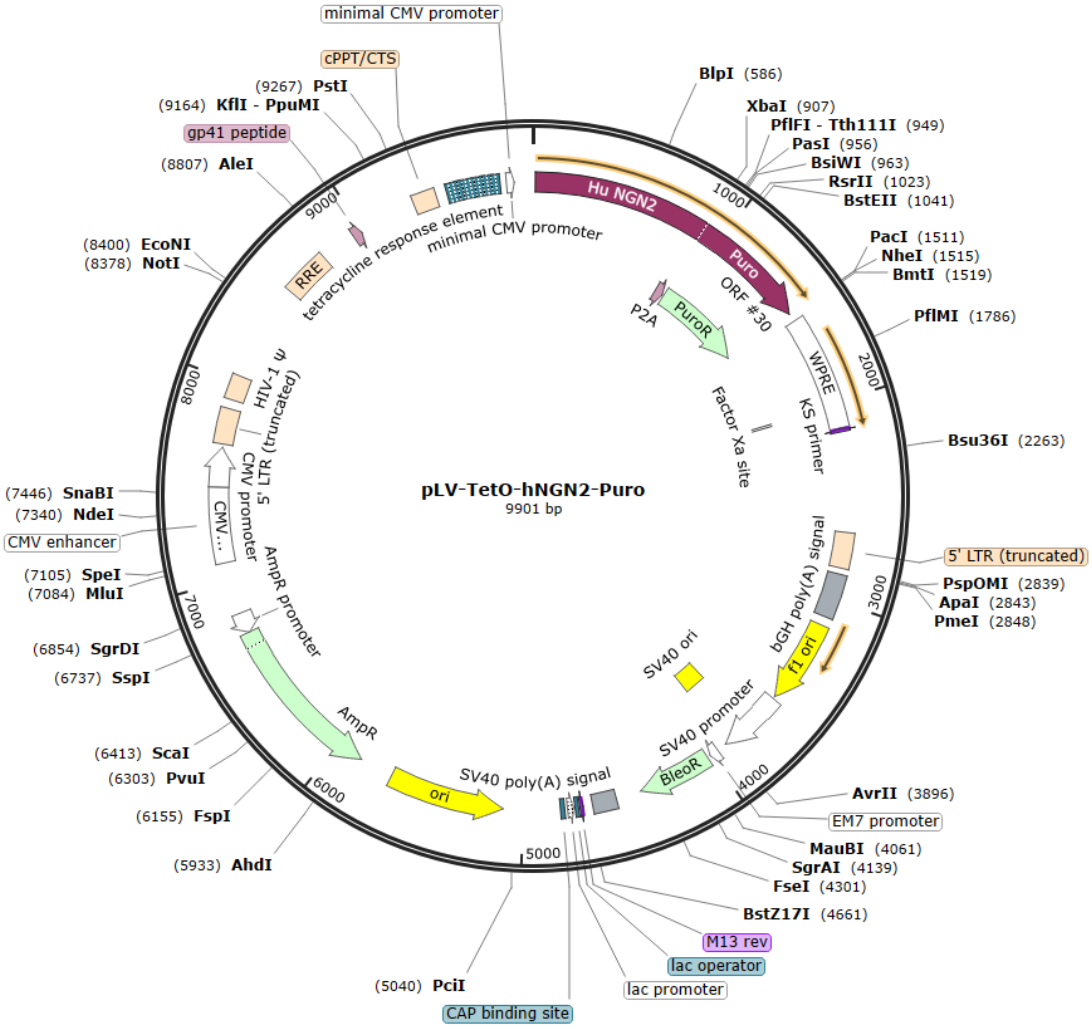

Figure A.9 pLV-TetO-hNGN2-Puro plasmid map. This plasmid was provided by Addgene and includes the human neurogenin2 gene (Hu NGN2), the puromycin resistance gene (Puro), the Tet-On system including the tetracycline response element, and ampicillin resistance gene. (Made in SnapGene)

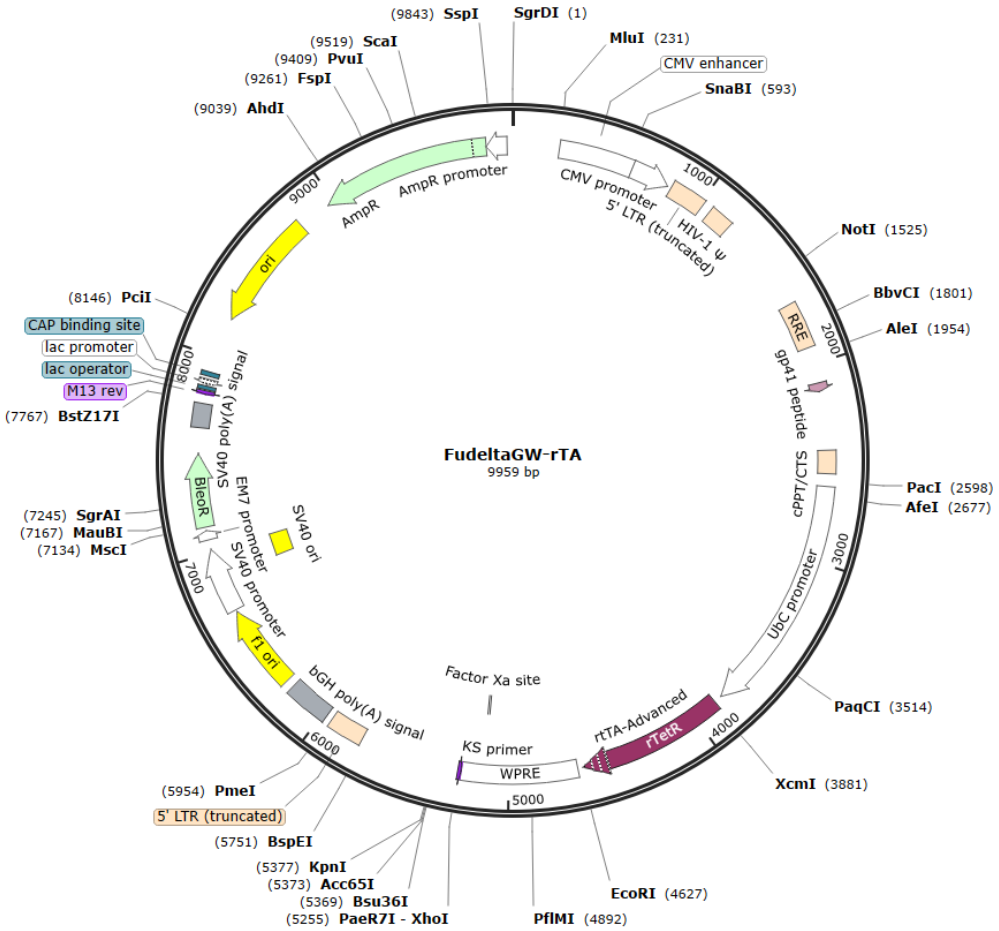

Figure A.10 FudeltaGW-rTA plasmid map. This plasmid construct was provided by Addgene and contains the human cytomegalovirus immediate early promoter (CMV), the reverse tetracycline-controlled transactivator (rtTA) gene, and the ampicillin resistance gene. (Made in SnapGene)